

AD-A050 091

NAVAL POSTGRADUATE SCHOOL MONTEREY CALIF

F/G 17/7

THE EFFECTS OF MULTIPATH PROPAGATION ON THE RANGE MEASUREMENT S--ETC(U)

DEC 77 H STURHAN, W P HAVENSTEIN

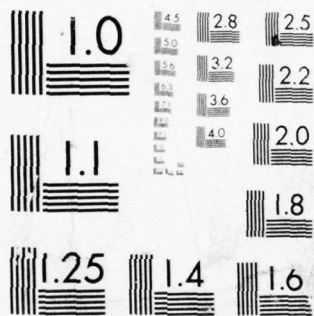
UNCLASSIFIED

NL

1 OF 3

AD
A050 091





MICROCOPY RESOLUTION TEST CHART
NATIONAL BUREAU OF STANDARDS-1963-A

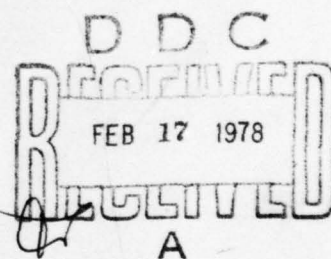
AD A 050091

AD No. _____
DDC FILE COPY

NAVAL POSTGRADUATE SCHOOL
Monterey, California



THESIS



THE EFFECTS OF MULTIPATH PROPAGATION
ON THE RANGE MEASUREMENT SYSTEM
AT FORT HUNTER LIGGETT

by

Hans Sturhan
Walter Perry Havenstein

December 1977

Thesis Advisor:

M. L. Wilcox

Approved for public release; distribution unlimited.

UNCLASSIFIED

SECURITY CLASSIFICATION OF THIS PAGE (When Data Entered)

REPORT DOCUMENTATION PAGE		READ INSTRUCTIONS BEFORE COMPLETING FORM
1. REPORT NUMBER	2. GOVT ACCESSION NO.	3. RECIPIENT'S CATALOG NUMBER
4. TITLE (and Subtitle) THE EFFECTS OF MULTIPATH PROPAGATION ON THE RANGE MEASUREMENT SYSTEM AT FORT HUNTER LIGGETT		5. TYPE OF REPORT & PERIOD COVERED Master's thesis
7. AUTHOR(s) Hans/Sturhan Walter Perry/Havenstein		6. PERFORMING ORG. REPORT NUMBER
9. PERFORMING ORGANIZATION NAME AND ADDRESS Naval Postgraduate School Monterey, California 93940		8. CONTRACT OR GRANT NUMBER(s)
11. CONTROLLING OFFICE NAME AND ADDRESS Naval Postgraduate School Monterey, California 93940		10. PROGRAM ELEMENT, PROJECT, TASK AREA & WORK UNIT NUMBERS
14. MONITORING AGENCY NAME & ADDRESS (if different from Controlling Office)		12. REPORT DATE Dec 77
		13. NUMBER OF PAGES 195 (12) 194 p.
		15. SECURITY CLASS. (of this report) Unclassified
		15a. DECLASSIFICATION/DOWNGRADING SCHEDULE
16. DISTRIBUTION STATEMENT (of this Report) Approved for public release, distribution unlimited.		
17. DISTRIBUTION STATEMENT (of the abstract entered in Block 20, if different from Report)		
18. SUPPLEMENTARY NOTES		
19. KEY WORDS (Continue on reverse side if necessary and identify by block number) Range Measurement System Multipath Propagation Range-Pulse Distortion		
20. ABSTRACT (Continue on reverse side if necessary and identify by block number) Instrumentation was developed for investigating the radio frequency link between the A station and the B unit in the Range Measurement System. Propagation effects were characterized using a multipath simulation in a laboratory environment. Field experiments were conducted to investigate the presence of a multipath environment at Fort Hunter Liggett. The effects of		

DD FORM 1473
1 JAN 73
(Page 1)EDITION OF 1 NOV 68 IS OBSOLETE
S/N 0102-014-6601

1

UNCLASSIFIED

SECURITY CLASSIFICATION OF THIS PAGE (When Data Entered)

751 450

JL

UNCLASSIFIED

SECURITY CLASSIFICATION OF THIS PAGE/When Data Entered

varying the ambient temperature on the A station and the B unit were measured.

ACCESSION for	
NTIS	White Section <input checked="" type="checkbox"/>
RDC	Dark Section <input type="checkbox"/>
UNANNOUNCED	
IDENTIFICATION	
BY	
DISTRIBUTION/AVAILABILITY CODES	
DIST.	AVAIL. CODE/OF SPECIAL
A	

DD Form 1473
S/N 0102-014-6601

UNCLASSIFIED

SECURITY CLASSIFICATION OF THIS PAGE/When Data Entered

Approved for public release; distribution unlimited.

THE EFFECTS OF MULTIPATH PROPAGATION ON THE RANGE
MEASUREMENT SYSTEM AT FORT HUNTER LIGGETT

by

Hans Sturhan
Lieutenant Commander, Federal German Navy
E.S.E.E. Naval Postgraduate School, 1976

Walter P. Havenstein
Captain, United States Marine Corps
B.S.A.E. United States Naval Academy, 1971

Submitted in partial fulfillment of the
requirements for the degree of

MASTER OF SCIENCE IN ELECTRICAL ENGINEERING

from the
NAVAL POSTGRADUATE SCHOOL
December 1977

Authors:

Hans Sturhan

W. P. Havenstein

Approved by:

Milton L. Wilson Thesis Advisor

Charles H. Kothmann Second Reader

Donald E. Kirk
Chairman, Department of Electrical Engineering

George J. Haltiner
Dean of Science and Engineering

ABSTRACT

Instrumentation was developed for investigating the radio frequency link between the A station and the B unit in the Range Measurement System. Propagation effects were characterized using a multipath simulation in a laboratory environment. Field experiments were conducted to investigate the presence of a multipath environment at Ft. Hunter Liggett. The effects of varying the ambient temperature on the A station and the B unit were measured.

TABLE OF CONTENTS

I.	INTRODUCTION.....	8
A.	BACKGROUND.....	8
B.	THESIS OBJECTIVES.....	9
C.	RMS SYSTEM DESCRIPTION.....	9
II.	THEORY.....	12
A.	MULTIPATH PROPAGATION PHENOMENA AT UHF.....	12
1.	Definitions.....	12
2.	Effects of Multipath on Pulse Systems....	14
B.	SURVEY OF ANALYSIS METHODS.....	15
1.	Prediction Models.....	15
2.	Empirical Results of Previous Tests.....	15
3.	Laboratory Simulation.....	16
III.	EXPERIMENTATION DEVELOPMENT.....	17
A.	GENERAL CONSIDERATIONS.....	17
1.	Signal Waveforms.....	18
2.	A Station/B Unit RF Link Specifications..	22
B.	INSTRUMENTATION.....	30
C.	SINGLE-PATH EXPERIMENTS.....	32
D.	MULTIPATH SIMULATION EXPERIMENTS.....	36
E.	EXPECTED RESULTS IN THE FIELD.....	39
IV.	RF LINK MEASUREMENTS IN THE FIELD.....	43
A.	GENERAL CONSIDERATIONS.....	43
B.	TEST PROCEDURES.....	50
1.	AB Arrangement.....	50
a.	Range Mode.....	51
b.	SCOM Mode.....	53
2.	BA Arrangement.....	53
C.	RESULTS.....	54
1.	Reliability Studies.....	54
a.	Field Tests.....	54

b. Temperature Sensitivity Tests.....	55
c. Alignment Comparison Test.....	55
2. AB Range Mode.....	56
3. BA Range Mode.....	58
V. CONCLUSIONS.....	59
VI. RECOMMENDATIONS.....	60
Appendix A: B UNIT CHECKOUT SET.....	61
Appendix B: TEKTRONIX 7834 STORAGE OSCILLGSCCPE.....	65
Appendix C: SINGLE-PATH EXPERIMENTS.....	69
Appendix D: MULTIPATH SIMULATION EXPERIMENTS.....	94
Appendix E: HELMET ANIENNA MODIFICATIONS.....	123
Appendix F: FIELD TESTS.....	133
Appendix G: A STATION/B UNIT TEMPERATURE TESTS.....	173
Appendix H: ALIGNMENT INVESTIGATIONS AT FHI/EDM.....	186
-LIST OF REFERENCES.....	191
INITIAL DISTRIBUTION LIST.....	194

ACKNOWLEDGEMENT

The authors are sincerely grateful to Professor Charles H. Rethauge and Professor Milton L. Wilcox for their professional guidance and dedicated counsel during the preparation of this thesis. Other members of the Naval Postgraduate School staff who provided valuable assistance include Professor Robert W. Burton, Mr. Victor McCullough and Mr. Jose N. Velasquez. The members affiliated with the United States Army Combat Development Experimentation Command who provided technical assistance and logistic support include Major David R. Park, Mr. Joseph A. Egger, Second Lieutenant Allan R. Marney and SP5 Prabodh K. Patel. Finally, the completion of this thesis is due in no small part to the moral support provided by the authors' wives, Sabine and Judith.

I. INTRODUCTION

A. BACKGROUND

The United States Army Combat Development Experimentation Command (USACDEC) employs the Range Measurement System (RMS) at Fort Hunter Liggett. The RMS system is used to provide accurate position/location information and digital data communication capabilities between tactical ground and airborne units for combat evaluations. In previous years several persistent problems were identified, the solution of which could potentially lead to a significant improvement in the overall effectiveness and reliability of the RMS system.

One of the significant difficulties identified was in electromagnetic anomalies. The uniquely rugged terrain at Fort Hunter Liggett led to the speculation that multipath propagation could be causing system errors. It was apparent that a systematic investigation of the effect of multipath phenomena on the RMS system was needed. A more detailed background is presented in Ref. 1.

B. THESIS OBJECTIVES

The object of this work was to determine if errors in data collected by the RMS system, such as 'wild' ranges could be attributed to multipath phenomena. Also, to identify and document any previously unknown problems encountered during the investigation.

C. RMS SYSTEM DESCRIPTION

The determination and provision of position/location information of tactical ground and airborne units to the central control facility is accomplished by deploying interrogation stations (A stations) at surveyed locations. The A stations communicate on a discrete address basis with responding units (B units) located in ground or airborne elements. Then, the B units transmit range pulse and instrumentation data to the A stations. The A stations operate under the direction of a computer-controlled central station (C station), which communicates directly with the A stations or via a relay/distribution station (D station). Figure 1 (extracted from Ref. 2) shows the general operating arrangement of the RMS system.

The RMS system is a pulse code modulation/amplitude modulation system that transmits formatted messages and range pulses at a carrier frequency of 918 MHz. Messages in digital form are transmitted via tone bursts at subcarrier frequencies of 1.35, 2.25, 3.14 and 4.05 MHz. Each subcarrier represents a channel, which is further subdivided into upper and lower sidebands for transmission of ones and

zeroes. This means that, on channel 1 (1.35 MHz), a tone burst on the upper sideband represents a one and a tone burst on the lower sideband is a zero. Thus, the simultaneous triggering of both the upper and the lower sidebands of a channel does not occur. This technique is used to eliminate intersymbol interference. A half-duplex mode is used in the A-B link in which channels 2 and 3 are used for transmitting information from the A station to the B unit and channels 1 and 4 transmit information from B to A. Ranging is accomplished by pulses at the carrier frequency. The system uses omnidirectional vertically polarized antennas with the maximum gain in the horizontal plane for the B unit and approximately 10 degrees below the horizontal for the A station. A detailed description of the system operation and the individual elements is contained in Ref. 3.

The system has four modes of operation; Ranging (Range), Short Communication (SCOM), Extended Communication A to B (EAB) and Extended Communication B to A (EBA). A detailed description of each mode and digital message format is contained in Ref. 3. The data reduction/distribution techniques that are carried out by the C station for each mode are described in detail in Ref. 4.

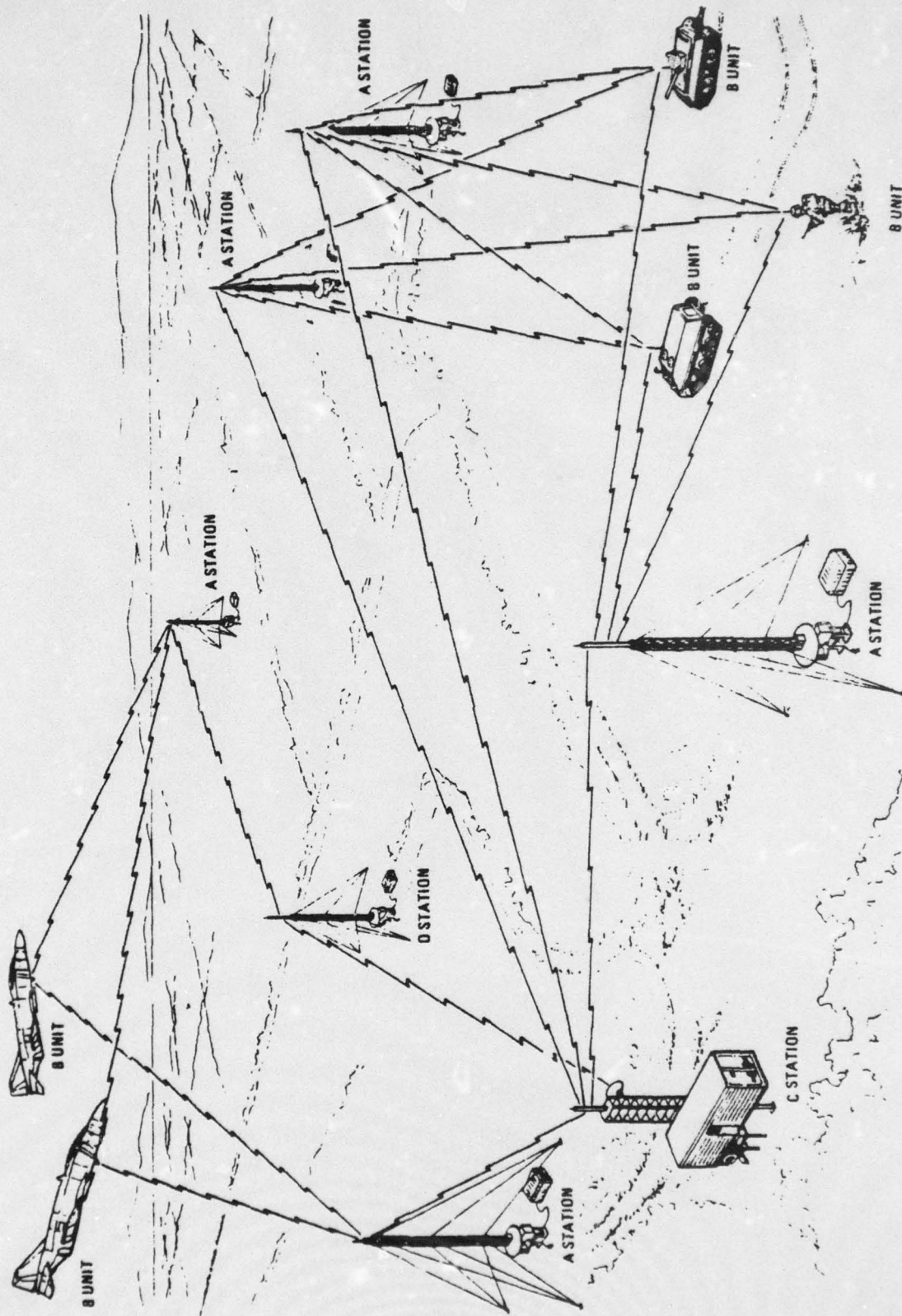


Figure 1 - RMS GENERAL ARRANGEMENT

II. THEORY

A. MULTIPATH PROPAGATION PHENOMENA AT UHF

1. Definitions

Multipath propagation normally exists in irregular terrain, but it is also likely to be found in any area where obstacles are present (buildings, trees, vehicles, etc.). Multipath propagation is the phenomenon that occurs when there are many rays (paths) along which electromagnetic energy can travel from the transmitting point to the receiving point. The propagation times, amplitudes and phases differ in these rays at the receiving point. These variances will sometimes enhance and sometimes tend to cancel the original signal at the receiver, resulting in signal-strength variations known as 'fading'. At ultra-high frequencies (UHF) two types of multipath that produce fading are atmospheric-multipath and reflection-multipath (Ref. 5). Atmospheric-multipath is caused by two or more rays arriving by slightly different paths. These different paths are caused by abnormal variations in the characteristics of the lower atmosphere. If the atmosphere is uniform in the propagation area then this type of multipath does not exist. Reflection-multipath is from the interaction of direct and reflected rays. In line-of-sight (LOS) propagation the reflecting surface may be the ground or any obstacle not in the LOS path. Figure 2 illustrates multipath propagation in the atmosphere.

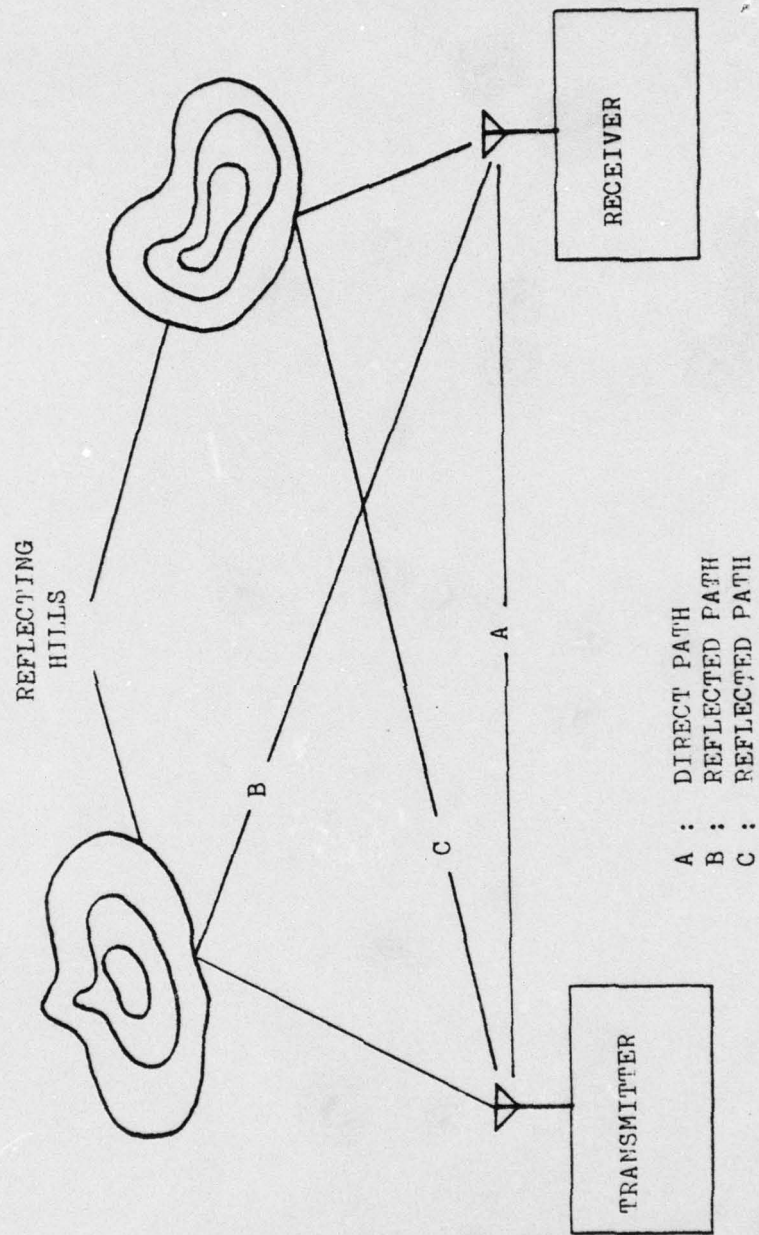


Figure 2 - MULTIPATH PROPAGATION IN THE ATMOSPHERE

The influence of multipath on a communication system is described in terms of two effects; selective fading and intersymbol interference (Ref. 6). Selective fading is related to the relative radio frequency (RF) phases of the signals arriving at the receiving antenna via the various paths. For any frequency, the total received signal is the vector sum of all the individual path components. Since the amplitudes and phases of the reflected signals vary with the reflection coefficient of the reflecting surface and delayed path length, the resultant received signal will also vary. Moreover, if a signal is composed of different frequencies, each vector sum for a particular frequency will be different, since losses and time delays are frequency dependent as well. Thus, there are signal-strength variations of the received signal with respect to time and frequency which is termed selective fading.

Intersymbol interference is associated with the time delay between the first and last significant signals. If the modulation is rapid enough, the signal interference will result in a smearing of the intelligence, for any signal waveform. For example, if a particular modulation technique is used to transmit digital signals, interference may cause the information contained in a symbol for a 'one' to be shifted enough to cause a detection error in a following symbol for a 'zero'.

2. Effects of Multipath on Pulse Systems

Pulse communication systems are generally tolerant of multipath propagation that produces a reflected pulse whose delay, with respect to the direct-path signal, is small compared with the pulsewidth. In this case intersymbol interference will be slight although distortion

of individual pulses may be significant. Schmid (Ref. 7) showed that intersymbol interference problems arise when reflected pulses are as large or larger than the pulsewidth. In single-pulse systems where pulses are used for timing, as in some radars, detection of the arrival of the leading edge of the pulse is critical. Distortion of the pulse due to multipath in such a system may lead to errors.

B. SURVEY OF ANALYSIS METHODS

In trying to quantitatively analyze the effects of multipath on communication signals several techniques have been developed.

1. Prediction Models

The nature of the multipath problem is probabilistic and lends itself to prediction models based on probability theory. Several authors (Refs. 7, 8 and 9) have developed models for specific environments and communication systems. Prediction models are normally designed for a particular requirement and are therefore limited in their general application.

2. Empirical Results of Previous Tests

Comparative analysis of previous tests of multipath effects to the system being considered can be valuable. In many cases where modelling of a system is impractical systems are tested in actual multipath environments. Although this is a very accurate method, it normally requires more time than modelling. Therefore, if previous

testing of similar systems has been conducted their results may provide the desired information. There has been a significant amount of data collected concerning the effects of multipath on numerous communication systems and in a variety of environments.

3. Laboratory Simulation

This method is particularly useful since it does not depend on other sources of information. Although simulations may not correspond to the actual environment the communication system will be operating in, they do provide an understanding of the system sensitivity to vary signals. Jakes (Ref. 8) has developed two fading simulations for mobile communication systems operating at microwave frequencies.

III. EXPERIMENTATION DEVELOPMENT

A. GENERAL CONSIDERATIONS

Although there has been extensive work and large amounts of empirical data compiled on the multipath problem dealing with mobile communication systems and pulse communications in general (Refs 10-12) very little data was found that could be applied to the RMS system. It was further determined that statistical modelling of the multipath environment at Ft. Hunter Liggett was impractical. Therefore, actual field measurements were conducted to provide accurate multipath data and at the same time uncover other RMS problems. In an effort to become more familiar with the RMS system operations and to develop measurement techniques prior to going to the field a laboratory simulation was designed. It was apparent that the RF link most likely to be affected by multipath was the A station to B unit link. Therefore, it was the only link in the system considered in the experiments. The Range and to a lesser extent SCCM modes of operation were the only modes considered. By observing the actual detected signals at the A station/B unit receivers and noting the variation from the specified waveforms an understanding of the effects of the multipath environment was realized.

1. Signal Waveforms

Prior to determining what type of instrumentation was going to be used a basic understanding of the signal waveforms was necessary. In the Range mode the A station upon command from the C station transmits a formatted signal to a B unit. The signal consists of an initializing pulse, 10 address bits, two mode bits and a range pulse. The initializing pulse sets the required automatic gain control (AGC) level in the B unit receiver. The 10 address bits determine the B unit that is being interrogated. The mode bits indicate that the ranging mode is being used and the range pulse provides a timing marker from which ranges are determined. All B units that are operating will 'listen' for the A station transmission, but only the B unit that can identify the address will respond.

Upon receipt of a range command the B unit starts a calibrated internal delay after which it transmits a message back to the A station. The internal delay in the B unit is triggered by the leading edge of the received range pulse. The message that is transmitted back to the A station consists of a message flag bit and a range pulse. The slant range between the A station and the B unit is determined by a 15 bit clock in the A station that measures the time between the transmission of a range pulse (leading edge) by the A station and the detection of the leading edge of the range pulse from the B unit at the A station. The A station then accounts for the internal delay of the B unit and forwards the 15 bit range to the C station. The least significant bit in the range corresponds to a range of 2 meters.

The SCOM mode is a communication mode by which the C station can send a four bit message to a B unit via an A station. For the AB link, the A station transmits a message to the B unit that consists of an initializing pulse, 10 address bits, two mode bits and four message bits. The B unit response to the A station is a signal consisting of 13 message bits. At the B unit the four received message bits are displayed on an input/output (I/O) device (Figure 3). Reference 3 presents a more complete description of the waveforms and explains how they are generated. Figure 4 shows the signal waveforms that are transmitted by the A station for the Range and SCOM modes.

The application of some of the basic multipath theory led to the assumption that distortion of the signal waveform by selective fading of the signal due to multipath could be responsible for some of the errors in RMS data. It was clear that significant distortion of address bits in any mode of operation might cause the B unit to fail to identify its own address. This would cause a 'no B unit response' result. In a less likely case, distortion of the address might be sufficient to cause an incorrect B unit to respond. It was also apparent that significant distortion of the range pulse might cause errors in slant range data. In the SCOM mode distortion in the address and/or message bits could lead to no or incorrect B unit responses or errors in the received message.

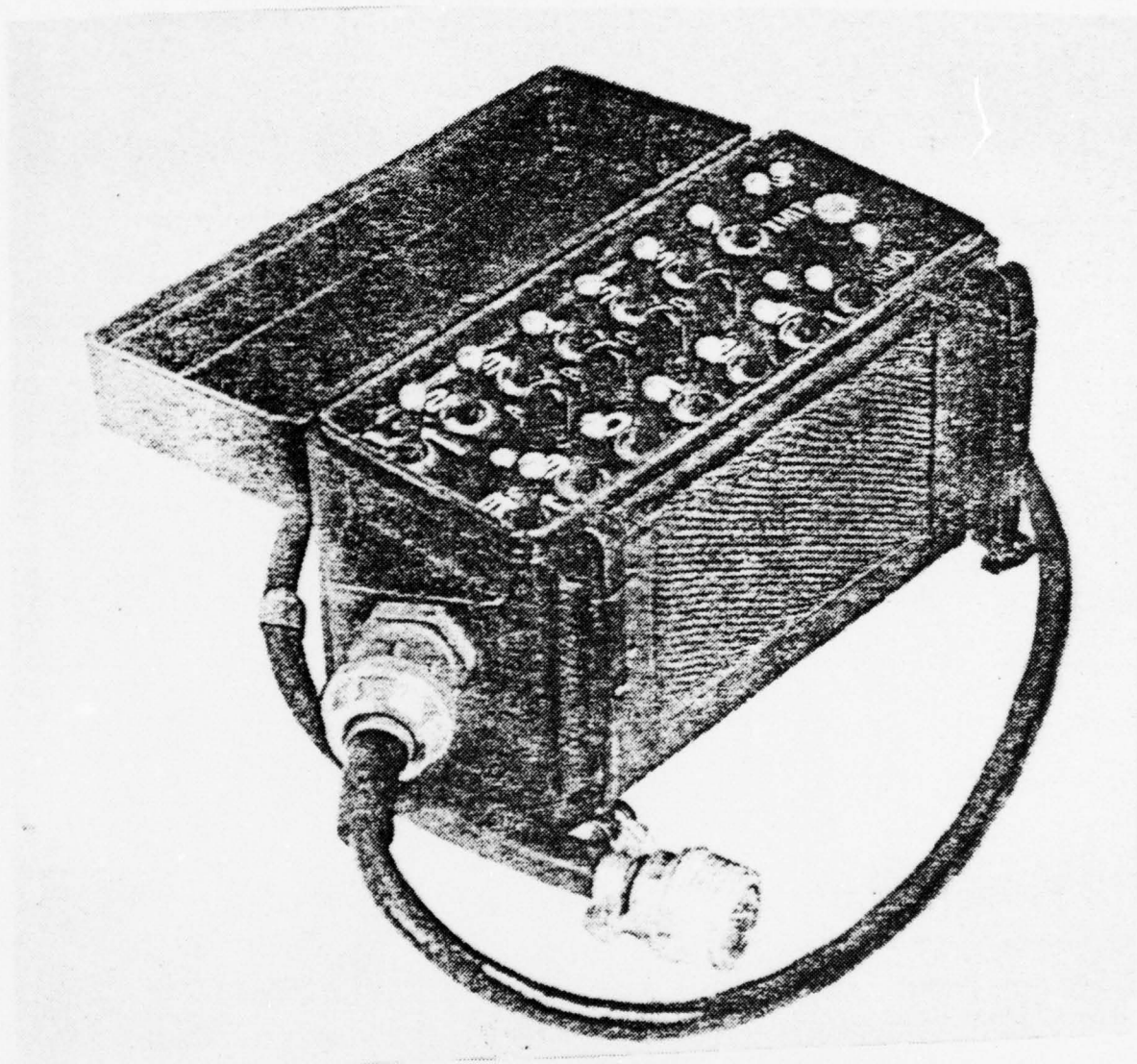


Figure 3 - MONITOR INPUT/OUTPUT DEVICE

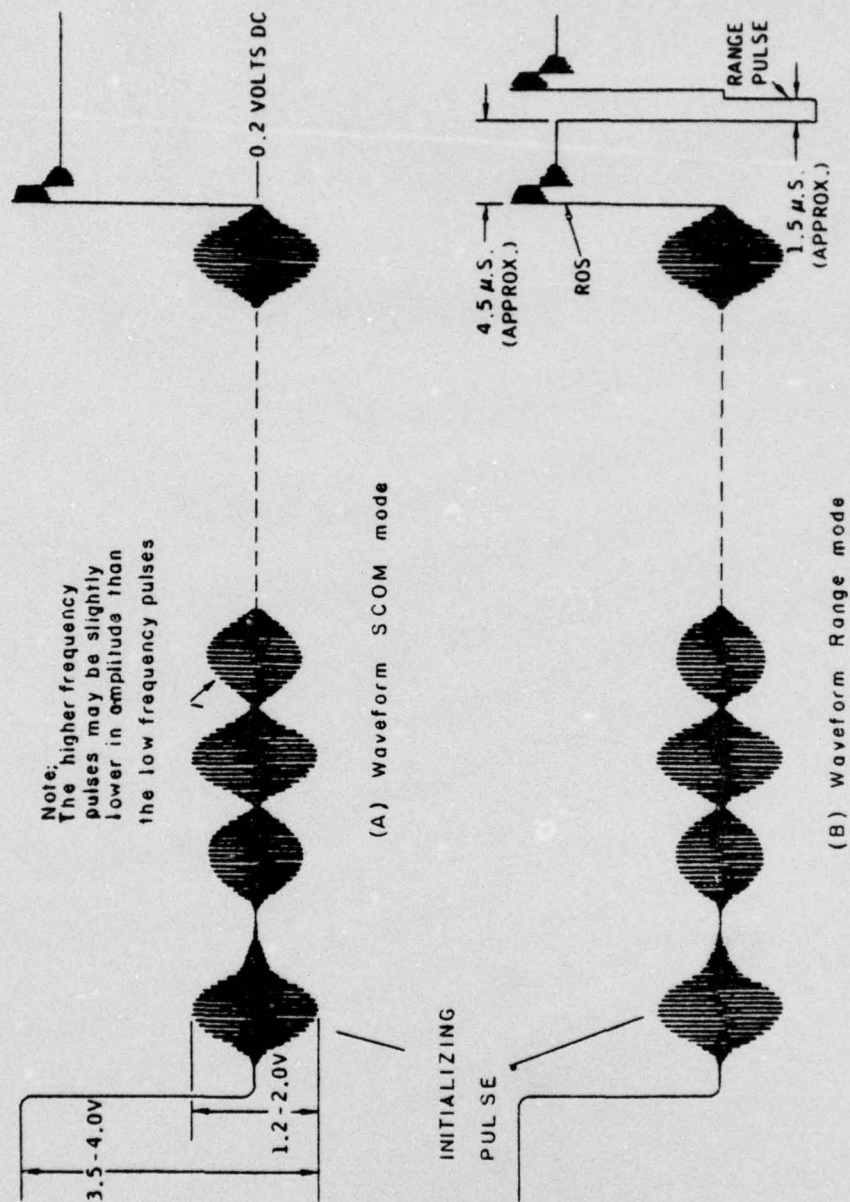


Figure 4 - A STATION TRANSMITTED SIGNAL WAVEFORMS

2. A Station/B Unit RF Link Specifications

The following characteristics are those specified by the designer for properly operating and aligned A stations and B units. The minimum transmitter output power is 37 dBm for the A station and 40.8 dBm for the B unit. The B unit receiver operation is from -23 dBm to -67 dBm. The A station antenna is an eight dipole pair colinear array with swamper elevated 24 feet above the ground. Reference 13 gives the vertical and horizontal patterns for the antenna, which are reproduced in Figures 5 and 6. There are several antennas designed for use with the B unit. However, the helmet mounted quarter-wave monopole was the only antenna considered. Laboratory and field measurements (Refs. 1 and 14) have shown significant variations in the antenna patterns from one helmet antenna to another. Therefore, the design specifications were somewhat suspect in determining the B unit antenna gain. Figures 7 and 8 show representative vertical and horizontal patterns for the helmet antenna.

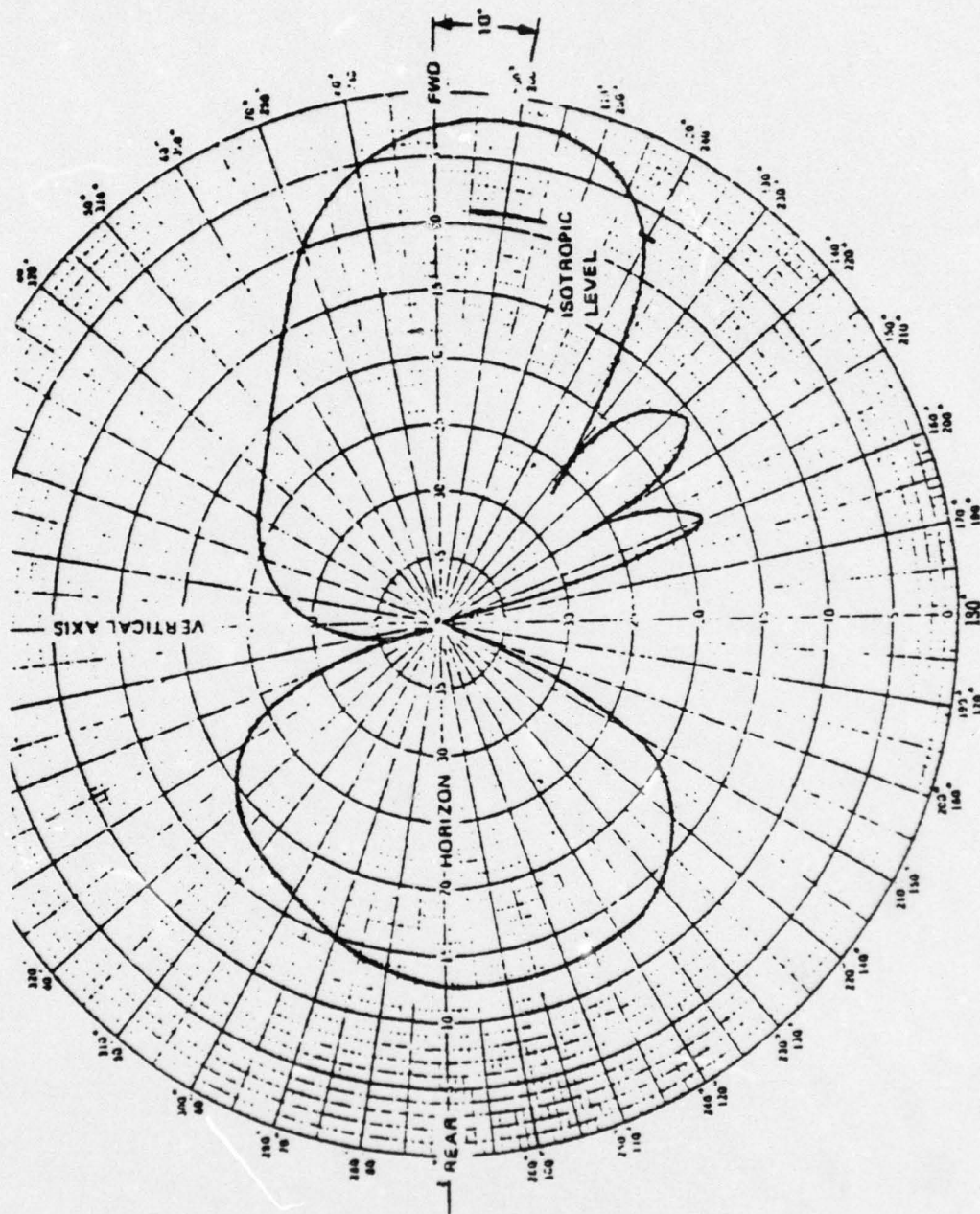


Figure 5 - VERTICAL PATTERN A STATION ANTENNA

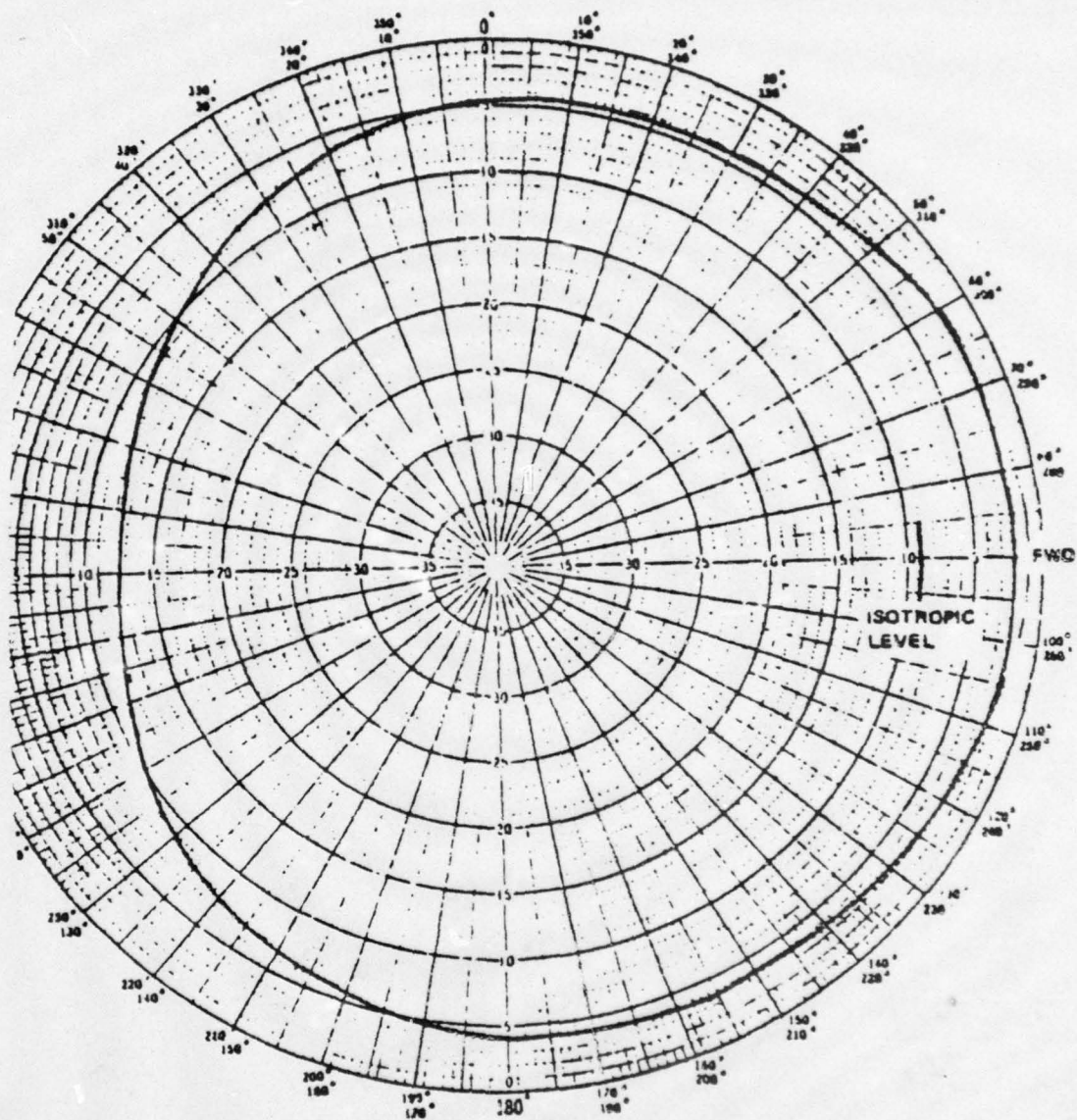


Figure 6 - HORIZONTAL PATTERN A STATION ANTENNA

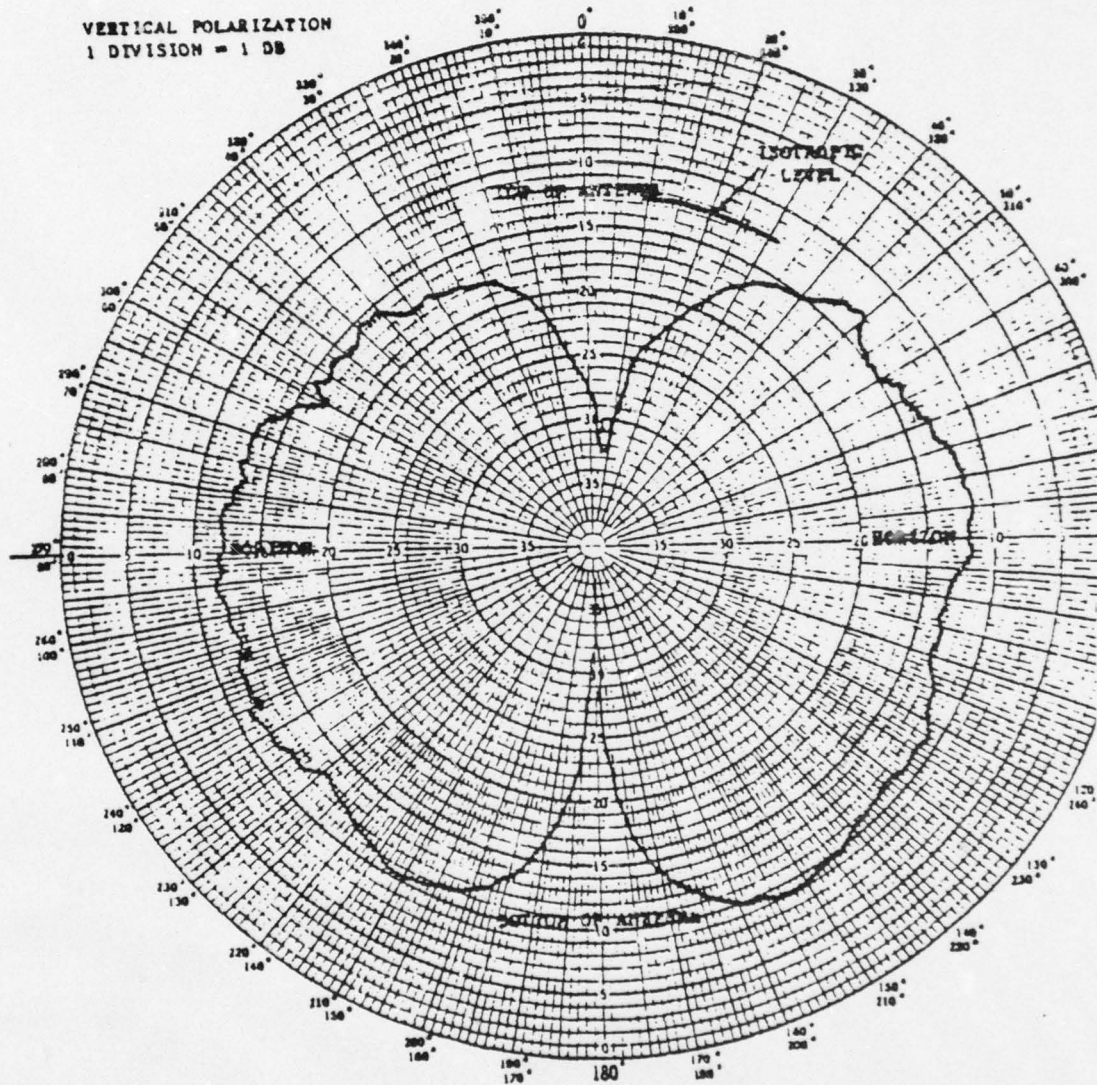
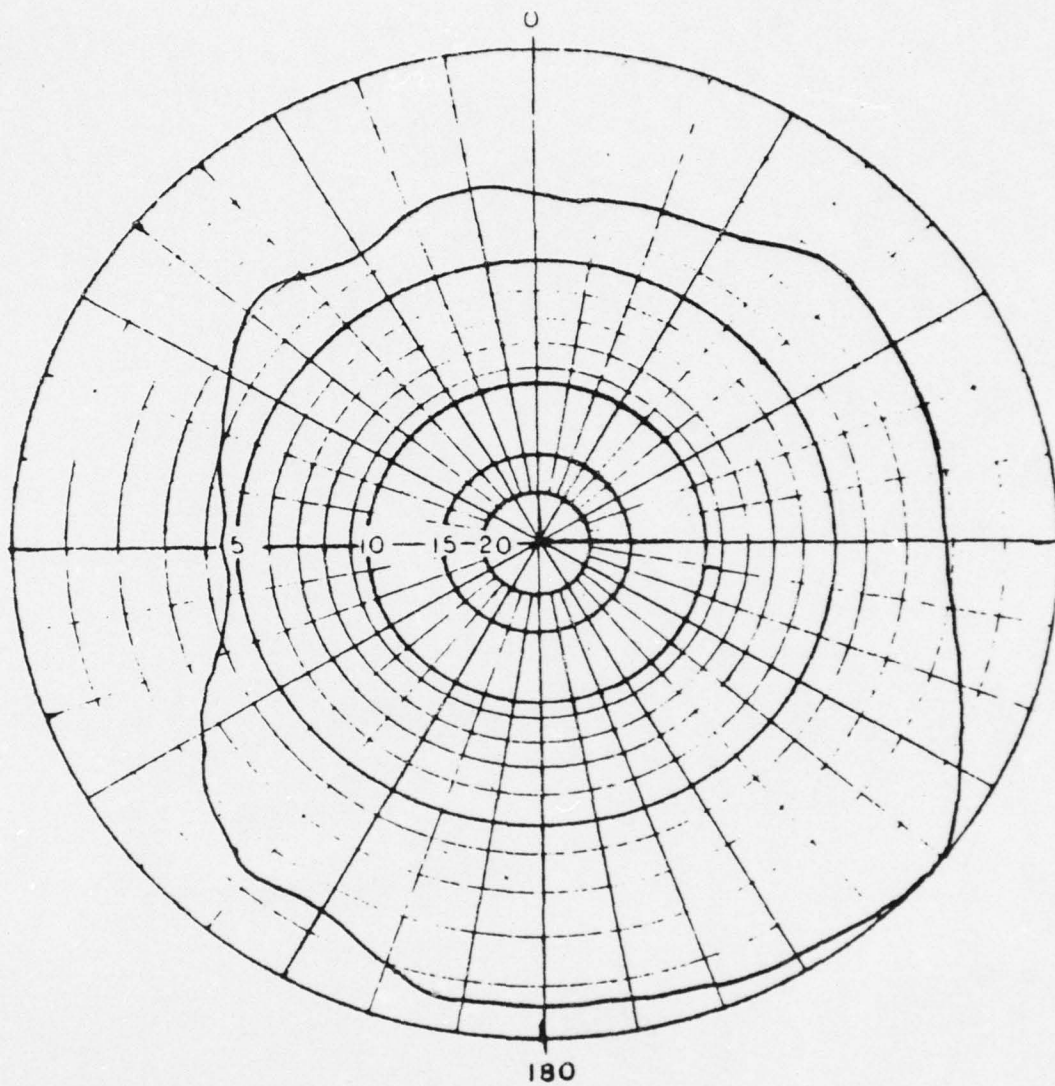


Figure 7 - VERTICAL PATTERN HELMEI ANTENNA



1 db per division.

Figure 8 - HORIZONTAL PATTERN HELMET ANTENNA

The height of the A station with respect to the B unit is an important factor as is readily apparent from the antenna patterns. Figure 9 is a diagram of the relative positions of the A station and the B unit and shows the 30° angle at which the gain of the A station antenna has dropped to +2 dB. Designating any area where the A station antenna gain is below +2 dB as an 'apparent' null the minimum distance (S) to a B unit for any given relative height (H) can be calculated from the equation

$$S = H \tan 60^\circ$$

Table 1 gives some representative values of this distance for typical A station antenna heights.

The transmission loss in free space, that is, in a region free from all objects that might reflect or absorb RF energy (Ref. 15) is given by

$$L = 10 \log \frac{(4\pi d)^2}{\lambda^2}$$

where λ = the wavelength in meters

d = the distance between antennas in meters

This loss provides a good estimate to the operating range (distance) of the system (AB link), which is specified from a minimum of 30 meters to a maximum range of 9,000 meters.

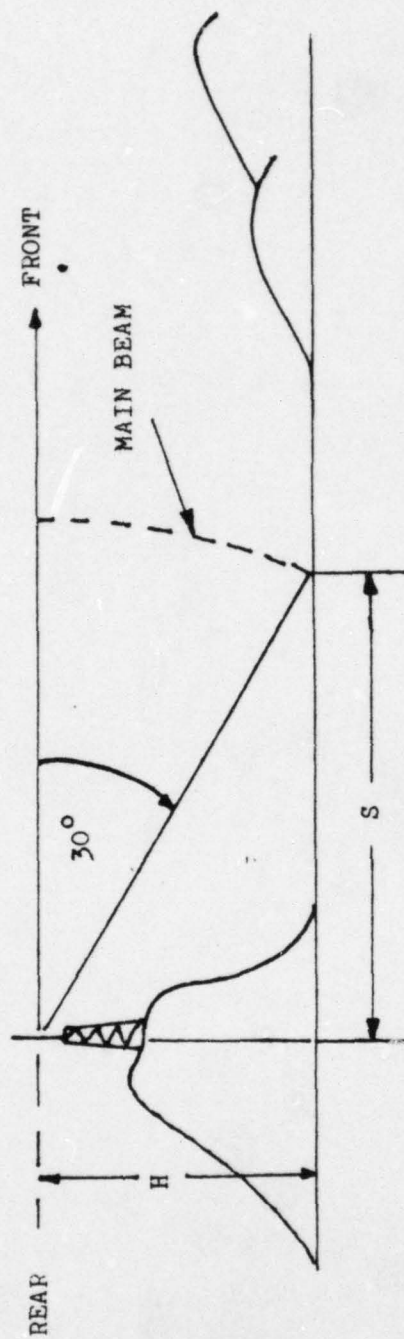


Figure 9 - AB LINK DIAGRAM

Table 1 MINIMUM DISTANCES FROM ELEVATED A STATION

<u>H (feet)</u>	<u>S (feet)</u>
30	52
50	87
100	173
200	346
400	693
600	1039
800	1386
1000	1732
1200	2079
1400	2425
1600	2771
1800	3118
2000	3464

E. INSTRUMENTATION

The basic RMS components required for the experiments were a standard A station and a micro B unit. In addition, a B Unit Checkout Set was necessary to trigger the A station to interrogate the B unit. References 2 and 16 present a complete description and a detailed operation of the micro B unit and the A station respectively. Appendix A presents a complete description and the operating procedures for the B Unit Checkout Set (checkout set). Several other items were used for specific tests such as the Monitor Input/Cutput Device (I/O device), antennas and the B unit Power Breakout Box. Prior to commencing any experiment the A station was checked for proper alignment in accordance with procedures set forth in Ref. 16.

The primary measurement instrument was the Tektronix 7834 Storage Oscilloscope (Figure 10). This mainframe together with accompanying plug-ins provided a fast writing speed, variable persistence display and signal storage capability. Its use was dictated by the specified characteristics of the signal waveforms under investigation. Appendix B gives some of the performance characteristics of the 7834 and the procedures used to make both laboratory and field measurements. In addition to the oscilloscope, various attenuators, directional couplers, envelope detectors, power meters, DC power sources and coaxial cables were used as required by individual experiments. These items were checked to meet required bandwidth and power ratings prior to being used in actual experiments. Because of its relatively low loss characteristics (9 dB/100 ft at 900 MHz), RG-213/U coaxial cable was used whenever cable was needed for the transmission path.

C. SINGLE-PATH EXPERIMENTS

A simple single-path arrangement (Figure 11) was set up with coaxial cable used as the RF link. Several laboratory experiments were conducted with this setup to measure the performance of the A station and the B unit in an 'ideal' propagation environment. The procedures and data collected for the single-path experiments are presented in Appendix C. The A station and B unit were kept at an ambient temperature of 20°C during all of the single-path and multipath simulation experiments.

The experiments verified that the system operates according to specifications in a single-path environment. Figure 12 presents typical signal waveforms that were measured with the 7834 oscilloscope. The figure shows an entire cycle in the Range mode with the upper trace being the signals transmitted by the A station. The lower trace is the detected video signal of the B unit and consists of both the received and transmitted signals. The numbers displayed are the vertical scales (200 mV and 50 mV) for each trace and the horizontal scale (50 microseconds) for both traces. A picture of a range pulse that has been expanded to measure rise time is presented in Figure 13. The experiments clearly showed that distortion of the range pulse could cause errors in the slant range data. In addition, it was determined that the B unit I/O device had no degrading effect on the system performance.

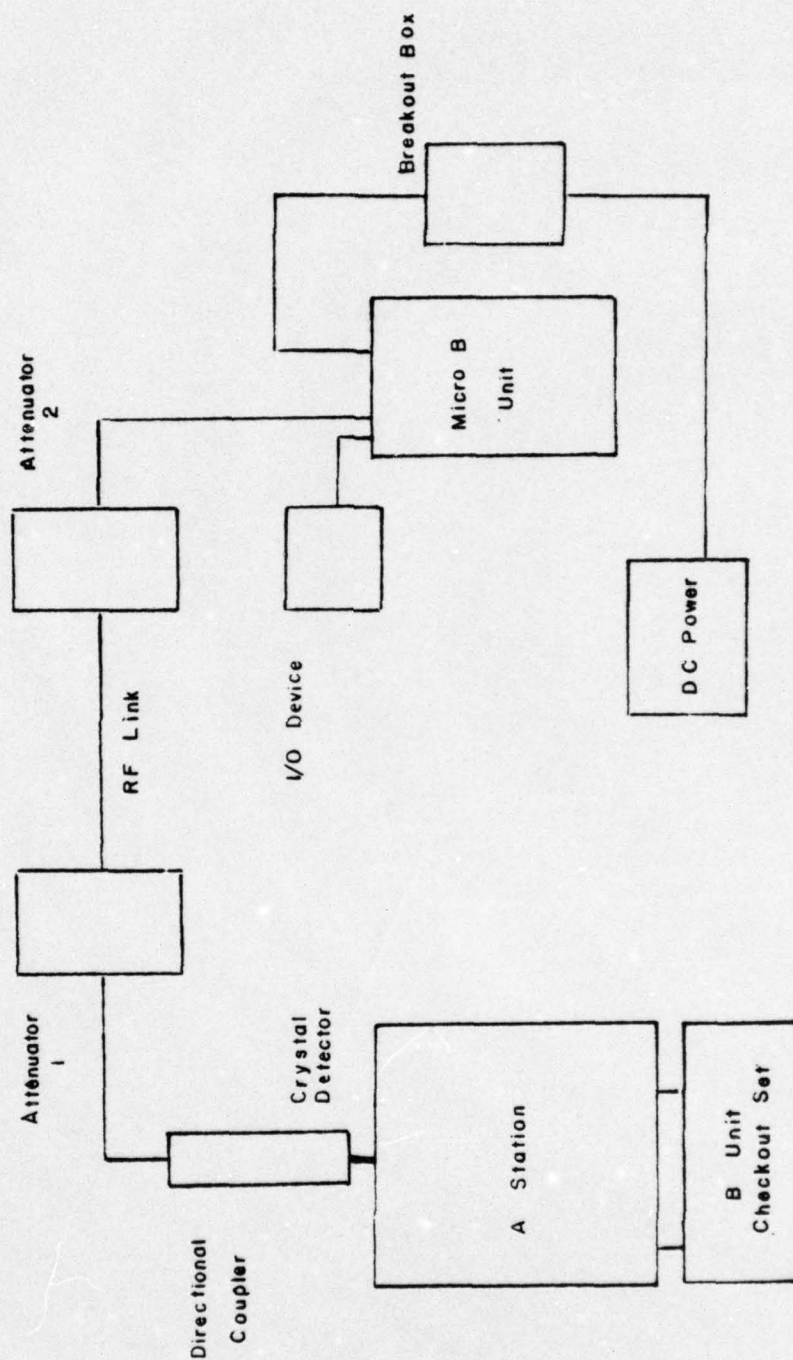


Figure 11 - SINGLE-PATH SETUP

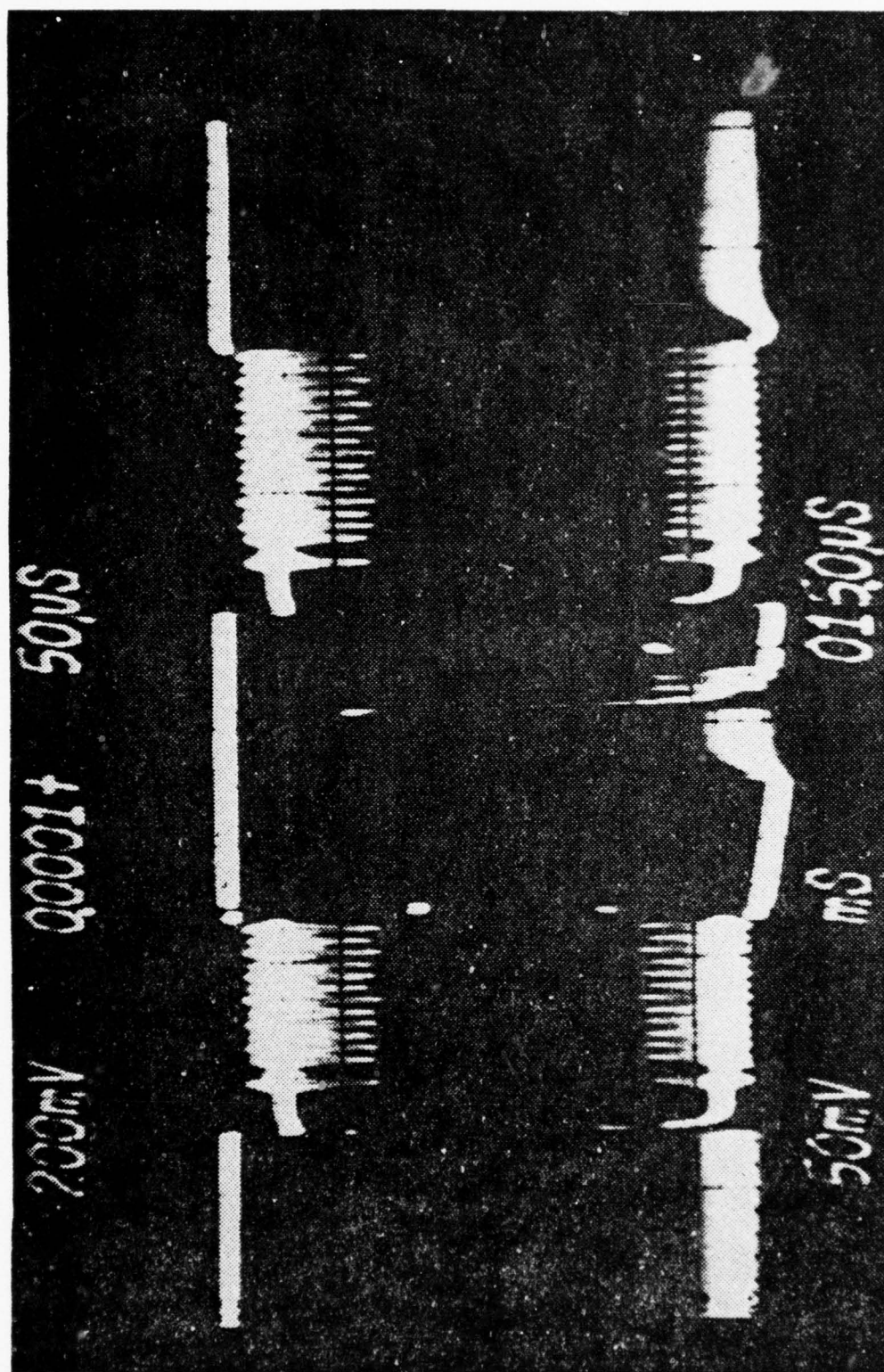


Figure 12 - TYPICAL SIGNAL WAVEFORMS

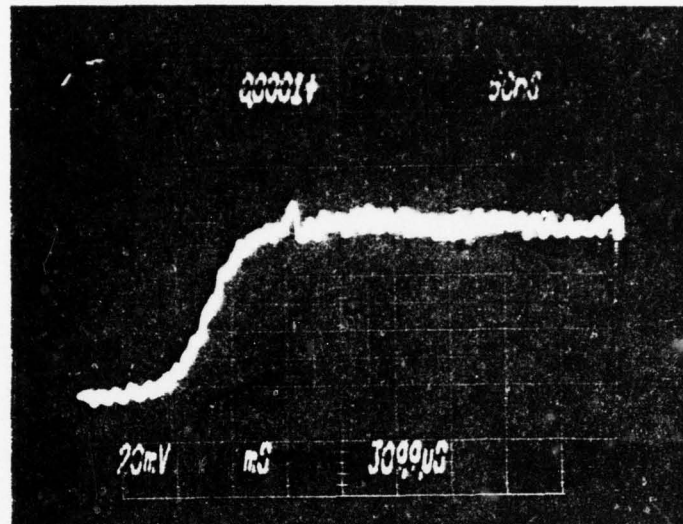


Figure - 13 EXPANDED RANGE PULSE

The system operating time during the single-path tests totalled over 60 hours most of which was in the continuous command mode. During this period there were no failures of the A station and one failure of the B unit. This failure was attributed to a breakdown in the power supply component of the B unit. The B unit checkout set failed near the end of the testing. The failure was due to a malfunction in the EC power supply for the logic unit of the set. Repair of these failures was timely and did not delay the testing.

D. MULTIPATH SIMULATION EXPERIMENTS

To simulate a multipath environment a two-path arrangement (Figure 14) was developed in the laboratory. The longer path was designated as the 'delayed' path and the shorter path was the 'direct' path. The direct path contained a section of variable coaxial cable that could be extended to provide up to 25 cm additional path. By changing the length of the direct path a small amount with respect to a wavelength the phase addition of the two signals could be varied. Variable attenuators were used to control the signal strength of each path.

The experiments conducted with this setup demonstrated that it was possible to distort the signals arriving at the A station and B unit enough to cause significant errors in the system. Figure 15 is an example of a distorted range pulse that led to a 'no B response' result though the system was working well within its specified operating range. The procedures and data collected for the multipath experiments is presented in Appendix D. The only system failure that occurred during these tests was a reoccurrence of the problem in the B unit checkout set. An external 5 VDC source was hooked up to the logic unit and this remedied the problem.

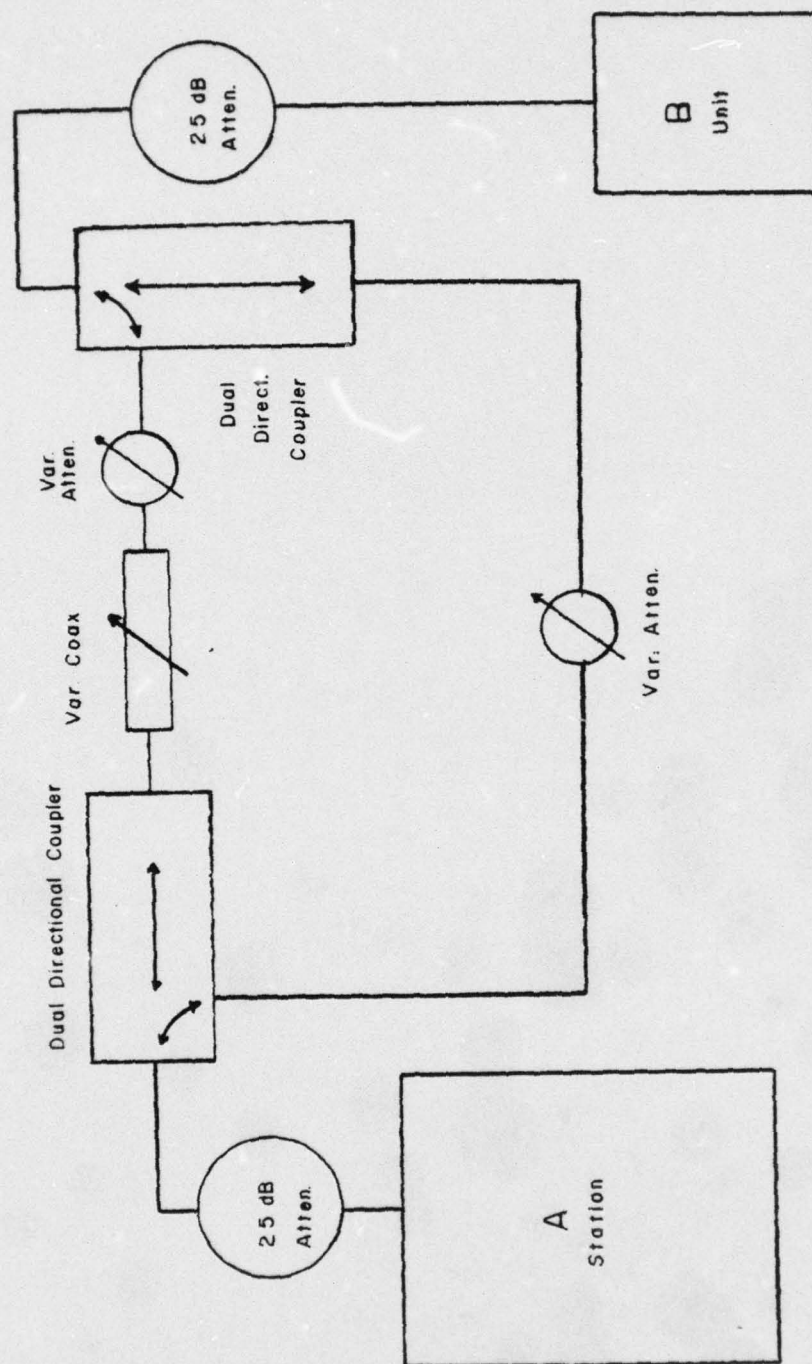


Figure 14 - MULTIPATH SIMULATION SETUP

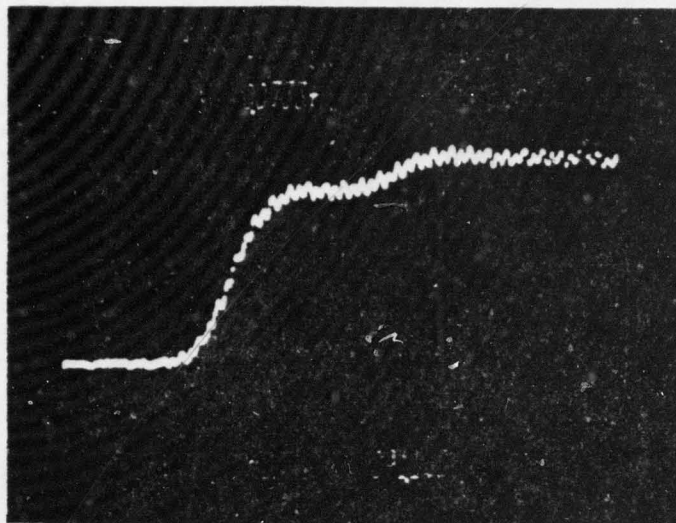


Figure 15 - DISTORTED RANGE PULSE

E. EXPECTED RESULTS IN THE FIELD

The results of the single-path and multipath simulation experiments indicated that it was possible to have errors in the RMS data if certain unusual propagation phenomena cause distortion of the signal waveform by selective fading. It was also clear that due to the non omnidirectional characteristic of some helmet antennas a signal arriving at the antenna via a delayed or reflected path might be as large as the direct path signal. The multipath simulation showed how this condition could result in RMS errors. Intersymbol interference was not experienced in any of the laboratory experiments.

The unique terrain at Ft. Hunter Liggett is characteristic of a multipath environment. Figures 16-20 show some typical B unit locations with respect to an A station. Figure 16 shows the B unit located close to the A station with no reflecting objects in the vicinity of the B unit antenna. In this case the reflected path signal would be expected to be significantly less than the direct path signal, thus selective fading should not be a problem. The situations depicted in Figures 17, 19 and 20 might produce direct and reflected path signals of equal magnitude arriving at the A station and B unit. It was considered unlikely that the reflected path signal of Figure 18 would be of the same order of magnitude as the direct path signal. These situations do not consider the possibility that a reflecting surface may be within a few wavelengths of the antenna as would be the case if the antenna were mounted on or near a vehicle or near trees or buildings. However the field tests did not consider those types of situations.

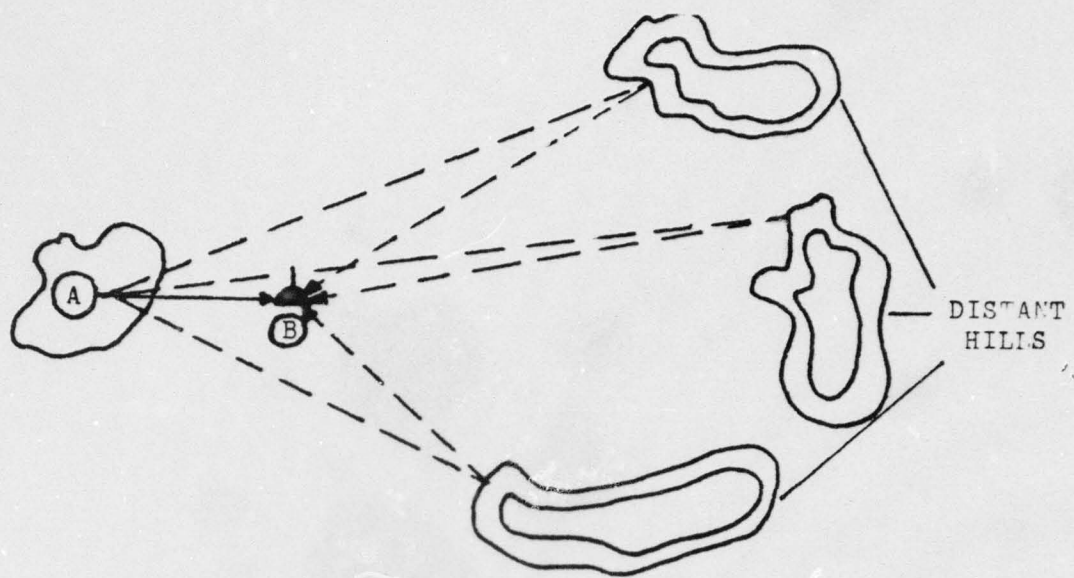


Figure 16 - AB LINK SITUATION 1

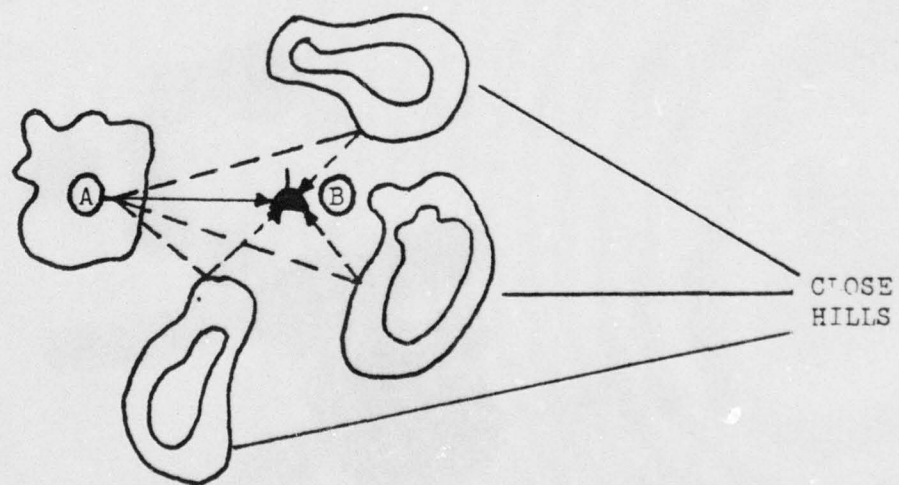


Figure 17 - AB LINK SITUATION 2

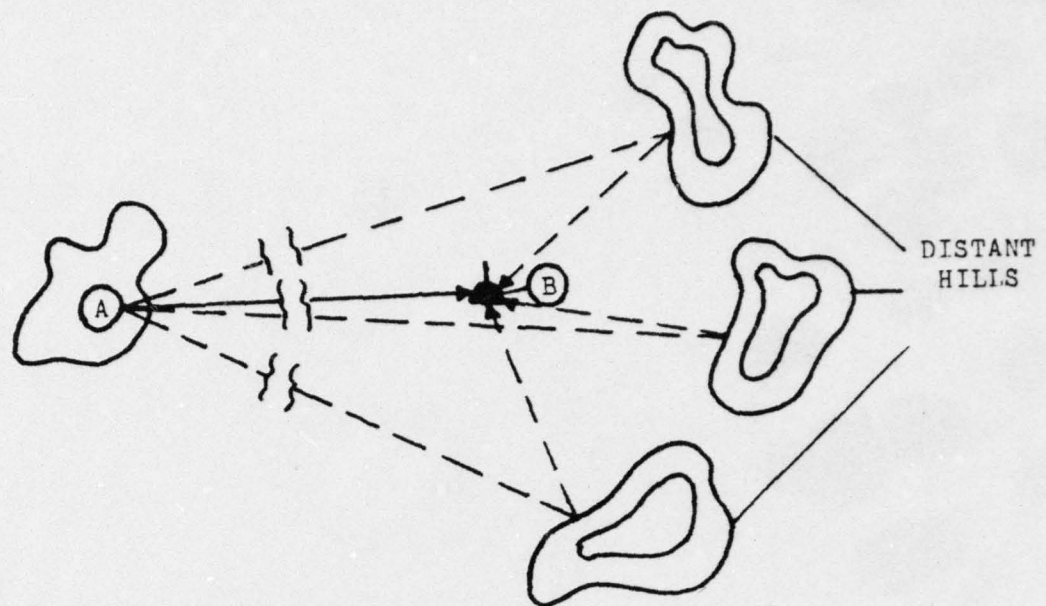


Figure 18 - AB LINK SITUATION 3

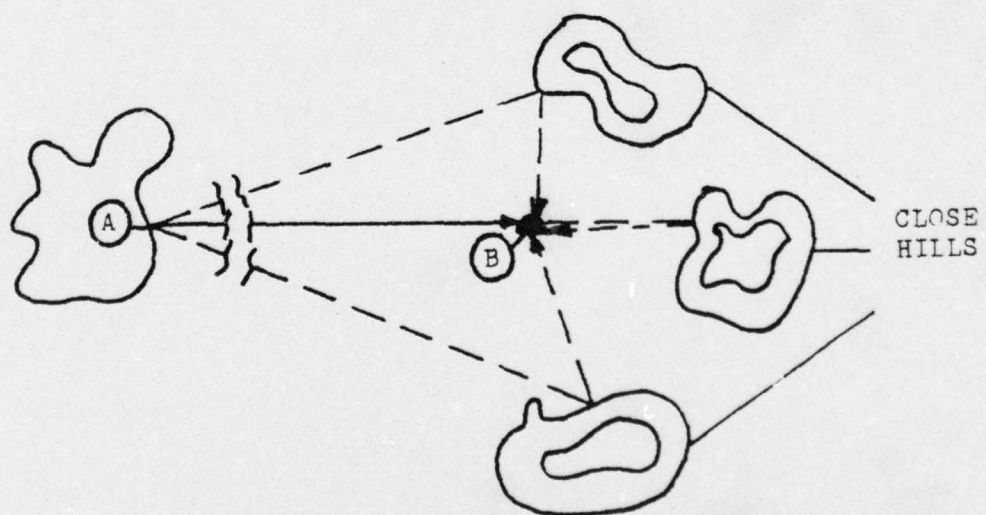


Figure 19 - AB LINK SITUATION 4

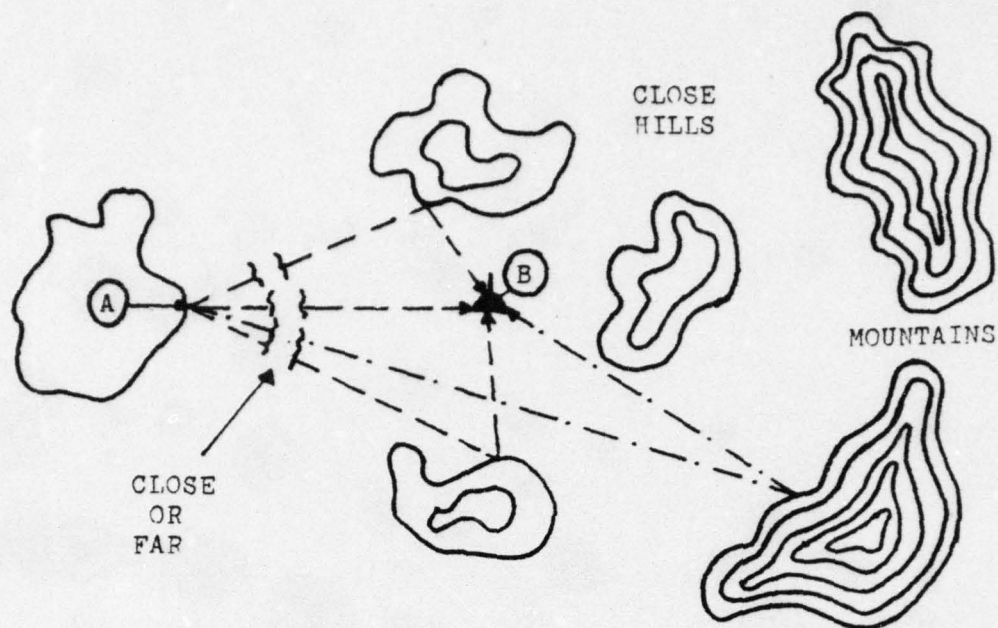


Figure 20 - AB LINK SITUATION 5

In summary selective fading was most likely to occur, if the direct and reflected path lengths were almost equal and apparent nulls of the A station and B unit antennas lie in the direct path. Intersymbol interference was considered very unlikely since the requirement of a large time delay implies significantly larger path attenuation of the delayed signals. So in general the long delayed signals will not be strong enough to distort the next symbol of similar frequency.

IV. RF LINK MEASUREMENTS IN THE FIELD

A. GENERAL CONSIDERATION

To determine the effect of multipath propagation on the AB link in the field a technique was developed that limited the signals that were being received and transmitted by the B unit. The helmet antenna was modified with shielding material to limit the B unit to a direct path signal only (configuration A) or to an indirect path signal only (configuration B). By measuring the system response in these configurations and comparing the results to the system response with an omnidirectional helmet antenna (configuration C) a realization of the effects of multipath was anticipated. Appendix E presents the different helmet antenna configurations and how they were developed. Additionally, the height of the helmet antenna above the ground was varied during the field tests to determine the effect this would have on the system. Three heights were considered 72 inches, 36 inches and 18 inches above the ground.

Two basic experimental arrangements were designated to simplify the data collection process. In the 'AB' arrangement all measurements were taken at the A station with the exception of the B unit I/O device readings. The primary objective of this arrangement was to analyze the signals detected by the A station. In the 'EA' arrangement all measurements were made at the B unit except the slant range readings taken from the B unit checkout set at the A

station. Figures 21 and 22 show schematically the standard 'AB' and 'BA' test arrangements. Series of 'AB' or 'BA' experiments were distinguished by number subscripts as shown in the following example:

$$A E_{i j} \quad \text{where } i = 1, 2, \dots, n \text{ (A station location \#)} \\ j = 1, 2, \dots, m \text{ (B unit location \#)}$$

Only one experiment was performed at each $A B_{i j}$ or $E A_{j i}$ location.

Extensive logistic support and coordination was required during all phases of the field experiments. The areas of Ft. Hunter Liggett that were used for most of the preliminary reliability investigations are shown in Figures 23 and 24. The tests conducted in these areas were limited to the weekends due to USACDEC experimentation schedules. Thus, any RMS component failure usually forced a delay in the testing to the next weekend. Later in the testing a mobile A station antenna was made available at Camp Roberts (Figure 25) where the terrain is very similar to that at Ft. Hunter Liggett. Testing at Camp Roberts was not restricted to any time period and allowed for easier support.

Communications between operators at the A station and B unit sites was achieved with battery powered hand-held radios. Portable generators were used to provide AC power at sites where there was not an AC power outlet. Additionally, provisions had to be made for storing Polaroid film, shading measurement equipment, and transporting the equipment to the field. The time spent transporting and setting up equipment in the field proved to be one of the limiting factors in the total number of field experiments that were conducted. The data collected during the field experiments is presented in Appendix F.

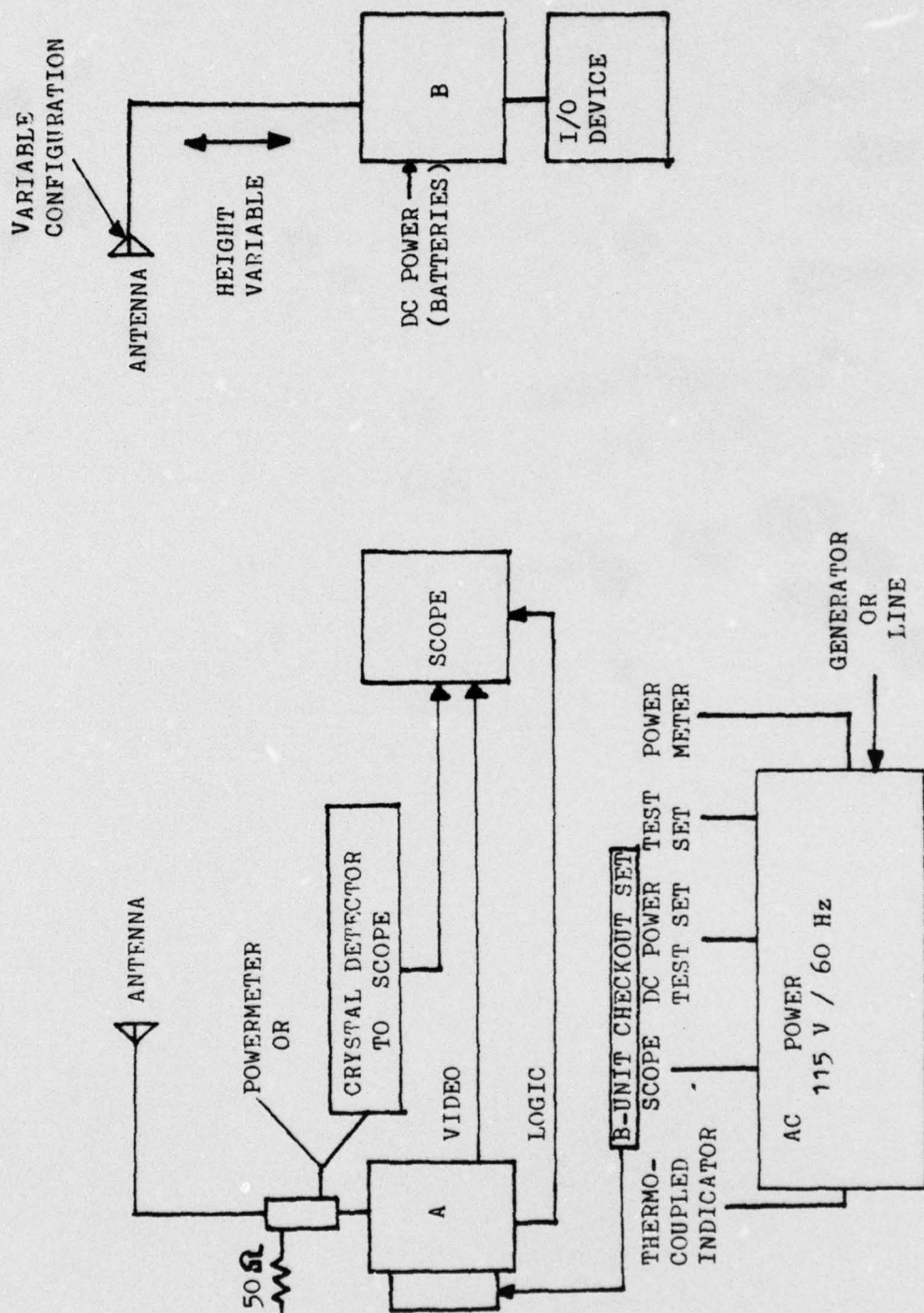


Figure 21 - STANDARD AB ARRANGEMENT

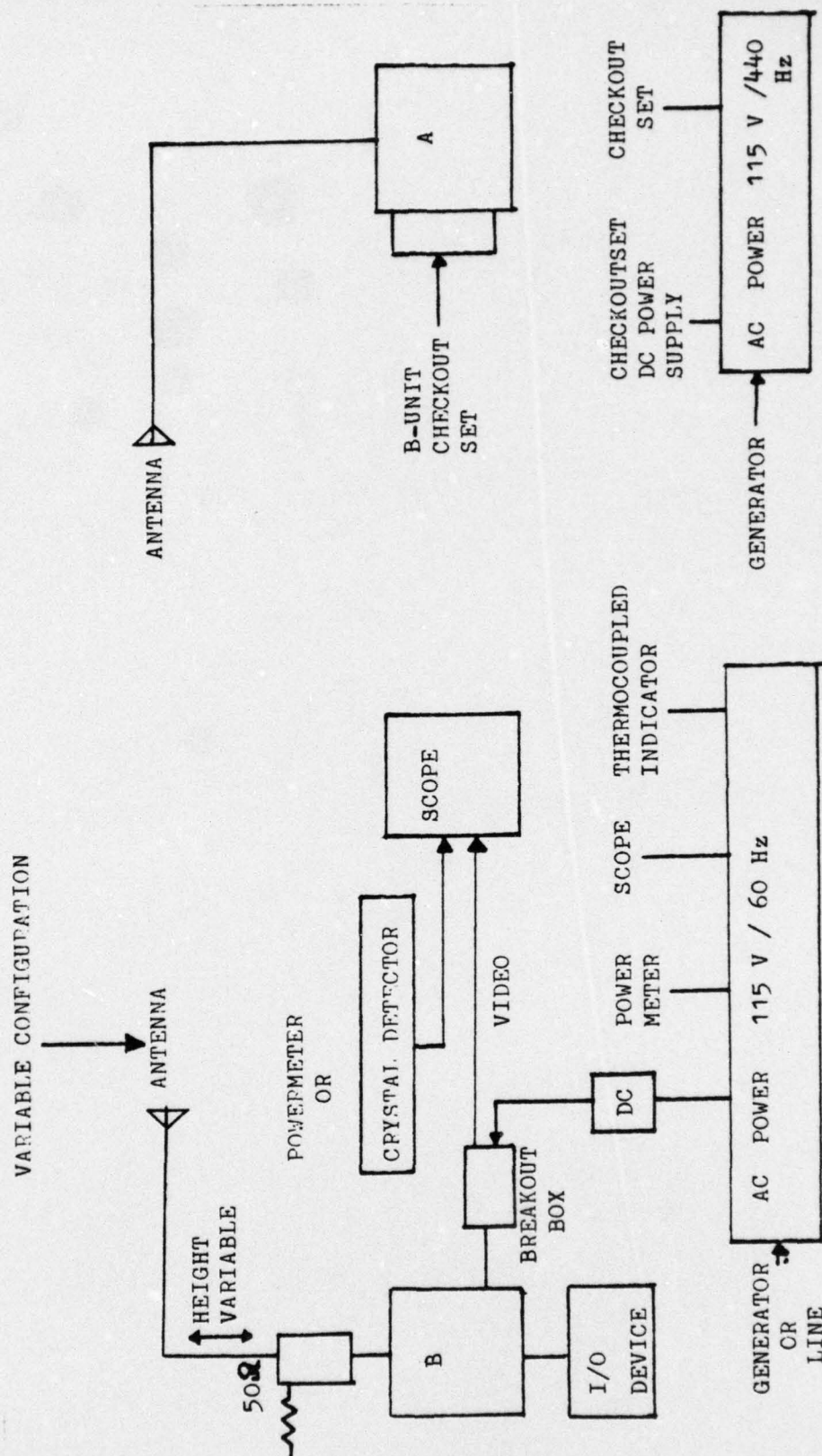


Figure 22 - STANDARD BA ARRANGEMENT

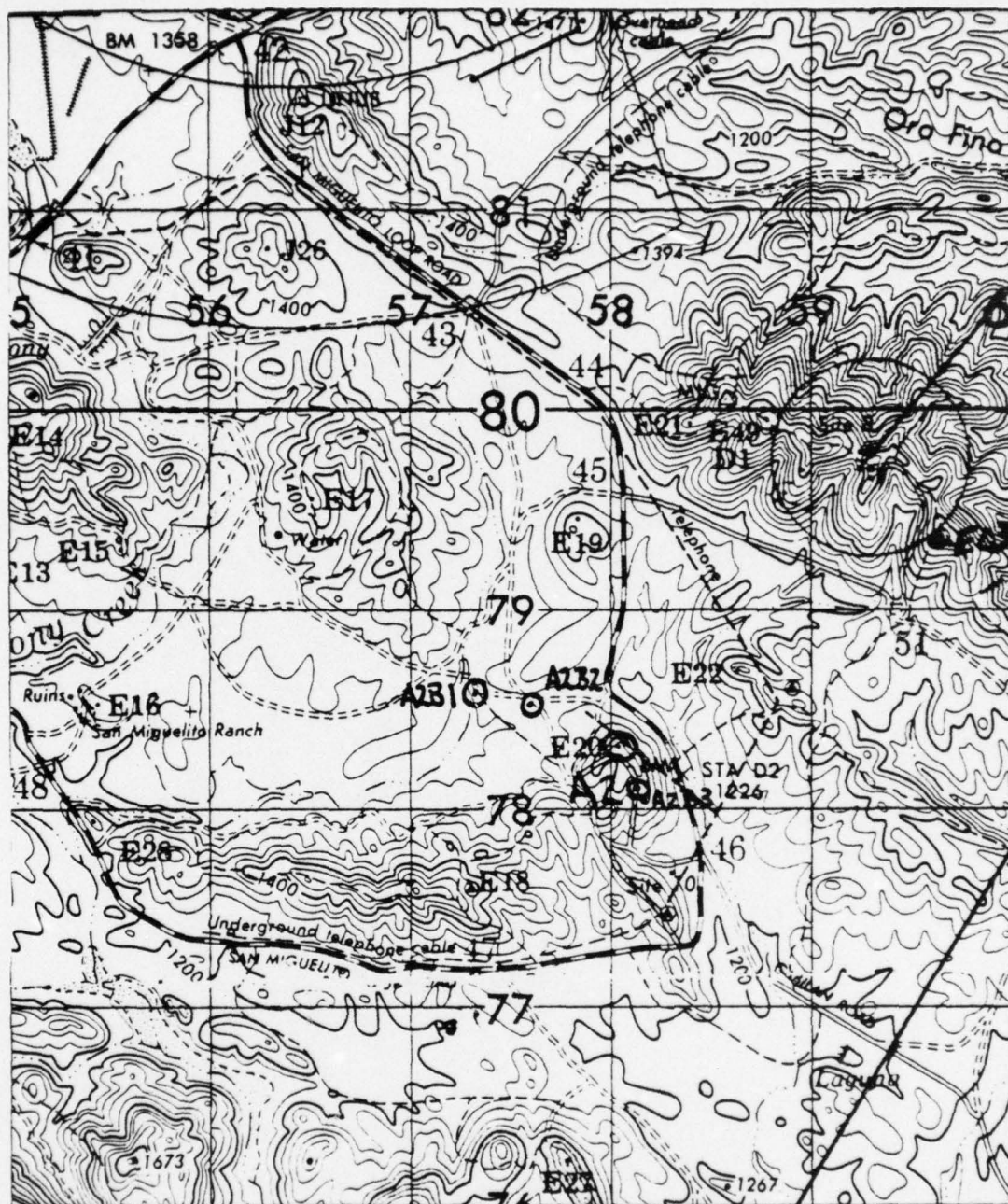


Figure 23 - FT HUNTER LIGGETT OPERATING AREA

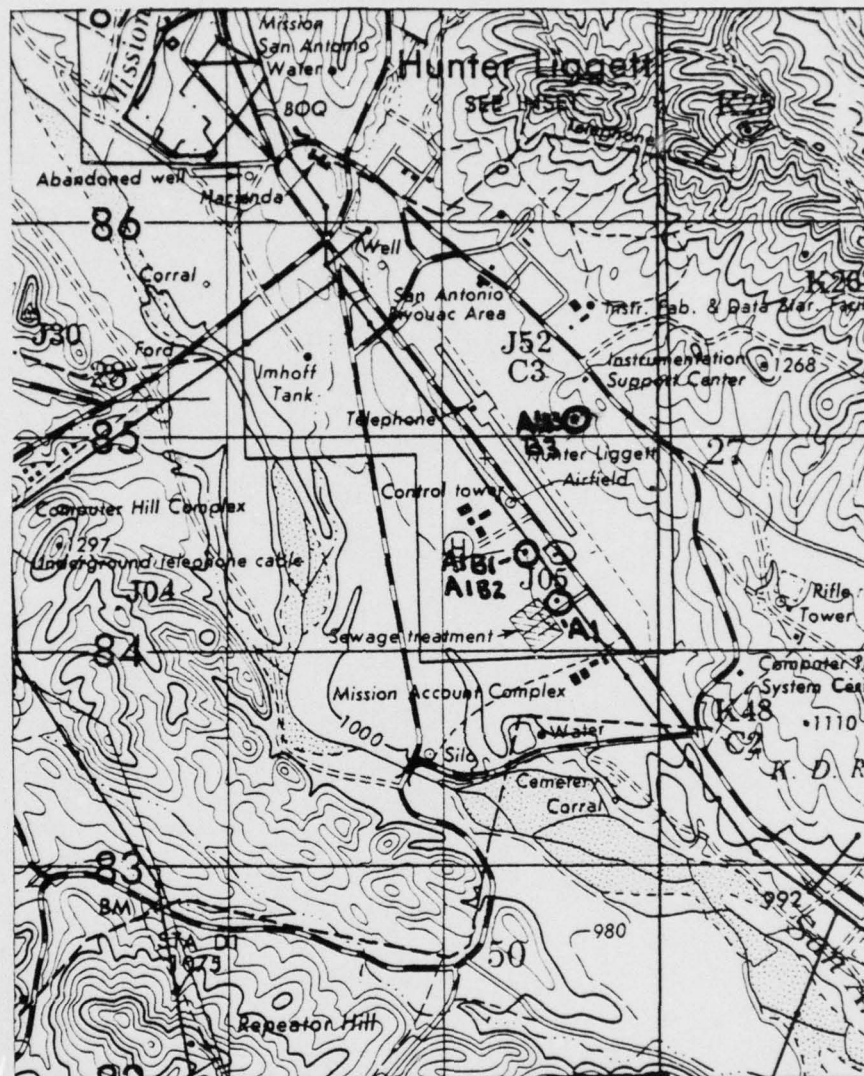
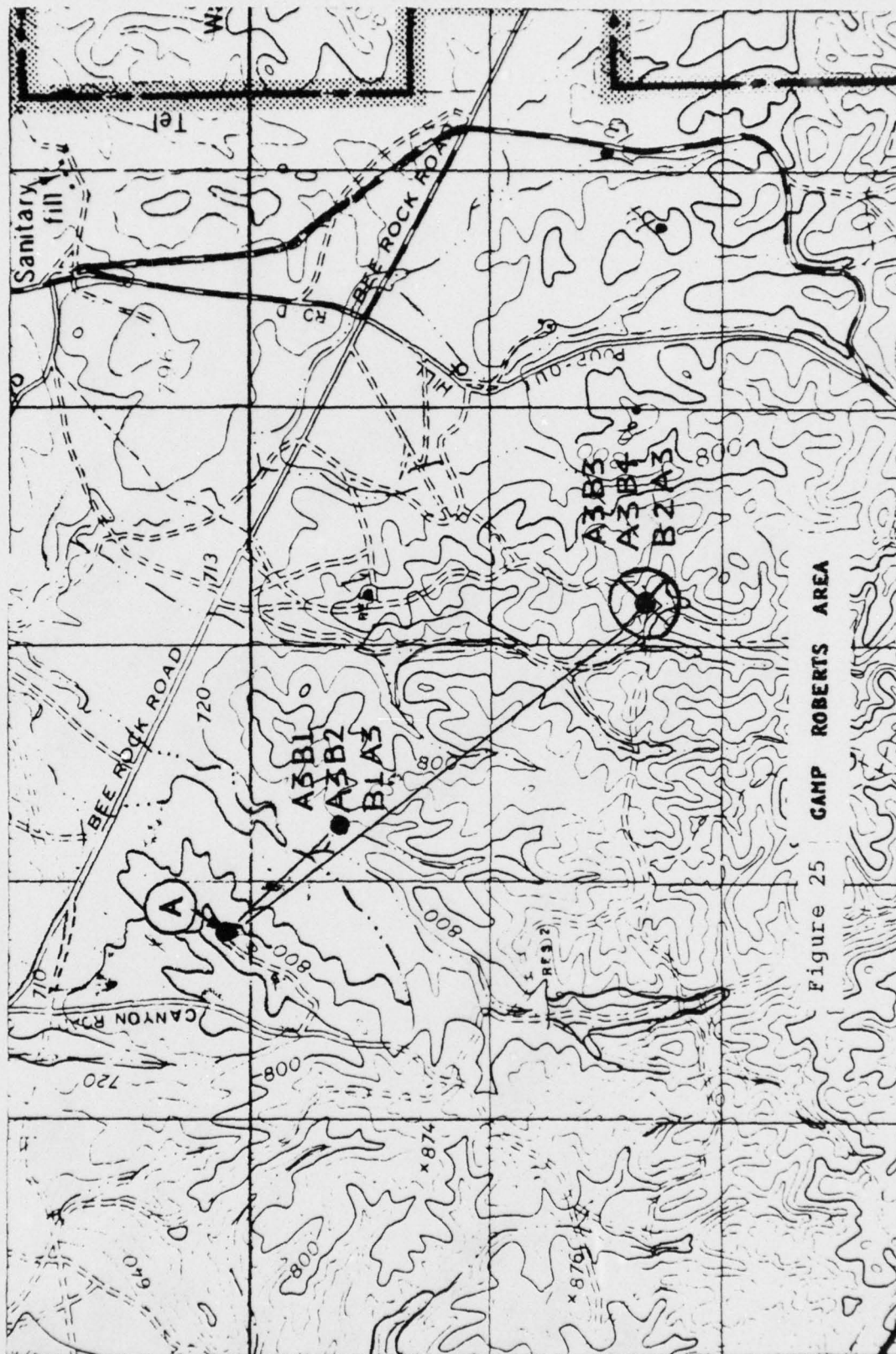


Figure 24 - FT HUNTER LIGGETT OPERATING AREA



E. TEST PROCEDURES

The data collection procedures required for each experiment depended upon the arrangement (AE or BA) and the mode of operation (SCCM or Range) being used. However, the initial portion of the procedure was the same for all the field experiments. The locations of the A station and B unit under test were recorded and the B unit was set up with the helmet antenna at a height of 72 inches and in configuration C. Operating in the Range mode with continuous commands it was verified that the B unit was responding to the interrogations of the A station. Finally, the 7834 oscilloscope was set up for recording repeated events as described in Appendix B.

1. AE Arrangement

The equipment was set up as shown in Figure 21 and the initialization procedures were conducted. The case temperature and average output power of the A station were measured and recorded. The A station transmitted waveform was observed on the 7834 oscilloscope and compared with laboratory standard to ensure that the A station was transmitting properly. Next, the signal waveform of the A station video detector (Pin #7) was displayed on the 7834 and the oscilloscope was prepared for recording single-shot events. The B unit checkout set was put in the single command mode and the helmet antenna changed to configuration A at 72 inches. At this point the system was ready to begin measuring single events in either the Range or SCOM mode of operation. Figure 26 is a picture of the A station site during a test conducted in the AB arrangement.

a. Range Mode

Operating in the Range mode ten single commands were initiated and the resulting slant ranges recorded. Pictures of at least two returning range pulses relating to particular slant ranges were taken. If the oscilloscope could not record in the single-shot mode due to low signal to noise ratio the B unit checkout set was switched to the continuous command mode and the two pictures taken. In this case the photos could not be related to a particular slant range.

Upon completion of taking data with the helmet antenna in configuration A at 72 inches the antenna was lowered to 36 inches. At this height 5 single events were observed and one photo of a range pulse was taken. The helmet antenna was then moved to 18 inches above the ground and 5 more events were observed and one photo taken. The same procedures were used for the helmet antenna in configurations B and C.

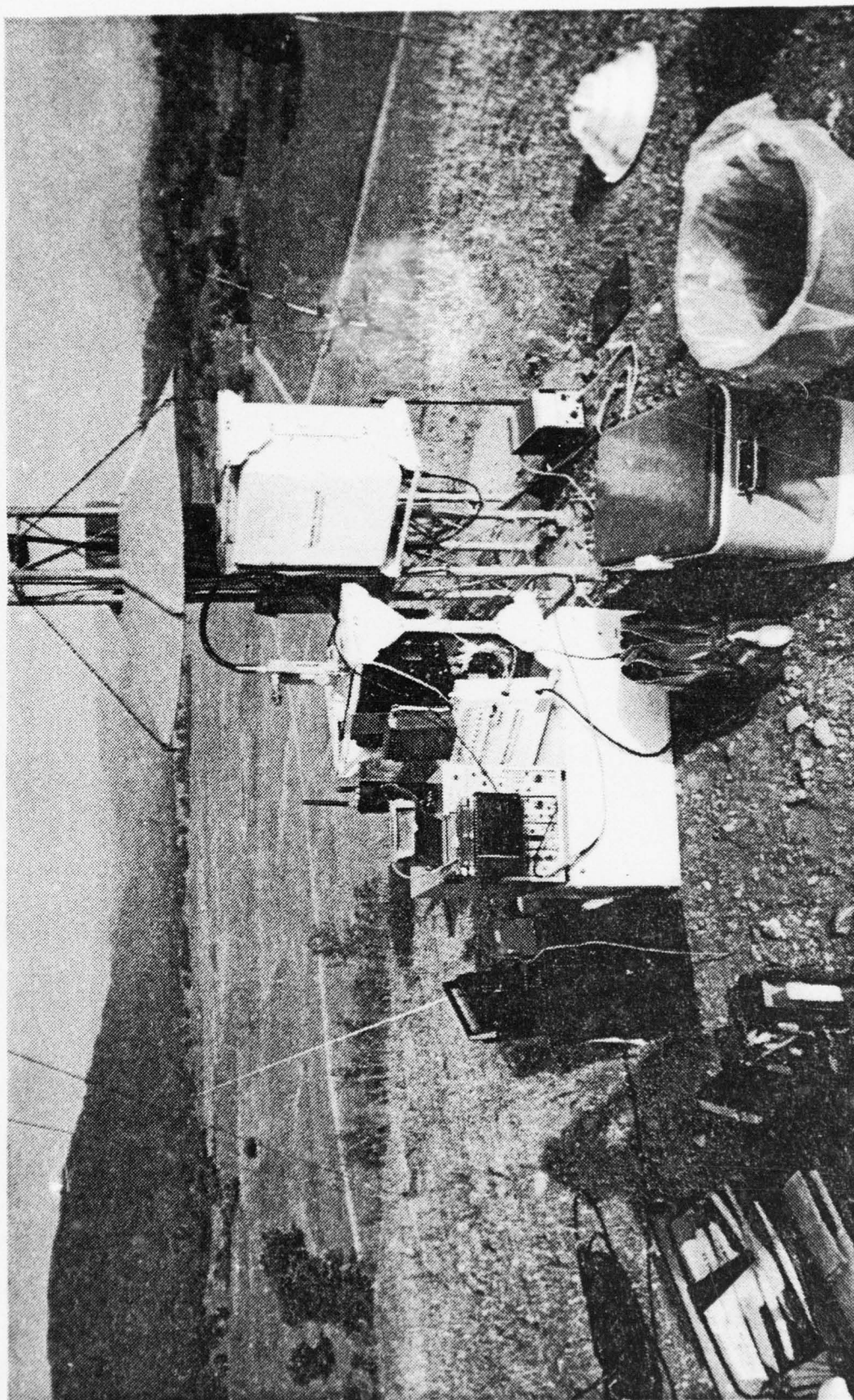


Figure 26 - A STATION SETUP FOR AE TEST CONFIGURATION

b. SCOM Mode

Time limitations prevented extensive field testing in the SCOM mode however, a technique was developed for measuring individual bits in the SCOM message. Message data are transmitted from the B unit to the A station and vice versa on four different frequency channels. These four channels were sensed after detection and logic level conversion at the A station logic module test points 24-27 on electronic board number 1. The signals were then summed by a diode summing circuit and displayed on the oscilloscope. For each helmet antenna configuration and height five interrogations, each with a different message from A to B and B to A, were made. The four bit and thirteen bit messages transmitted and received by the A station and B unit were recorded for each interrogation. In addition, at least one photo of the summed logic signals was made.

2. EA Arrangement

The equipment was arranged as shown in Figure 22 and the initialization procedures conducted. The B unit power breakout box provided the necessary test points for monitoring the detected video signals but there was not a readily accessible point for monitoring the data channels at the B unit. Therefore, experimentation for this arrangement was limited to the Range mode. In essence, the same experiments were conducted in the BA arrangement as in the AB arrangement. However, in this case the signal of interest was that detected by the B unit and only for the Range mode.

C. RESULTS

1. Reliability Studies

The initial field experiment objective to investigate multipath distortion effects on the RMS signal waveforms could not be pursued immediately, since severe equipment reliability problems had to be solved first.

a. Field Tests

The familiarization tests, A1B1, A1B2 and A1B3, verified that the projected field experiments could be done with the available measurement equipment. Since the two B units used worked only about two hours each, the effective test time was limited. Either more units had to be made available or the reliability of the units improved. Since one of the B units (#237) worked properly during the entire laboratory phase with an average daily operation time of four hours, it was suspected that high ambient field temperatures might have caused the observed failures. The use of a larger sample of B units in experiments A2B1, A2B2, A2B3, A1E4, E1A1, A2B4 and A2B4 (Appendix F) added more unknowns to the overall system reliability problem. Some of the reliability problems were:

- A station receiver automatic gain control failures at high ambient temperatures
- Possible broken RF cable connections
- B unit checkout set indicator light instability
- RF interference

- Measurement equipment failures
- A station and/or B unit center frequency drift
as well as B unit receiver gain reduction with time
and increasing ambient temperature

Solutions for all but the last problem were found by trial and error during the second part of the reliability tests. The solution for the last problem was found during subsequent laboratory temperature sensitivity tests.

b. Temperature Sensitivity Tests

As described in Appendix G both the B unit and the A station showed no measurable center frequency drift with time or increasing temperature. The B unit receiver sensitivity stayed within specifications at room temperatures. At the high temperature chosen (50°C) all B units decayed rapidly in receiver sensitivity to values, which made them useless for field operation. Once a B unit broke down under high temperature it did not recover at room temperature to specified receiver sensitivity values. These results agreed with the field observations.

c. Alignment Comparison Test

The results of this series of tests, Appendix H, explained why B units checked out or aligned by maintenance personnel at Ft Hunter Liggett did not work properly for more than 30 to 45 minutes in the field. The receiver gain reduction at higher ambient temperatures investigated previously was related to the alignment method. A particular B unit under test was interrogated directly by a Test C Station, so eliminating the A station. It was found, that a B unit aligned to that C station did not respond to

an A station put into the test RF link. If the B unit was aligned to an A station using an C to A to B RF link, it was insensitive to high ambient temperatures and could be used reliably for field experiments. The latter test setup resembled the checkout procedure used during former field experiments.

2. AB Range Mode

The detailed results of the AB Range mode tests are given in Appendix F. It was found, that depending on the B unit antenna height above ground, location and antenna gain pattern severe range pulse distortion occurred due to multipath fading at the A station antenna. For short ranges (about 500 meters) multipath fading was observed for the omnidirectional B unit antenna transmission only. At longer ranges however, multipath fading could be observed for any antenna gain pattern configuration depending on the B unit location and antenna height. The effects of the multipath fading were either erroneous 'wild' ranges or 'no B response' message returns from the A station to the C station, simulated by the B unit checkout set.

Figure 27 shows a typical distorted leading edge of a range pulse return at the A station. A similarly distorted range pulse was obtained during the multipath simulation experiments, Appendix D, and is shown in Figure 28 for comparison. The waveform shown in Figure 29 generally resulted in an accurate slant range.

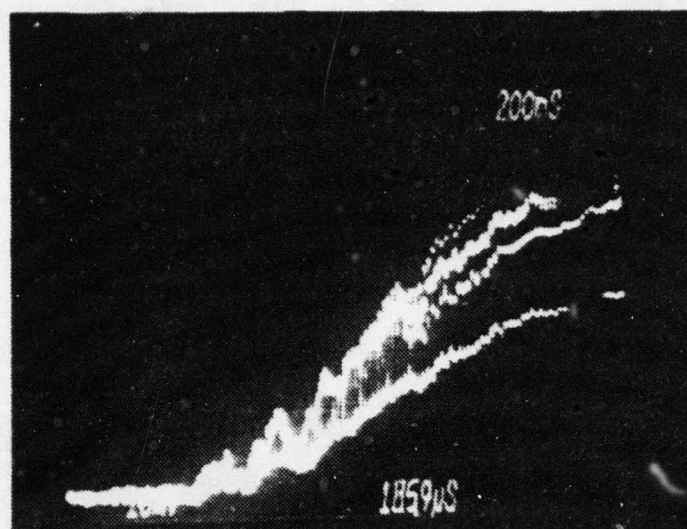


Figure 27 - DISTORTED RANGE PULSE
DETECTED AT THE A STATION DURING FIELD TESTS

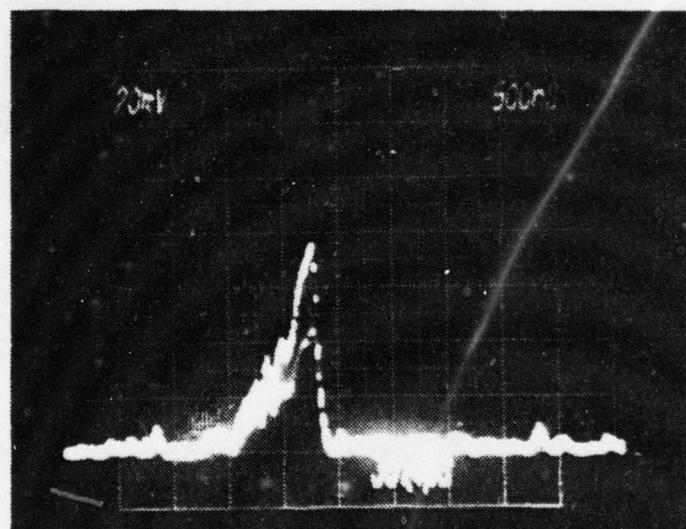


Figure 28 - DISTORTED RANGE PULSE
DETECTED AT THE A STATION DURING SIMULATION

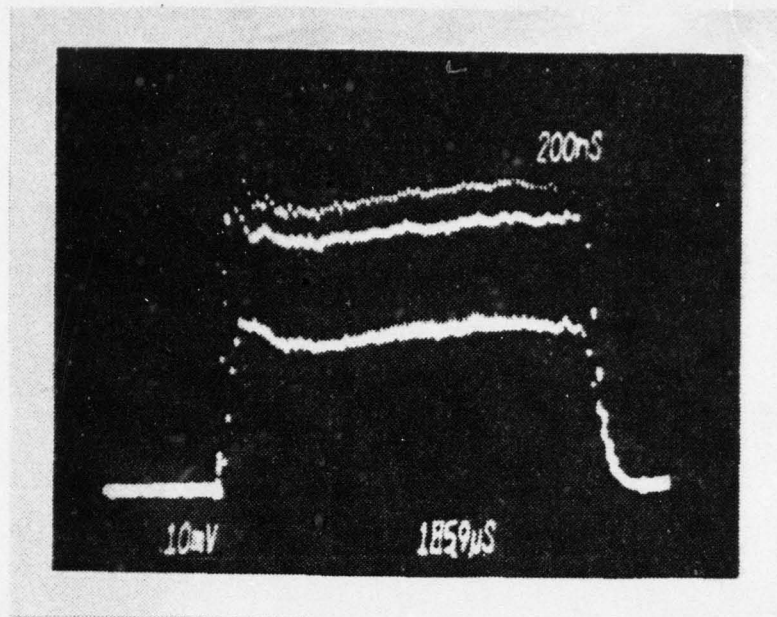


Figure 29 - STANDARD RANGE PULSE
DETECTED AT THE A STATION DURING FIELD TESTS

3. EA Range Mode

This series of tests showed that although 'wild' ranges could still be obtained at the A station, no severe range pulse distortion occurred at the B unit. moreover it was verified that B units used during the AE tests operated to specifications, such that waveform distortions were not caused by malfunctioning B units as observed during the reliability tests.

V. CONCLUSIONS

During the two path simulation experiment it was shown, that under proper phasing conditions RF fading did occur. The RMS system did not tolerate that situation and heavily distorted range pulse waveforms resulted in uncorrelated wild ranges. This simulation, although being an over simplification of the real multipath conditions in the field, proved to be a valuable method for predicting what would occur in the field. Comparison of the predicted and field results showed without any doubt, that the Ft. Hunter Ligett environment not only allows multipath to occur, but can seriously effect the RMS system performance in its present hardware configuration. Although mainly large Range mode errors have been shown, further investigations into the other communication modes are expected to result in telemetric errors as well.

The micrc-B units operated more reliably when they had been aligned to A stations. The Test C Station used to align both the A stations and the B units, did not provide a common alignment standard for the two different components. Thus, it seems only reasonable that many B units failed to operate in the field. The temperature sensitivity tests indicated that alignment drift occurs under field temperatures. The degree of drift was not determined, but it was obvious that B units aligned to an A station were less sensitive to large temperature deviations and were much more reliable in the field.

VI. RECOMMENDATIONS

The RF link between the A stations and the B units is a critical part of the RMS system. This link must be reliable if the system is going to provide accurate information. In an effort to make this link more reliable a common standard should be developed for aligning both the A stations and the B units. Investigating the origin and nature of the E unit alignment drift in the field may provide a guide as to the most flexible alignment standard.

The effects of multipath fading on the RMS system have been investigated and a technique for observing these effects has been developed. Time limitations restricted the amount of pertinent information that could be obtained. Further investigation of the operating areas of Fort Hunter Liggett should be conducted to include field strength tests to determine those areas that would be most susceptible to multipath effects.

APPENDIX A

B UNIT CHECKOUT SET

General Information

The B unit Checkout Set is designed to operate through any standard A station to provide an operational checkout of a B unit. The set acts in essence as a C station providing the necessary logic and triggering circuitry to cause the A station to interrogate the B unit. The set requires a 120 Volt/60 Hz power source and provides the necessary 28 VDC power for the A station. The set will cause the A station to interrogate the B unit in either the Range or SCOM mode with either a single command or continuous commands (approximately 60 commands per sec.). The front panel of the set (Fig 30) has the A and B address switches (octal address), a mode selection switch (RNG/SCM), a power on/off switch, four SCOM message bit switches and 12 message response lights. The additional large unmarked switch to the right of the address switches is the interrogation command switch. This is a three-position switch, off in the center position, single command in the spring loaded up position and continuous commands in the down position. On the right side of the upper panel are located three signal points. The two red points provide the transmitted and received data bits respectively. The larger white point is a synchronizing signal for use with oscilloscope work. The right side panel has three cables coming from it. The lower single cable is the power cable. The remaining two cables are the A station interface cables.

Operating Procedures

1. Remove the cover on the Logic Module side of the A station. Install the set using the carrying handles of the A station as supports. Disconnect the connectors A4J2 and A4P2, then connect A4J2 and A4P2 to the two interface cables of the checkout set. Be sure the set is properly grounded to the A station ground terminal. Do not connect AC power to the set yet.

2. Install desired matched (50 ohms) antenna to the A station. CAUTION: The antenna must be installed prior to powering the set. Powering the set without an antenna on the A station could cause a blow out in the A station pulse power amplifier.

3. Position the A address switch to match the A station address located on a tag on the Logic Module of the A station. Position the B address switches to correspond to the B unit address which is the serial number of the B unit Logic Module. Connect the AC power cord to a 120V/60Hz outlet and turn the power switch on.

4. Apply power to the B unit. Select Range or SCCM and either single or continuous command as desired. The message response lights are designed to indicate as follows:

Light Number	1	2	3	4	4	6	7	8	9	10	11	12
Range bits	S	5	6	7	8	9	10	11	12	13	14	15
SCOM bits	1	2	3	8	9	10	11	12	13	C	X	X
Nc B response	1	2	3	X	X	X	X	X	X	X	X	X

C = Message complete when lit

X = Not used

S = Status bit

15 = Least significant bit (2 meters)

Note: (1) Max range display is 4094 meters

(2) SCOM bits 4, 5, 6, and 7 are not displayed

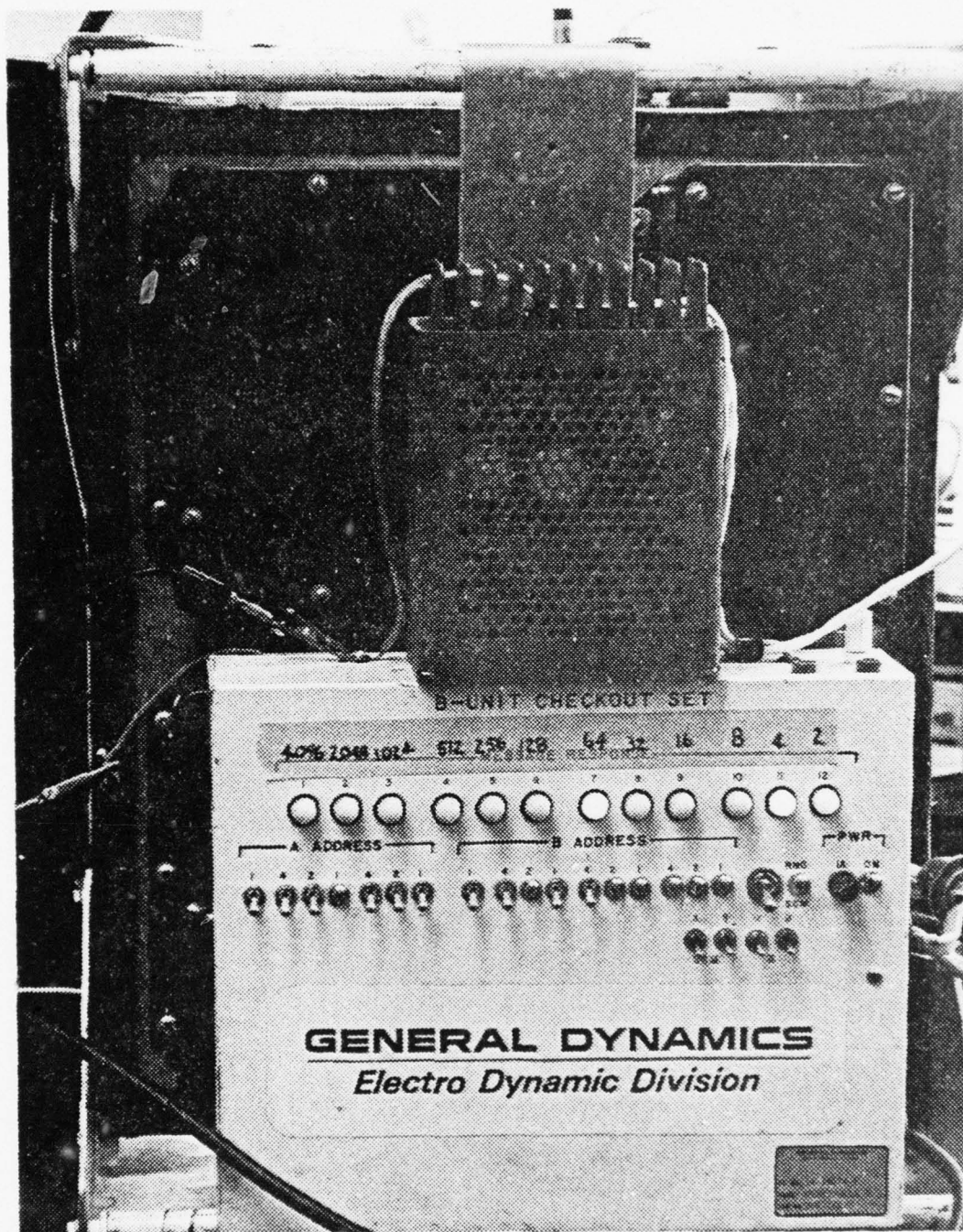


Figure 30 - B UNIT CHECKOUT SET

APPENDIX B

TEKTRONIX 7834 STORAGE OSCILLOSCOPE

The Tektronix 7834 Storage Oscilloscope is designed to store single events at a maximum writing speed of 2500 cm per microsecond. This enables the user to record single-shot rise times of up to 1.4 nanoseconds. The 7834 mainframe has a vertical bandwidth of 400 MHz and four plug-in compartments. Two of the compartments are for vertical systems and the other two are for horizontal systems. The four plug-ins used for experimentation were:

7A26	Dual Trace Amplifier
7D11	Digital Delay Unit
7B85	Delaying Time Base
7B80	Time Base

The overall operation of the mainframe and plug-ins is explained in detail in the instruction manuals (Refs 17-21). The following is intended to describe the basic modes of operation that were used during the experiments and assumes a previous familiarization of the oscilloscope features. A picture of the scope front panel is shown in Figure 10.

Measurement of Elapsed Time for Two Repeated Events

This operating mode was used in the laboratory to determine the average propagation time of the range pulse from the A station to the B unit and back.

1. On the mainframe, set the display mode to Non Store, adjust the A channel and readout intensity to display the baseline and digital readout.
2. On the mainframe, set the vertical mode to Left, A and B trigger source to Left Vertical.
3. Connect the input signal to either channel 1 or 2 of the vertical amplifier, 7A26, and set trigger source and display mode respectively.
4. Connect an external trigger source, which can be either the input signal itself or a synchronous signal from the B unit checkout set, to the external trigger input of the digital delay unit.
5. Connect the delayed trigger output to the external trigger input of the delaying time base, 7B85. On the 7D11 set the count mode to Time Interval Clock and the trigger mode to AC Coupling, source external. Only one time base is used for this mode. Set the delaying time base to Independent delay mode, trigger Coupling AC, source External, mode Normal.
6. Adjust the trigger levels of the 7D11 and the 7B85 for a stable display.
7. With the delay time knob of the 7D11 move the leading edge of the transmitted range pulse to any of the vertical graticules and expand the leading edge with Time/Div knob of the delaying time base. If the trace becomes too weak to see, put the display mode to Var Persist and adjust the channel intensity and storage level.
8. Line up the 50% point of the leading edge with a graticule and record the delay time readout off the CRT.
9. Move the delay time knob until the received range pulse falls onto the same graticule with its 50% leading edge point. Record the delay time readout off the CRT. The time difference to the first readout is the total time of travel. The actual propagation time can be determined by subtracting the internal B unit delay time.

Display of Entire Transmission Cycle, Preparation for Recording Single Event

The total transmission cycle display was used for initial RF link testing during laboratory and field experiments and is the mode from which preparation for a single-shot event recording could be made. The digital delay unit was not used for this measurement.

1. The initial mainframe settings are the same as those used previously, 1 and 2 above.
2. Connect the input video signal to one of the two channels of the vertical amplifier.
3. If operating at the A station connect the synchronous trigger signal from the B unit checkout set to the external trigger input of the delaying time base. For operation at the B unit use the signal itself as the external trigger source.
4. Set the delaying time base scale for display of the entire transmission cycle and adjust the trigger level for a stable display. Set the B delay mode to B Starts After Delay.
5. On the delayed time base, 7B80, check that the trigger controls are set the same as those on the delaying time base, 7B85.
6. Adjust the display intensity so that the delayed sweep intensified zone becomes visible. The intensified zone may be varied with the Time/Div knob on the delayed time base, 7B80.
7. If the display is not stable change the trigger mode on both time bases to Peak to Peak Auto and readjust the trigger level carefully.
8. To prepare the scope for a single event recording, move the intensified zone with the Delay Time knob of the delaying time base, 7B85, over the desired waveform section. On the mainframe, push the B horizontal mode button. This

causes the delayed time base to control the display.

9. Set the display mode to Fast Var Persist and maximum Auto Erase. This causes the display to be erased about every second.

10. Adjust the storage level, persistence and intensity for the desired readout and trace visibility.

11. Turn the Auto Erase button off. The scope is now ready to record a single-shot event.

Recording a Single Event

1. After the scope has been set up to record a single event push the Auto Erase button. This opens the input channel for a new recording.

2. The next signal into the input channel will trigger the scope. Push the Save button to store the display on the scope.

3. The C-12 camera and adapter are designed for use with the 7834 scope. They enable the user to take a Polaroid picture of the scope display. Make sure that the scope display is properly focused and set at the correct level of intensity prior to taking the picture.

APPENDIX C

SINGLE-PATH EXPERIMENTS

Two single-path signal experiments were conducted in this phase of the work. The first experiment provided a working knowledge of the RMS A station and B unit and some operational familiarity with the 7834 oscilloscope. The second experiment investigated the effects of path attenuation on the detected signal waveforms and the system response in general. Both experiments utilized the basic setup illustrated in Figure 11.

Experiment 1

Objectives

1. To investigate the signal waveforms of the A station and the B unit under test.
2. To determine the standard range bias of the A station/B unit checkout arrangement.
3. To investigate the internal delay of the B unit for stability.
4. To investigate the effects of noise contributions from the cabled single path and other sources.

Procedure

1. A station 010, micro-B unit 237 and the B unit checkout set were set up as shown in Figure 31. The nomenclature and serial numbers of the other experiment hardware is given.

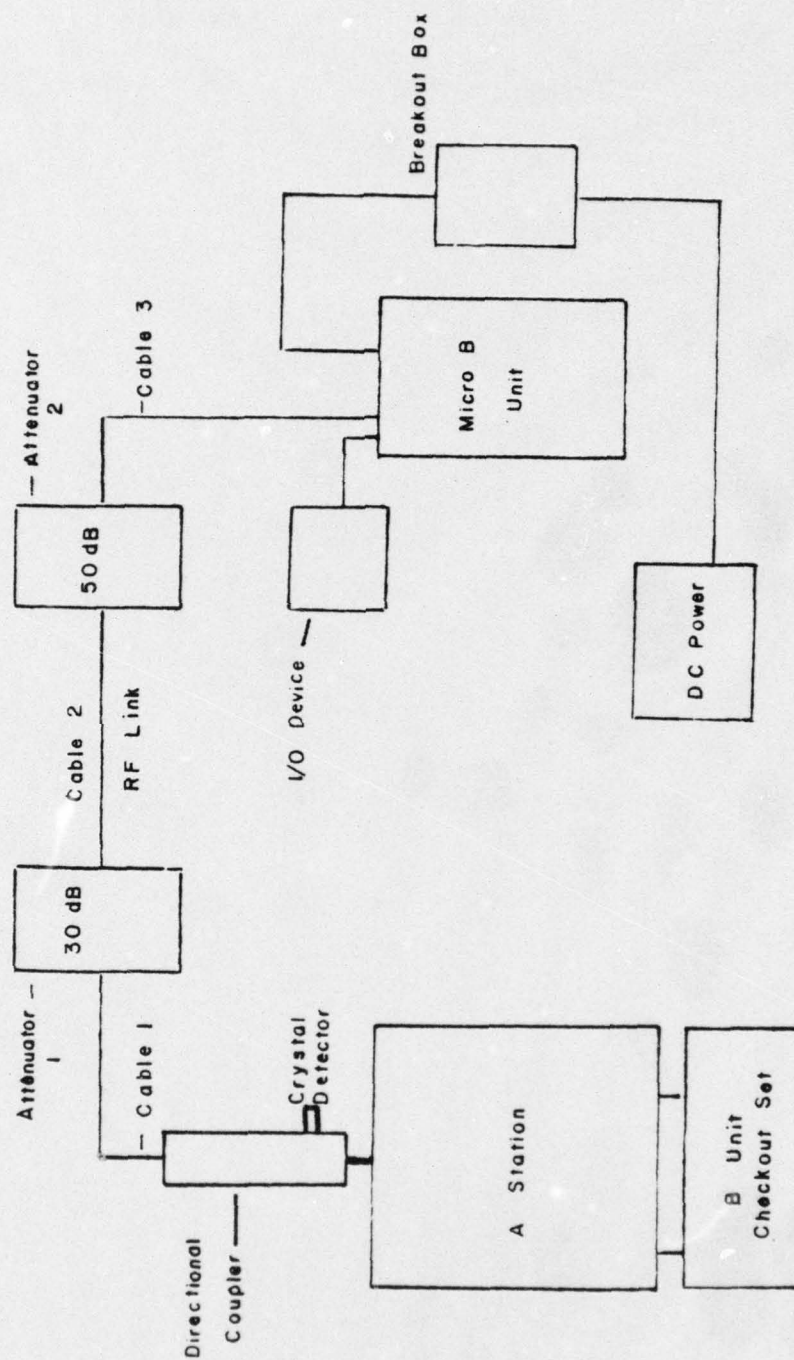


Figure 31 - EXPERIMENT 1 SETUP

<u>Item</u>	<u>Nomenclature</u>	<u>Serial No.</u>
Attenuator 1	KAY Variable Attenuator	9666
Attenuator 2	Telonic Variable Attenuator	9130
Cable 1	Belden RG 213/U	9.75 meters
Cable 2	Belden RG 213/U	1.04 meters
Cable 3	Helmet Antenna Cable	
Directional Coupler	HP 765D	9166
Crystal Detector	HP 420A	73
DC Power Source	PMC	26643

Note: All cables were RG 213/U with a relative permittivity of 2.26. The cables were measured in length with the Hewlett Packard 1815A TDR/Sampler and the AN/USM-310(V) 2 Oscilloscope. RG 213/U is specified to have 9 dB loss per 100 ft at 910 MHz. Attenuator 1 was set at 30 dB and attenuator 2 was set at 50 dB. A 3 dB loss due to cabling was calculated so there was a total of 83 dB of path attenuation. This was well within the specified operating range of 59 dB to 104 dB for the system.

The Hewlett Packard 765D Dual Directional Coupler attached to the A station antenna port provided a versatile test point. By putting a crystal detector at the forward direction branch port the transmitted signal of the A station could be monitored. If a thermistor coupled power meter were inserted at this test point, the average transmitted power of the A station could be monitored.

2. The micro-B unit requires a 24 to 30 VDC source which was provided by a PMC power supply via the B unit power breakout box. In addition, the breakout box provided several test points from which various B unit signals could be monitored. Pin 11 was of particular interest because it provided the B unit detected video signal. The video signal consists of both the transmitted and received video signals. To determine if the B unit was ON, the test button on the B unit I/O device was depressed. If the 4 lights on the I/O device were illuminated then the B unit was operating.

3. The E unit checkout set and the A station were set up as detailed in Appendix A and power was applied to the checkout set. The cover on the Transmitter/Receiver side of the A station was removed. Pin 7 located on the lower right-hand side of the squelch module is a test point used to observe the received signal of the A station. This is clearly explained on page 6-13 of Ref. 16. The probe in Figure 32 is attached to pin 7.

4. The B unit checkout set was set to Range and continuous command modes. A steady range reading of 64 meters was indicated by the checkout set.

5. The 7834 oscilloscope was set up to record repeated events as detailed in Appendix B. The input to channel 1 of the scope was the signal transmitted by the A station detected by a crystal detector at the directional coupler. The input to channel 2 of the scope was the E unit detected video signal. Figure 12 is a picture of the resulting signal waveforms.

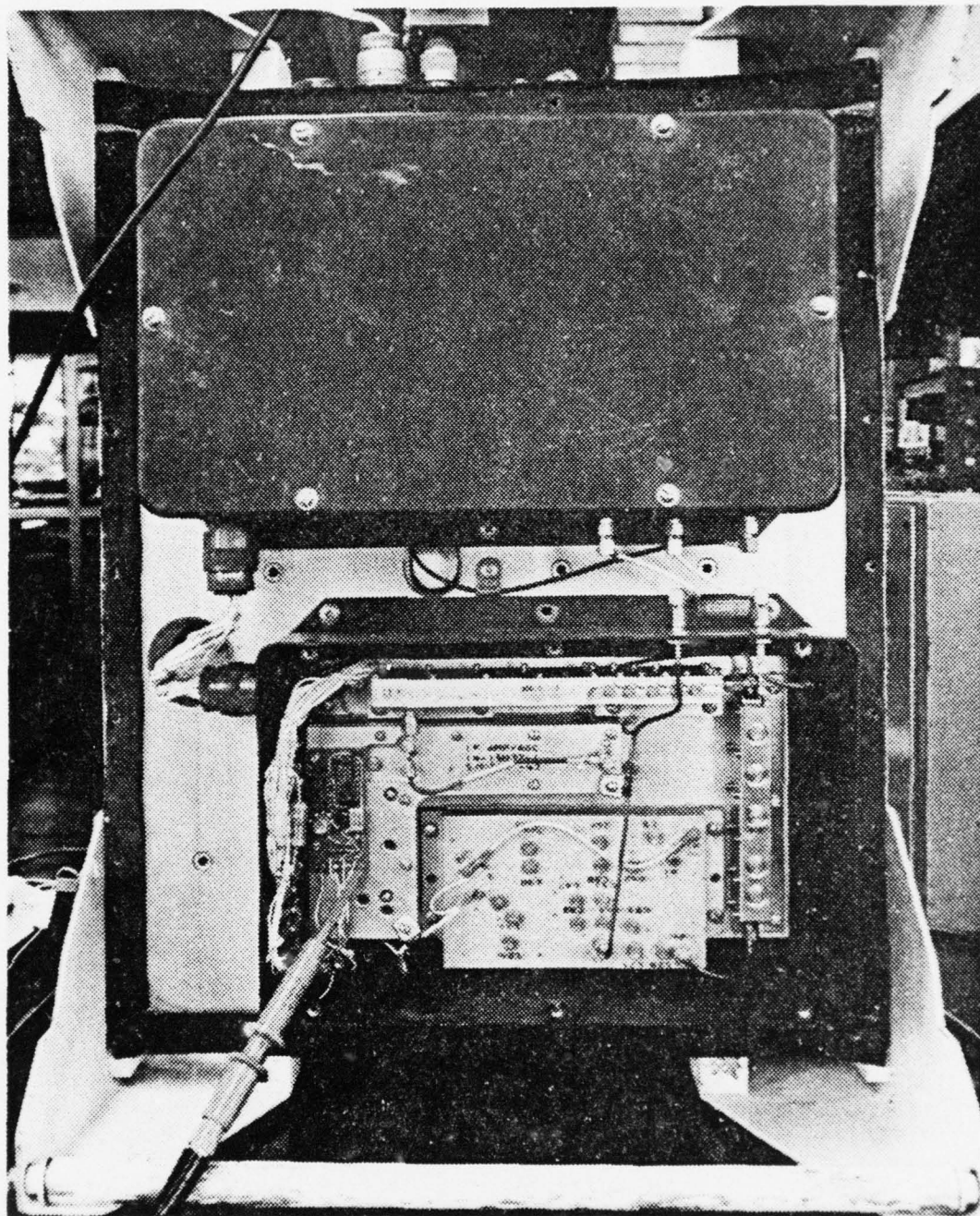


Figure 32 - A STATION TRANSMITTER/RECEIVER MODULE

6. The input to channel 1 was changed to the A station received signal (pin 7 on the squelch module). The signal waveforms were observed and several range pulses were photographed. Cable 2 was then changed to a length of 39.4 meters and a range reading of 122 meters was displayed on the checkout set. The extra cable length added 7 dB to the path attenuation but this was still within the operating range of the system. Several range pulses were photographed for this path length.

7. The internal delay time of the B unit was measured by putting the B unit detected video signal on both channels of the scope. Using the dual sweep delay on the scope both the received and transmitted range pulses could be expanded and displayed simultaneously, Figure 33. The upper trace of the figure is the detected A to B range pulse (100ns/div and 20mV/div) and the lower trace is the B to A range pulse. Merely by aligning the 50 percent point of each pulse to a common vertical graticule the time between receiving and transmitting a range pulse was read directly from the scope display as 109.1 microseconds.

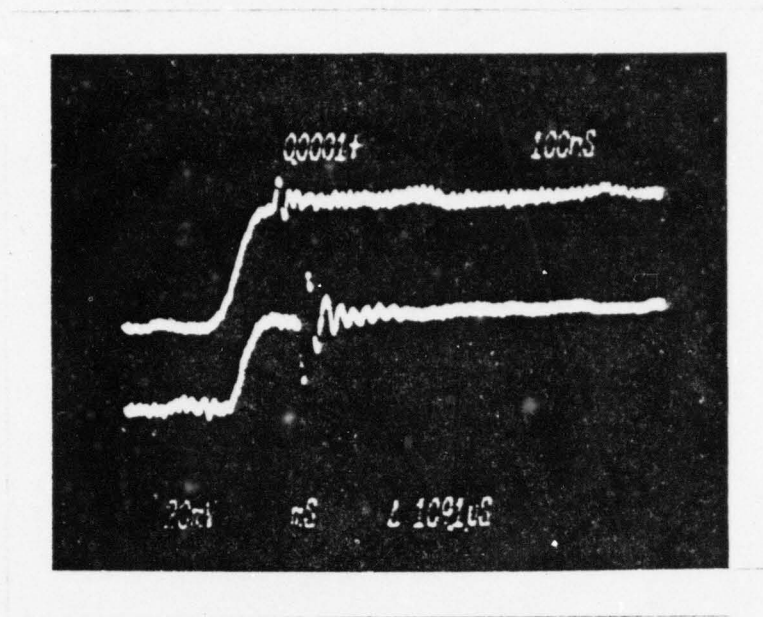


Figure 33 - B UNIT DELAY MEASUREMENT

Results

There is definitely a bias factor that must be applied to the slant range readings taken from the checkout set. The speed of transmission in coaxial cable differs from that of free space by a factor of the square root of the relative permativity of the center conductor of the cable. Therefore, it is easily shown that a given length of RG 213/U corresponds to a calculated path length in free space. A cable length of 1.04 meters corresponds to a free-space path length of 1.68 meters and a cable length of 39.4 meters corresponds to a free-space path length of 59.23 meters. Subtracting these free-space lengths from the respective slant ranges yielded a bias of about 62 meters. Since cable 1 and the attenuators remained the same throughout the single-path and multipath experiments their contributions to this bias was not considered.

The system operated according to specifications and the waveforms that were recorded were as expected. Figures 12 and 34 show the signal waveforms corresponding to the Range mode. As previously explained, Figure 12 has the signals transmitted by the A station on the upper trace and the B unit detected video signals on the lower trace. Figure 34 has the same B unit detected signals on its upper trace and the signal received by the A station on the lower trace. The two pictures show the complete signals received and transmitted by the A station and the B unit in the Range mode. Expanding the range pulse led to some interesting results.

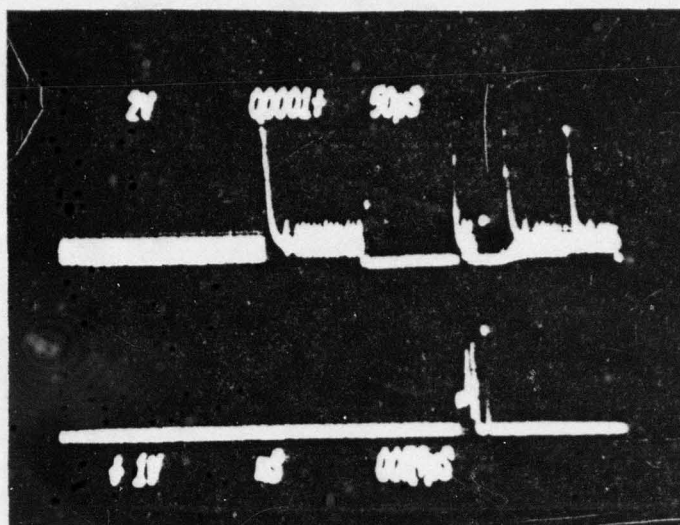
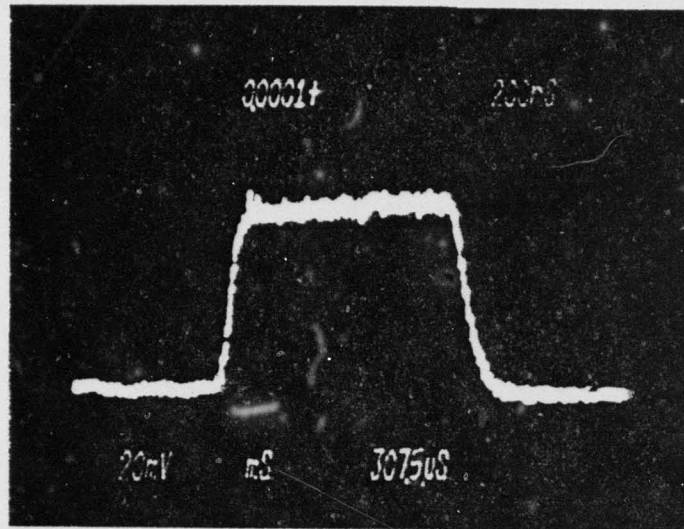


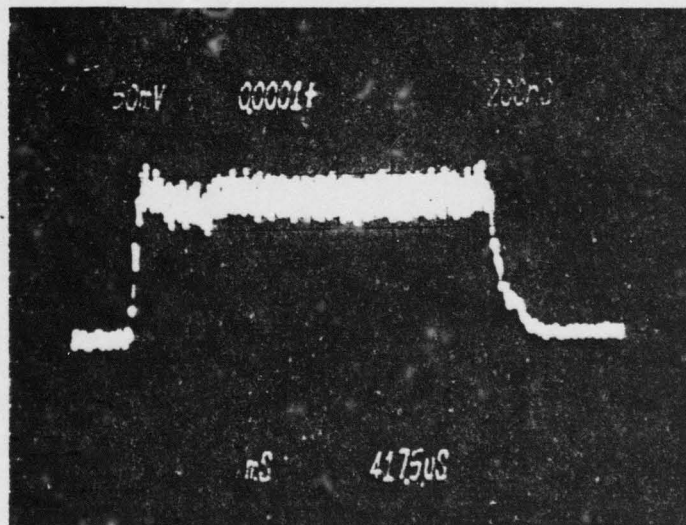
Figure 34 - RANGE MODE SIGNAL WAVEFORMS

The expanded range pulses detected at the B unit and the A station are shown in Figures 35A and 35B respectively. The range pulse detected at the B unit is sharp with a slight overshoot. The range pulse detected at the A station indicated a much noisier signal. By expanding the pulse more (Figure 36) it was determined that the additional noise was at the intermediate frequency (IF) of the A station receiver. It was concluded that the noise was due to leakage in the IF section of the receiver. This seemed to be characteristic of all A stations and had no effect on the range accuracy.

The internal delay of the B unit was measured several times during the experiment. It was clear that any variations of the internal delay during operation of the system in the field would cause ranging errors. However, the experiment indicated that the internal delay was stable at 109.1 microseconds.



(A)
Detected at the
A Station



(B)
Detected at the
B Unit

Figure 35 - EXPANDED RANGE PULSES

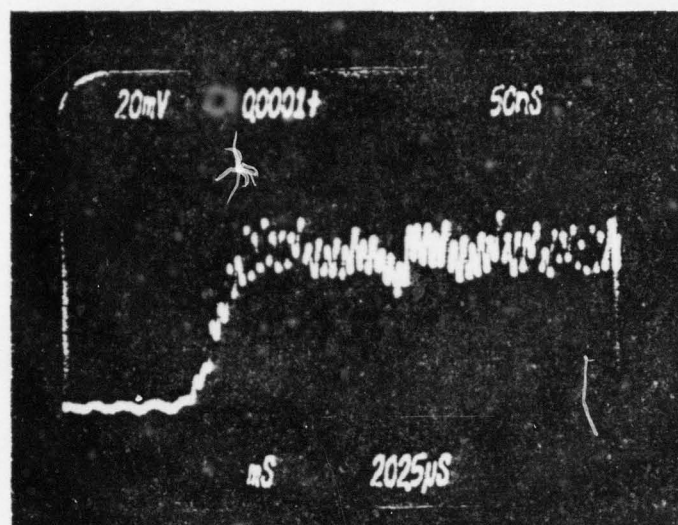


Figure 36 - RANGE PULSE WITH IF NOISE

Experiment 2

Objectives

1. To determine the operating range of the A station/E unit combination under test.
2. To determine the effect of path attenuation on range data and range pulse shape.

Procedures

1. The setup for this experiment was the same as that shown in Figure 31. The experiment hardware was the same as in the previous experiment. Cable 2, the RF link, was 1.04 meters in length.
2. Operating in the Range and continuous command modes Attenuator 1 was varied from 0 dB to 80 dB. This varied the total path attenuation from 53 dB to 133 dB. In each setting of attenuation the checkout set was placed in the single-command mode and photographs recorded the shape of the range pulses as detected at the E unit and the A station.
3. At each setting slant ranges were recorded in both the single and continuous command modes.
4. Range pulse rise times were measured from expanded range pulses detected at the B unit. Rise time was defined to be the time it took the leading edge of the range pulse to go from its ten percent amplitude point to its ninety percent point.

Results

Table C-1 gives a summary of the data collected during this experiment. For each value of total path attenuation the range of slant range readings is indicated and whether the response was 'steady' or 'not steady' in the continuous-command mode. A 'steady' response means that the B unit responded properly to every interrogation by the A station or that the B unit failed to respond to any of the interrogations. In addition, for each attenuation setting an average slant range is indicated. This value is the average of more than thirty single-command responses. Figures 37-44 present representative pictures of range pulses for selected values of path attenuation. Each figure consists of two pictures, one of a range pulse detected at the B unit and one of a range pulse detected at the A station. The slant range corresponding to a particular pulse is also indicated.

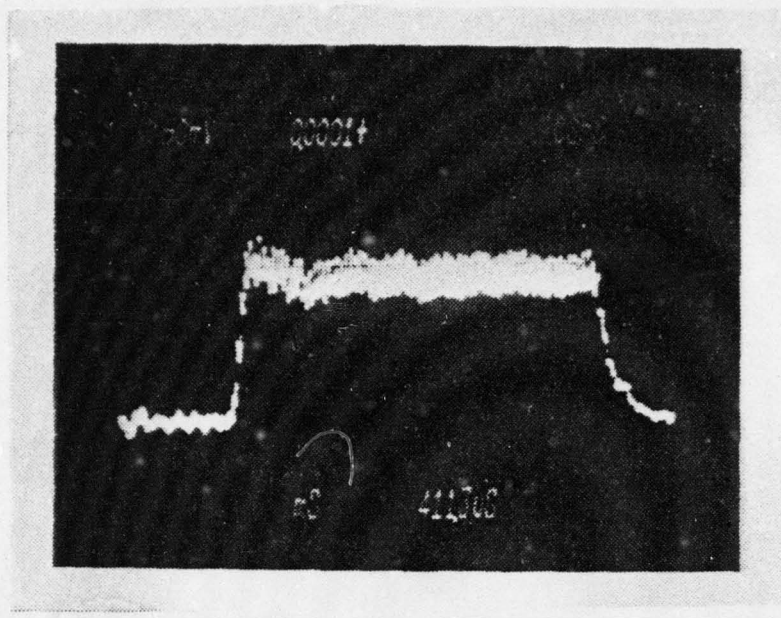
When the path attenuation was less than 60 dB there was never a response to the interrogations of the A station. This was expected and meets the specified limits of operation for the micro-B unit. That is, when the interrogating signal arriving at the B unit is too large the automatic gain control (AGC) of the B unit receiver is 'saturated' and a 'no B response' results. The tabulated data also shows that for values of path attenuation greater than 120 dB the B unit never responded. At a path attenuation of 118 dB the response of the B unit was not steady, sometimes the checkout set indicated a proper B unit response and slant range and other times a 'no B response' occurred. It was determined that leakage from the attenuators and cable connectors were creating alternate paths for the signals. When RF shielding material was placed around all the connectors this problem vanished.

Table C-1 SINGLE PATH SIMULATION ATTENUATION TEST

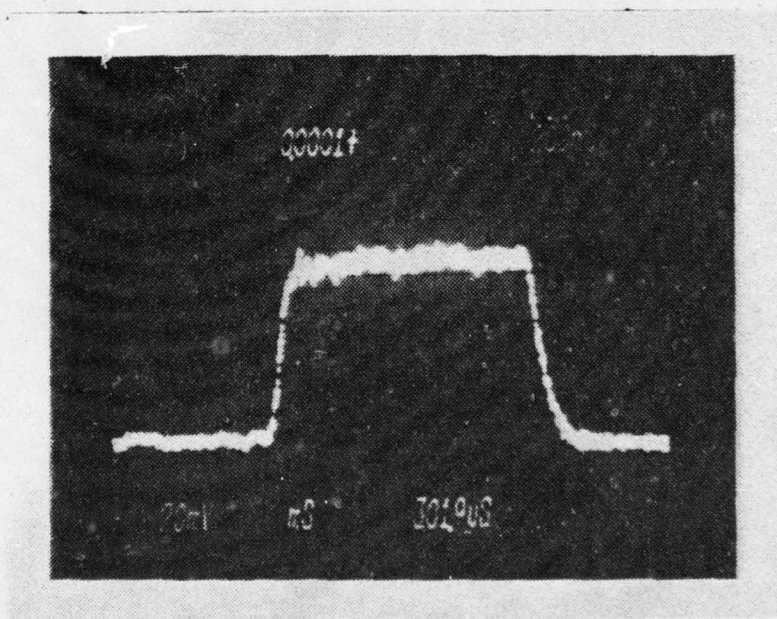
TOTAL PATH ATTENUATION (DB)	AVERAGE RANGE (METERS)	RESPONSE STABILITY
70	71.5	STEADY
75	72.5	STEADY
80	75.8	STEADY
85	76.9	STEADY
90	77.3	STEADY
100	78.6	STEADY
105	78.8	STEADY
110	82.0	NOT STEADY
115	88.2	NOT STEADY
120	NO B RESPONSE	STEADY

It is clear from Figures 37-44 that as the path attenuation was increased the average slant range increased and the range pulses became more distorted by noise. By expanding the range pulse to look at the leading edge it was apparent that in addition to overall range pulse distortion the increase in attenuation caused an increase in the rise time of the leading edge. Figures 45-47 are pictures of the leading edge of range pulses detected at the B unit for the indicated values of path attenuation and slant ranges. For each picture the rise time is given. Even for low values of path attenuation (70 dB) the rise time (60 nanoseconds) differs significantly from the specified value of 40-45 nanoseconds. Since slant ranges rely on the detection of the leading edge of the range pulses, the increase in slant range as the range pulse rise time increased was not unexpected. Assuming that both the A station and E unit range slicing levels were set at the fifty percent point a change in rise time of 10 nanoseconds for each range pulse would cause a 3 meters error in the slant range.

It was assumed that the deviation in rise time was due to the introduction of passive circuit elements into the system by the attenuators and not a shortcoming of the A station or the B unit. However, it is quite apparent that distortion of the range pulse, in particular the leading edge, causes errors in slant range data that may be significant depending on the amount of distortion.

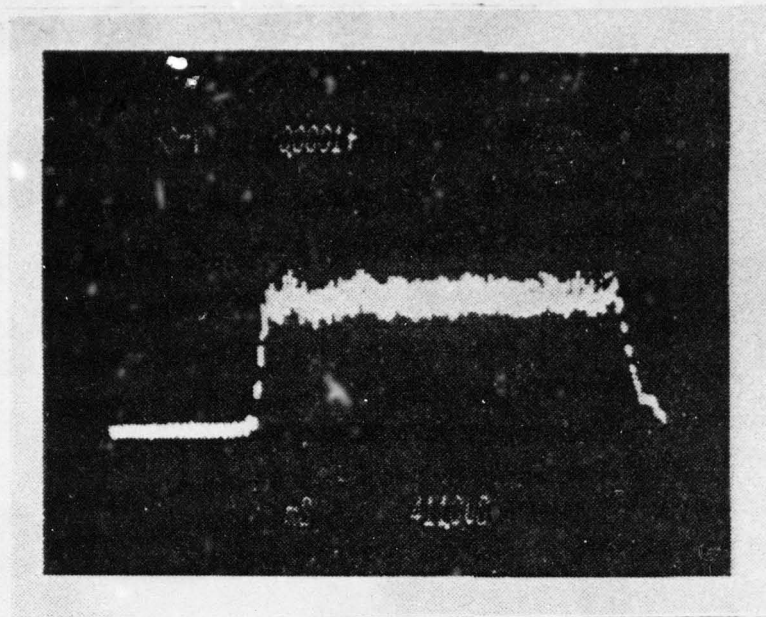


(A)
Detected at the
A Station
Range 66 meters

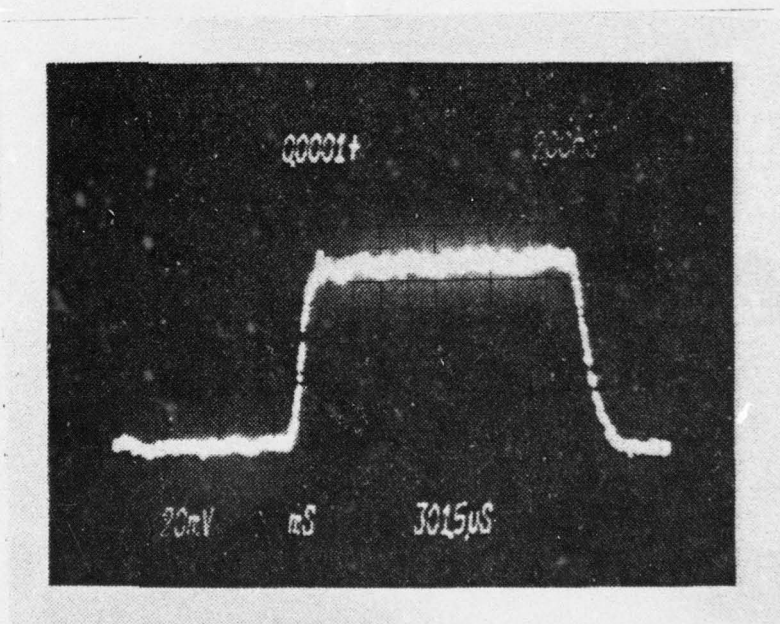


(B)
Detected at the
B Unit
Range 66 meters

Figure 37 - RANGE PULSES PATH ATTENUATION 62 DB

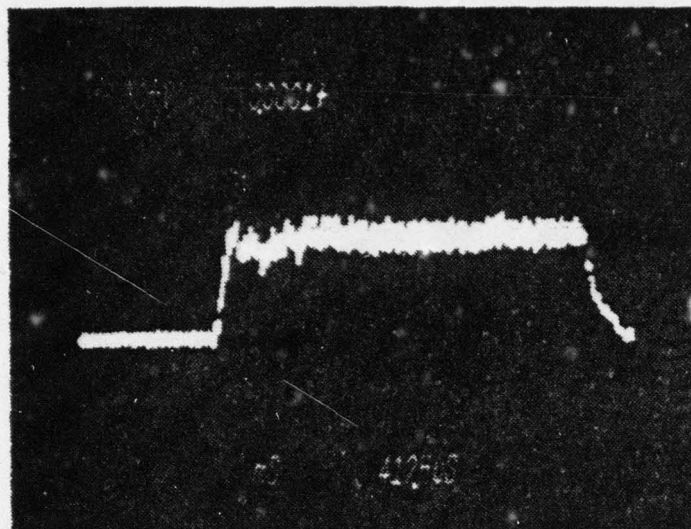


(A)
Detected at the
A Station
Range 68 meters

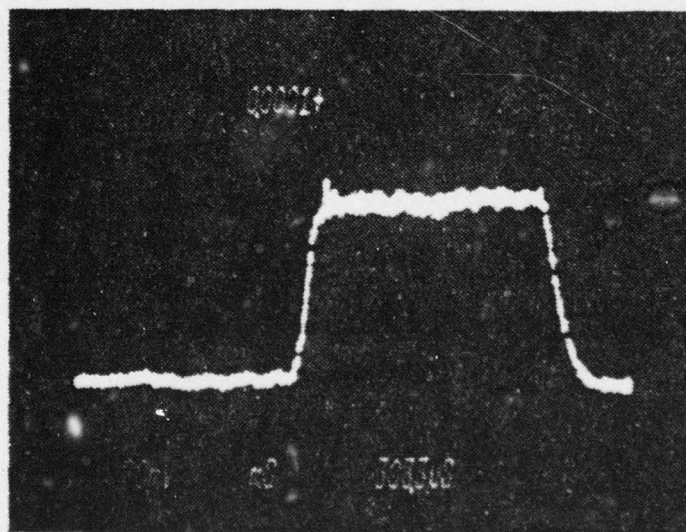


(B)
Detected at the
B Unit
Range 68 meters

Figure 38 - RANGE PULSES PATH ATTENUATION 73 DB

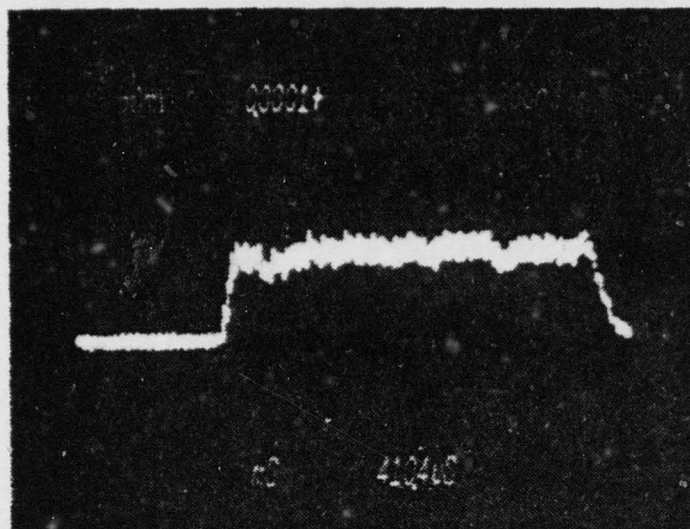


(A)
Detected at the
A Station
Range 70 meters

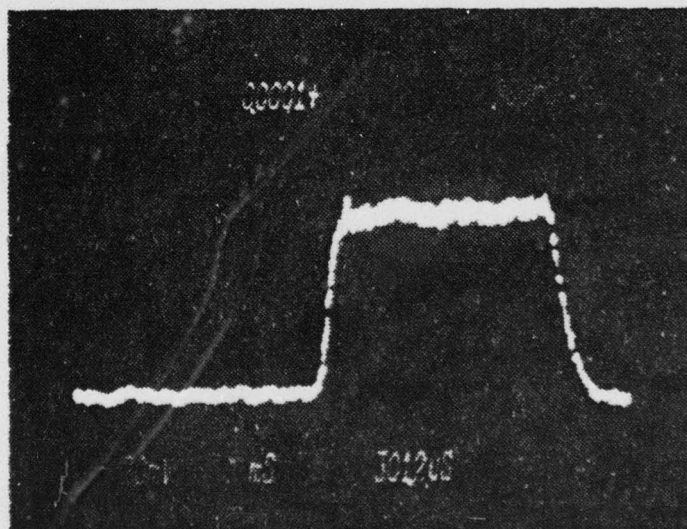


(B)
Detected at the
B Unit
Range 70 meters

Figure 39 - RANGE PULSES PATH ATTENUATION 83 DB

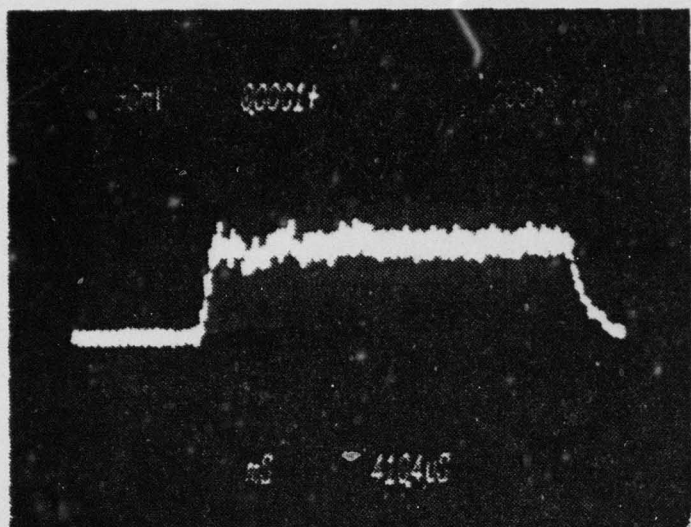


(A)
Detected at the
A Station
Range 70 meters

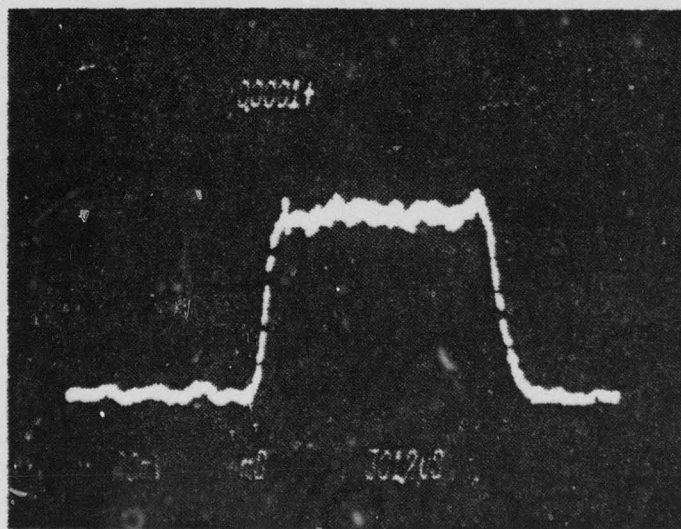


(B)
Detected at the
B Unit
Range 70 meters

Figure 40 - RANGE PULSES PATH ATTENUATION 93 DB

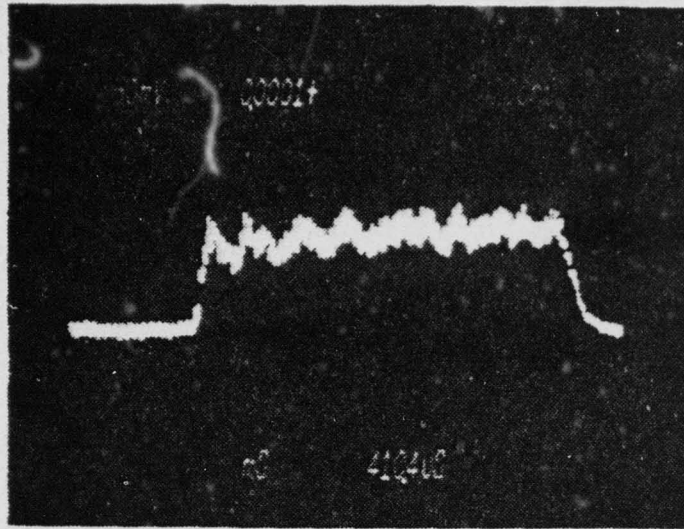


(A)
Detected at the
A Station
Range 70 meters

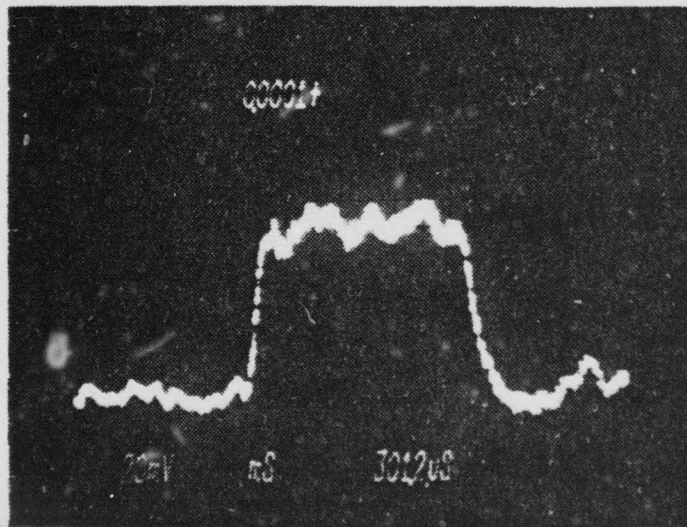


(B)
Detected at the
B Unit
Range 70 meters

Figure 41 - RANGE PULSES PATH ATTENUATION 103 DB

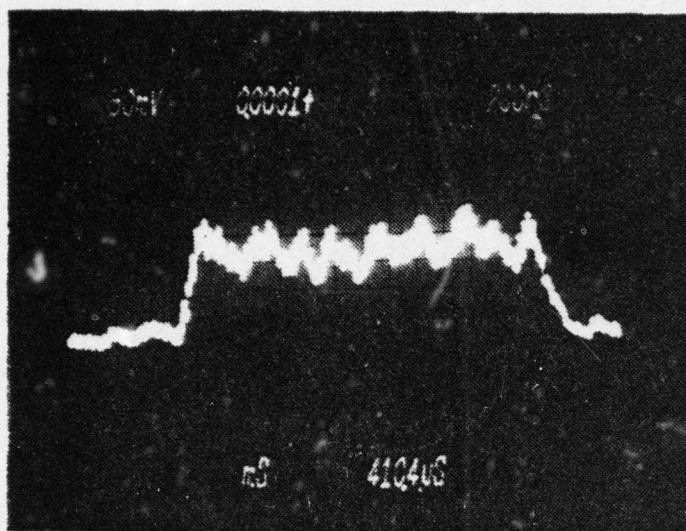


(A)
Detected at the
A Station
Range 72 meters

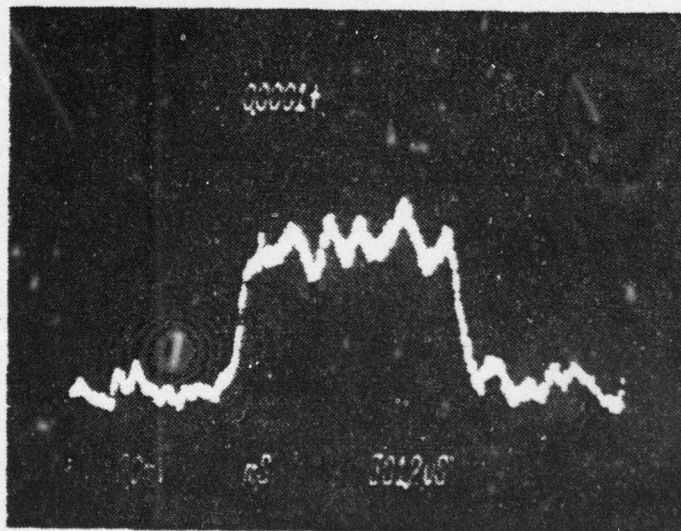


(B)
Detected at the
B Unit
Range 72 meters

Figure 42 - RANGE PULSES PATH ATTENUATION 113 DB

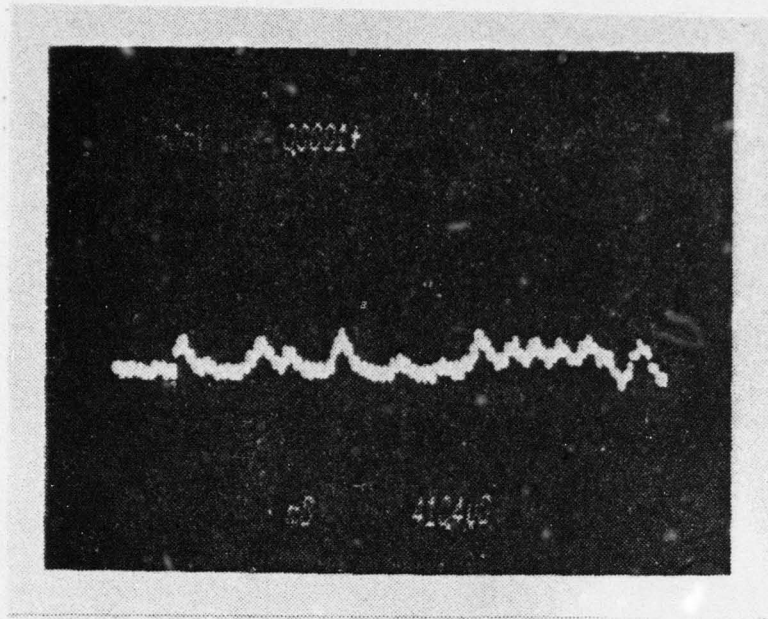


(A)
Detected at the
A Station
Range 72 meters

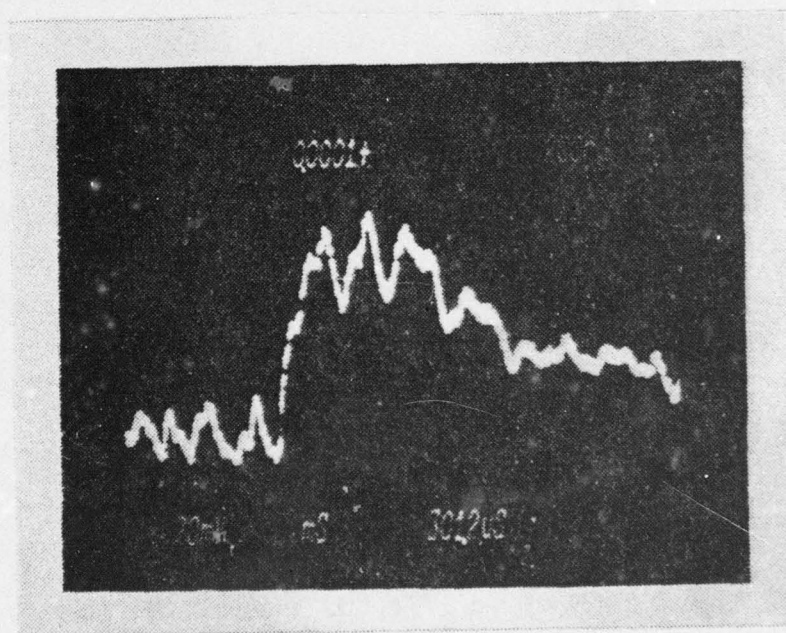


(B)
Detected at the
B Unit
Range 72 meters

Figure 43 - RANGE PULSES PATH ATTENUATION 118 DB



(A)
Detected at the
A Station
No B Response



(B)
Detected at the
B Unit
No E Response

Figure 44 - RANGE PULSES PATH ATTENUATION 118 DE

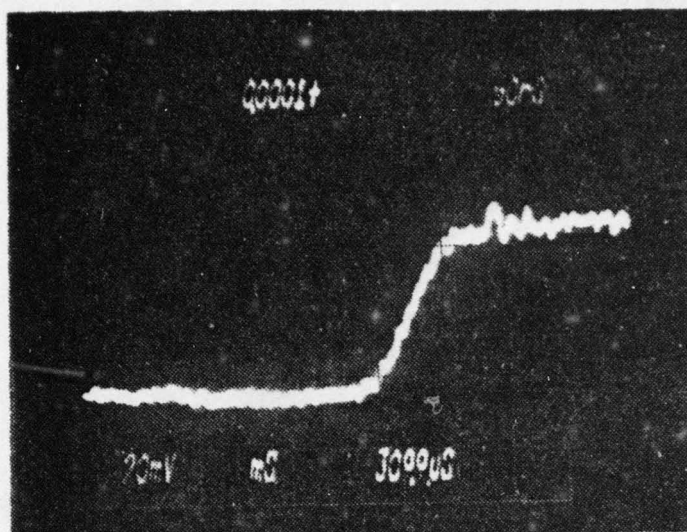


Figure 45 - RANGE DETECTED AT THE B UNIT
PATH ATTENUATION 73 DB RISE TIME 60 NS

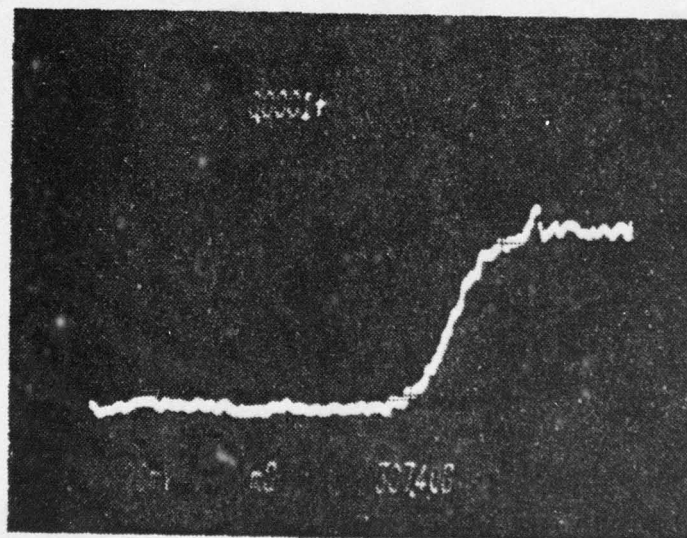


Figure 46 - RANGE DETECTED AT THE B UNIT
PATH ATTENUATION 93 DB RISE TIME 80 NS

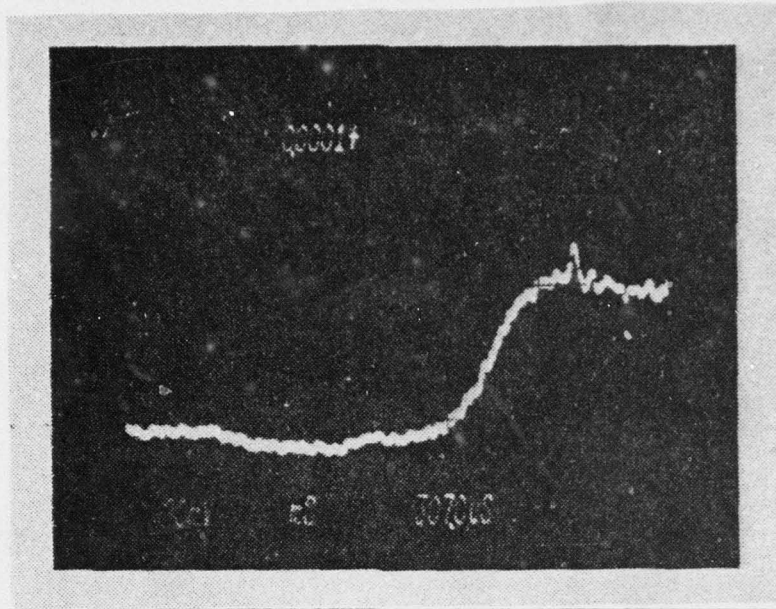


Figure 47 - RANGE DETECTED AT THE B UNIT
PATH ATTENUATION 113 DB RISE TIME 88 NS

A similar experiment was conducted operating in the SCOM mode. The results of this experiment were essentially the same as that for the Range mode. When the signal arriving at the B unit was too large a saturation condition existed and a 'no B response' resulted. Also, when the path attenuation was greater than 120 dB a 'no B response' resulted. There was no apparent bit shifting due to high attenuation nor was the noise in the channel large enough to cause bit errors.

APPENDIX D

MULTIPATH SIMULATION EXPERIMENTS

The basic multipath simulation of Figure 14 was used in several experiments to test the system response to two signals arriving at the A station or the B unit at about the same time. The overall objective of these experiments was to determine if it was possible to create conditions that might cause system errors such as 'wild' ranges. Dual directional couplers were used to isolate the two signals so different combinations of signal strength and path lengths could be investigated. A section of variable length coaxial cable inserted in the direct path allowed for the changing of the phase relation between the two signals as they combined at either the A station or the B unit. Figure 48 is the actual laboratory simulation setup with the RF shielding material removed.

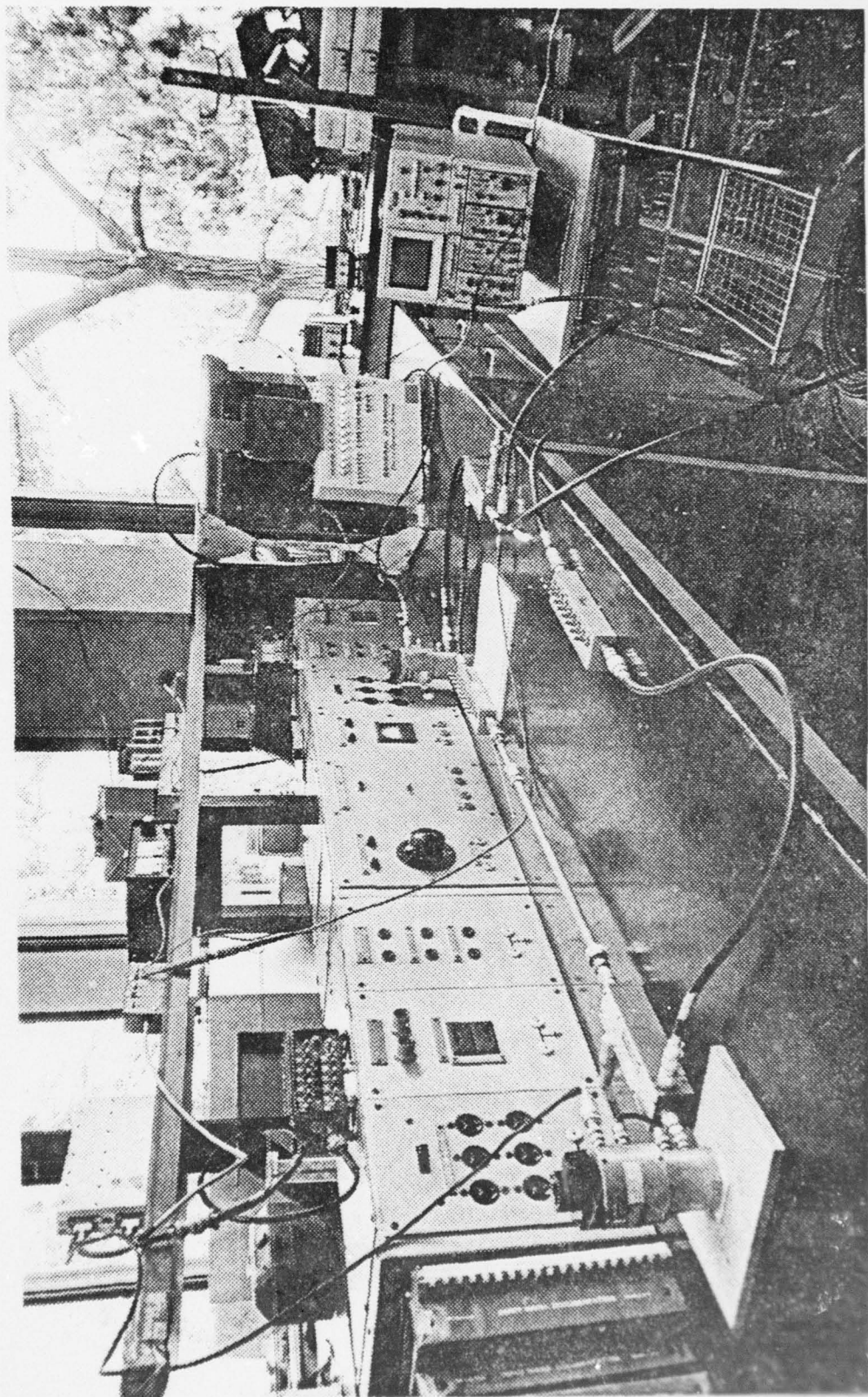


Figure 48 - MULTIPATH SIMULATION SETUP IN THE LABORATORY

AD-A050 091

NAVAL POSTGRADUATE SCHOOL MONTEREY CALIF

F/G 17/7

THE EFFECTS OF MULTIPATH PROPAGATION ON THE RANGE MEASUREMENT S--ETC(U)

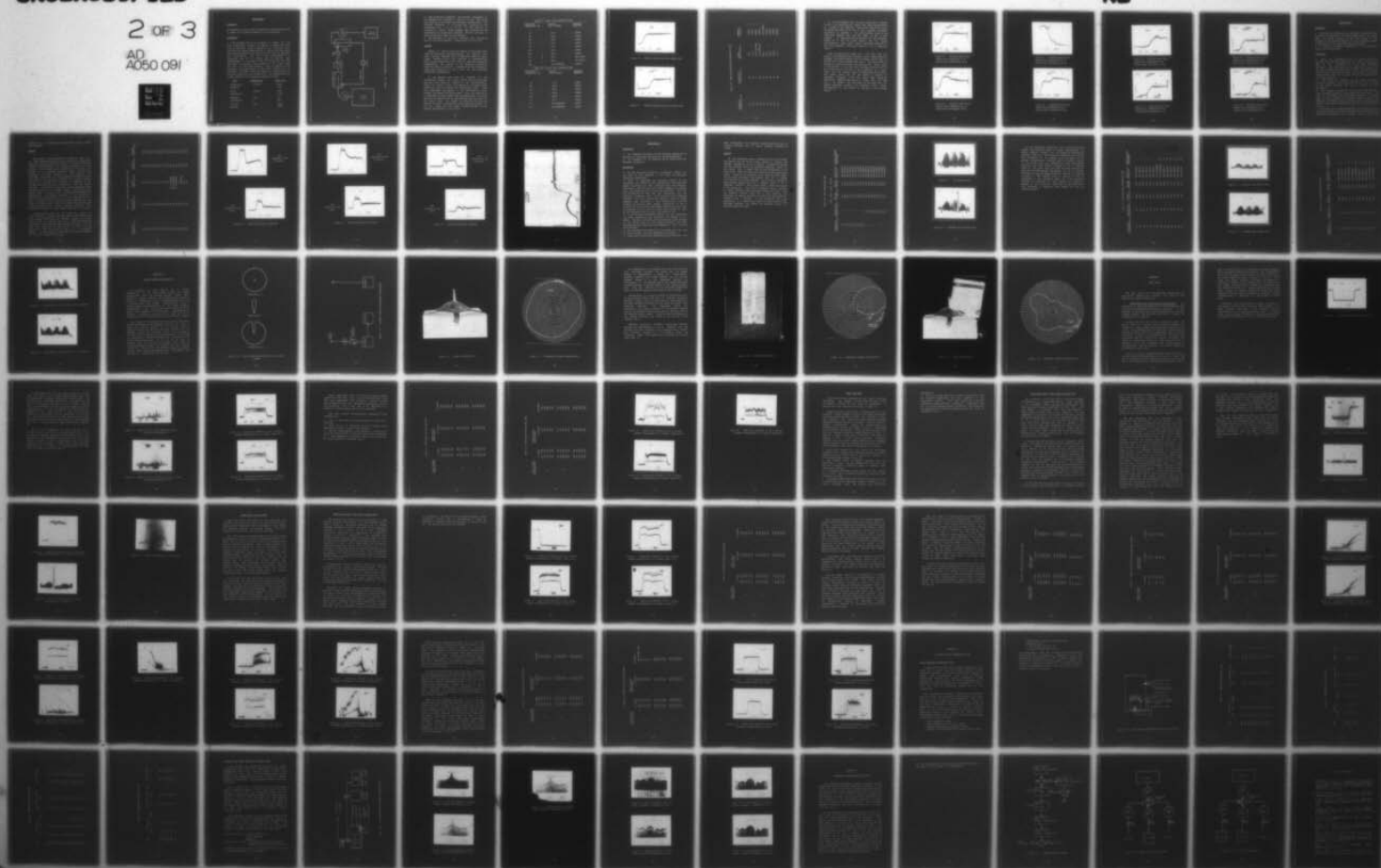
DEC 77 H STURHAN, W P HAVENSTEIN

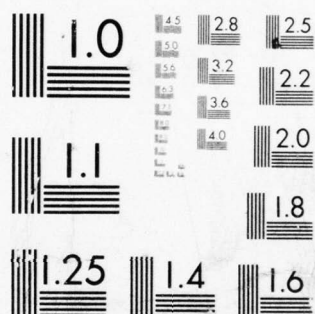
UNCLASSIFIED

NL

2 OF 3

AD
A050 091





MICROCOPY RESOLUTION TEST CHART
NATIONAL BUREAU OF STANDARDS-1963-A

Experiment 1

Objective

To determine at what signal strengths the delayed signal has an effect on the system response in the Range mode.

Procedures

1. The equipment was set up as shown in Figure 49. The dual directional couplers introduced an additional 20 dB loss to each path. Prior to beginning the multipath tests each path was tested independently to insure that both paths were operated properly and that the noise level in each path was satisfactory. The direct path corresponded to a free-space path of 10.1 meters and the delayed path corresponded to free-space path of 58.2 meters. For this experiment the variable length section of the direct path was kept in the closed position. Due to a failure in the internal 5 Volt power supply of the B unit checkout set, an additional DC power source was required to provide power to the logic section of the checkout set. The nomenclature and serial numbers of the remaining hardware is given.

<u>Item</u>	<u>Nomenclature</u>	<u>Serial No.</u>
Directional	HP 765D	9165
Couplers		9166
25 dB	Telonic	913U
Attenuators		5143B
Variable	KAY	871
Attenuators		9666
DC Power	PMC	36643
Sources		72577

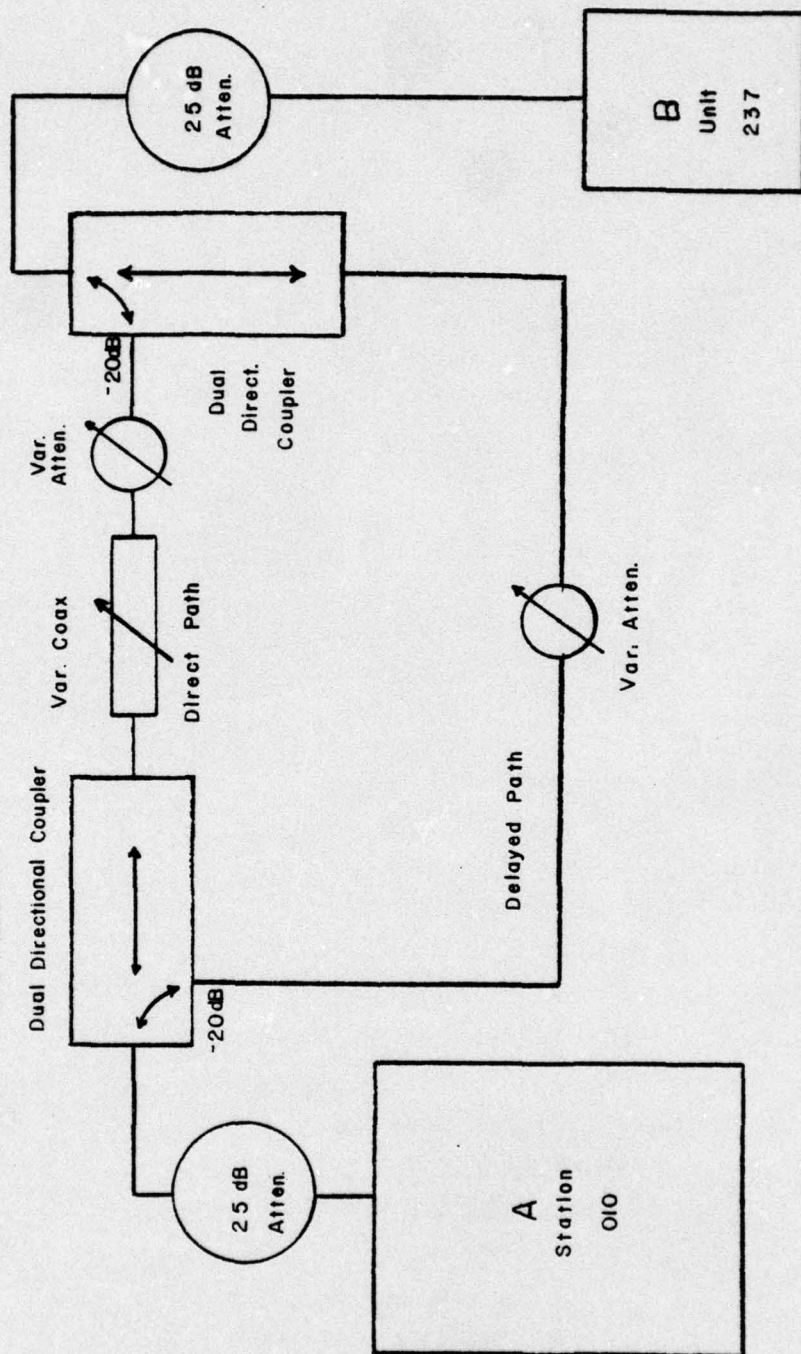


Figure 49 - MULTIPATH SIMULATION SETUP

2. Both paths were connected. The variable attenuator in the delayed path, attenuator 1, was set to 0 dB. The system was operated in the Range and continuous command modes. The variable attenuator in the direct path, attenuator 2, was incremented from 0 dB to 30 dB. At each setting of attenuation, twenty single commands were initiated and the resulting slant ranges were recorded. Several pictures of range pulses were taken at each setting.

3. The procedure in 2 above was repeated with attenuator set at 0 dB and attenuator 1 varied from 0 dB to 10 dB.

Results

Tables D-1 and D-2 show the results of the single-path tests for the direct and delayed paths. As expected, both paths operated properly over the specified range of signal levels. Figures 50 and 51 are pictures of representative range pulses detected at the B unit for each path operating independently. The results of the multipath simulation tests are shown in Table D-3. Figures 52-59 are pictures of range pulses detected at the B unit for the indicated attenuation combinations.

It was apparent that when the strength of the delayed-path signal was within 3 dB of that of the direct path the B unit failed to respond to the interrogations. Figure 54 clearly shows the presence of two range pulses arriving at the B unit about 160 nanoseconds apart. This time difference corresponds to the difference in length between the delayed and direct paths. Since the duration of a range pulse is much longer than 160 nanoseconds, the range pulse of the delayed path is superimposed upon the pulse of the direct path. The amount by which the second pulse effects the first is determined by the relative strength of the two signals and the phase relation between the two signals upon arrival at the B unit.

Table D-1 DIRECT PATH ATTENUATION TEST

TOTAL PATH ATTENUATION (DB)	AVERAGE RANGE (METERS)	RESPONSE STABILITY
70	71.5	STEADY
75	72.5	STEADY
80	75.8	STEADY
85	76.9	STEADY
90	77.3	STEADY
100	78.6	STEADY
105	78.8	STEADY
110	82.0	NOT STEADY
115	88.2	NOT STEADY
120	NO B RESPONSE	STEADY

Table D-2 DELAYED PATH ATTENUATION TEST

TOTAL PATH ATTENUATION (DB)	AVERAGE RANGE (METERS)	RESPONSE STABILITY
80	117.2	STEADY
85	120.9	STEADY
90	121.7	STEADY
95	122.2	STEADY
100	126.0	STEADY
110	127.1	STEADY
115	NO B RESPONSE	STEADY
120	NO B RESPONSE	STEADY

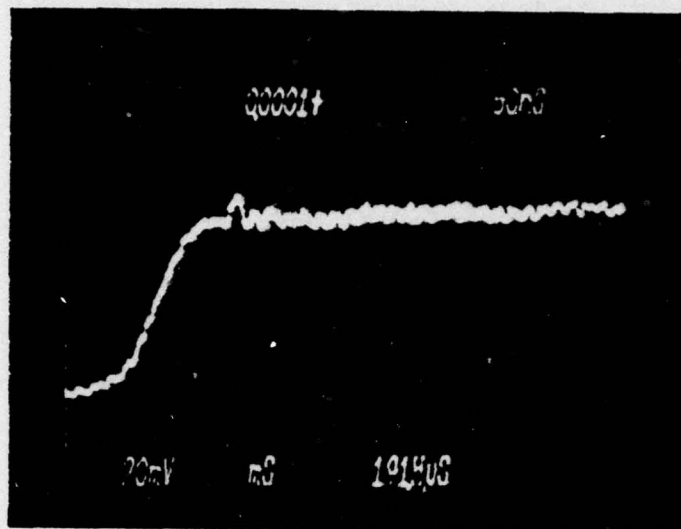


Figure 50 - DETECTED RANGE PULSE FOR DIRECT PATH

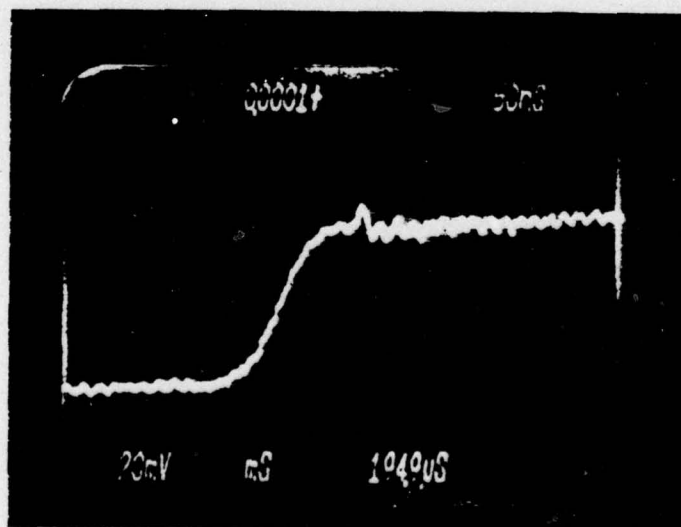


Figure 51 - DETECTED RANGE PULSE FOR DELAYED PATH

Table D-3 RANGE MODE MULTIPATH ATTENUATION TEST

DIRECT-PATH ATTENUATION (DB)	DELAYED-PATH ATTENUATION (DB)	AVERAGE RANGE (METERS)	RESPONSE STABILITY
70	80	70.4	STEADY
73	80	71.1	STEADY
76	80	NO B RESPONSE	STEADY
79	80	NO B RESPONSE	STEADY
85	80	456.0	NOT STEADY
90	80	114.0	STEADY
100	80	116.2	STEADY
70	85	69.75	STEADY
70	90	71.0	STEADY

It is also apparent that the pulse amplitude in Figures 53 and 54 are significantly greater than those corresponding to a proper B unit response. These large amplitudes create the saturated condition in the B unit receiver discussed previously in Appendix C. The initialization pulse of the Range mode message sets the AGC level in the B unit receiver. If superpositioning affected the initialization pulses as it did the range pulses, then the second initialization pulse would cause a saturated condition in the B unit receiver. This would lead to a 'no B response' result.

When the direct-path signal was 6 dB less than the signal of the delayed path erroneous 'wild' ranges resulted. Although the system response was not steady, better than 80 percent of the slant ranges were 'wild.' The range pulse in Figure 55 is quite distorted and resulted in a slant range of 458 meters. It is clear that the range slicing level of the B unit was set such that it was triggering on a point other than the leading edge of direct-path range pulse. This result shows that the RMS system is capable of producing erroneous range data under these simulated conditions. Whenever the signal of either path was more than 6 dB greater than the signal of the other path, the system responded properly and indicated slant ranges corresponding to the length of the path of the stronger signal.

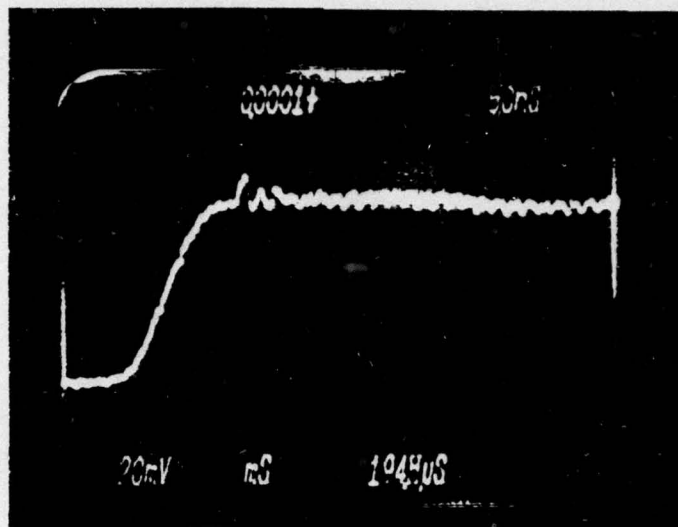


Figure 52 - DETECTED RANGE PULSE
DIRECT-PATH ATTENUATION 73 DB
DELAYED-PATH ATTENUATION 80 DB

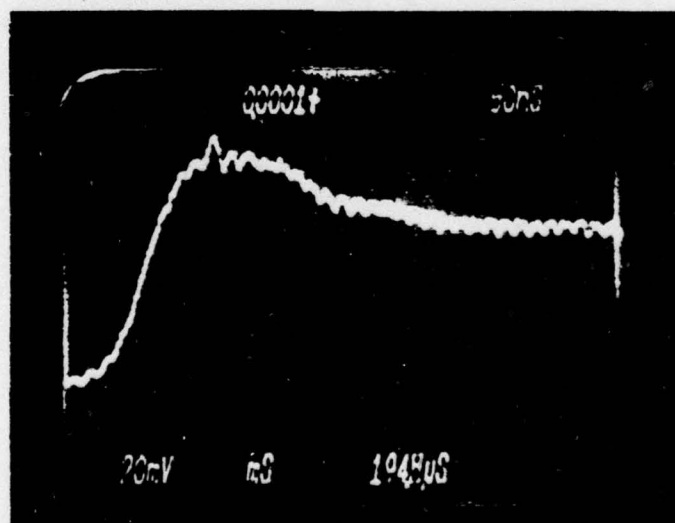


Figure 53 - DETECTED RANGE PULSE
DELAYED-PATH ATTENUATION 80 DB
DIRECT-PATH ATTENUATION 75 DB

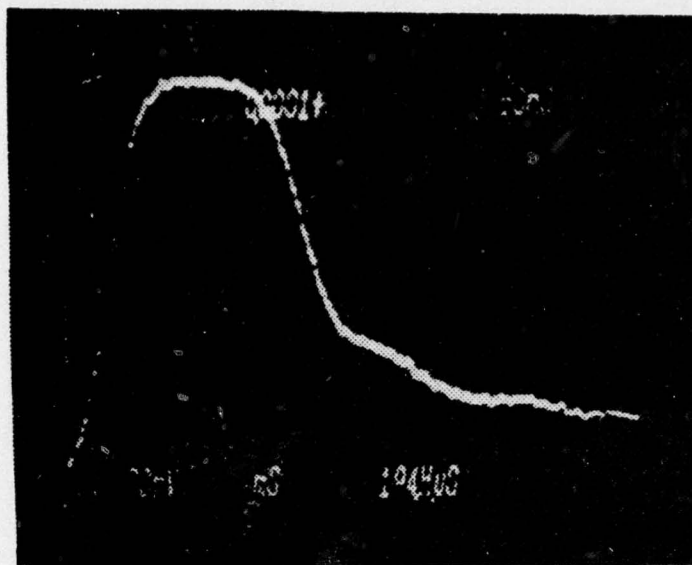


Figure 54 - DETECTED RANGE PULSE
DIRECT-PATH ATTENUATION 80 DB
DELAYED-PATH ATTENUATION 80 DB

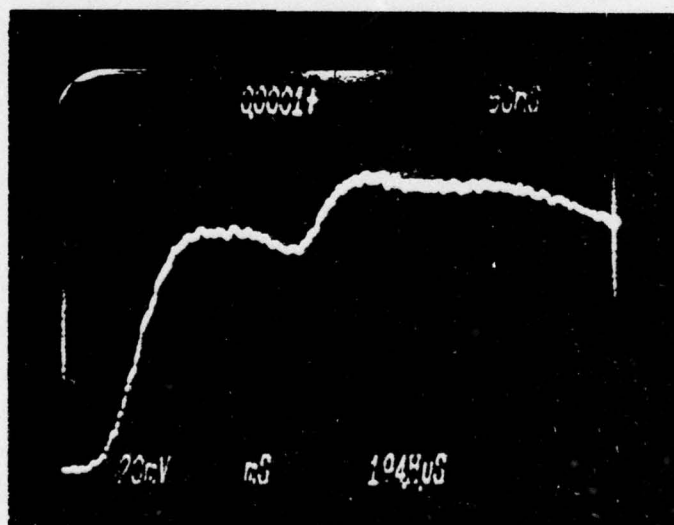


Figure 55 - DETECTED RANGE PULSE
DIRECT-PATH ATTENUATION 83 DB
DELAYED-PATH ATTENUATION 80 DB

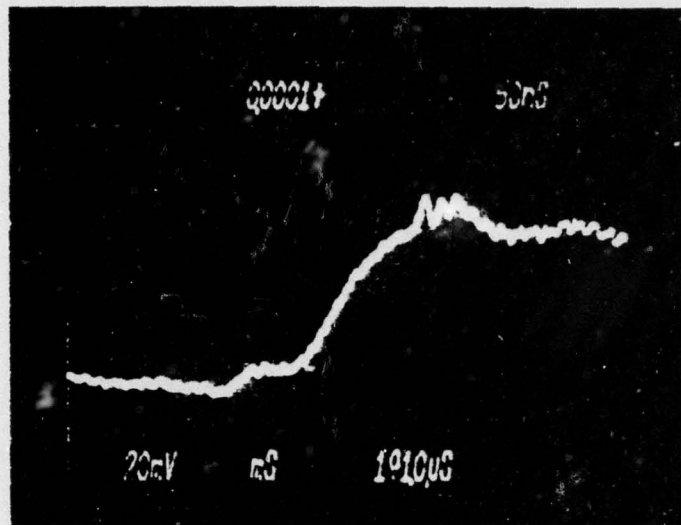


Figure 56 - DETECTED RANGE PULSE
 DIRECT-PATH ATTENUATION 85 DB
 DELAYED-PATH ATTENUATION 80 DB

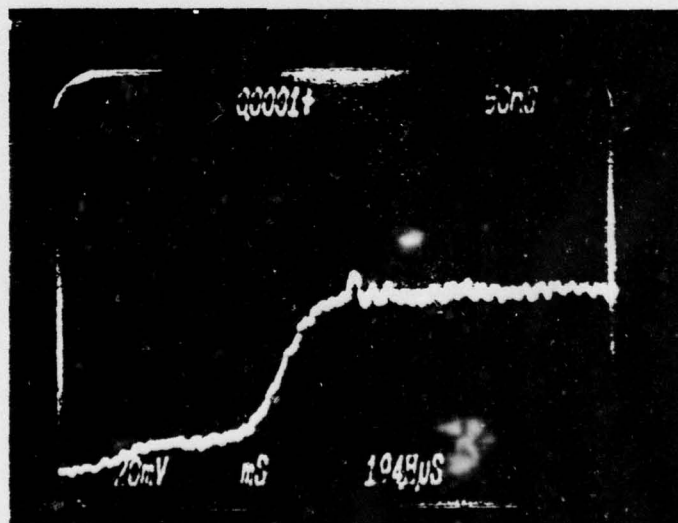


Figure 57 - DETECTED RANGE PULSE
 DIRECT-PATH ATTENUATION 86 DB
 DELAYED-PATH ATTENUATION 80 DB

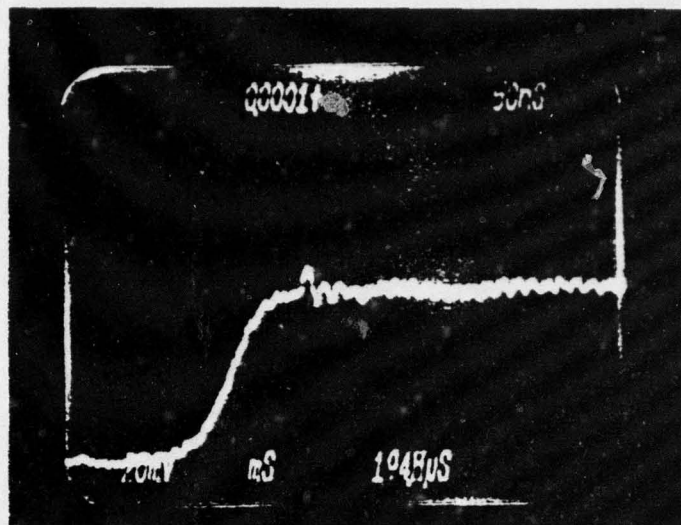


Figure 58 - DETECTED RANGE PULSE
 DELAYED-PATH ATTENUATION 80 DB
 DIRECT-PATH ATTENUATION 88 DB

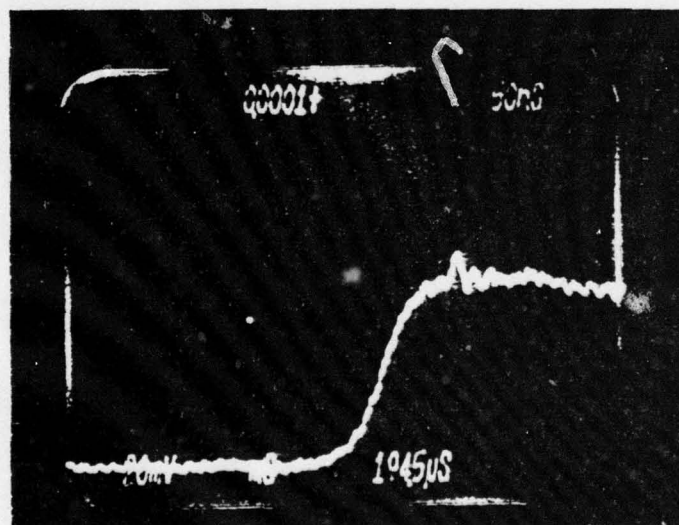


Figure 59 - DETECTED RANGE PULSE
 DIRECT-PATH ATTENUATION 95 DB
 DELAYED-PATH ATTENUATION 85 DB

Experiment 2

Objectives

1. To create an extreme case of multipath interference and determine the effects on the system operating in the Range mode. The phase relation of the two signals in the multipath simulation was adjusted to cause a maximum amount of distortion to the Range mode signal waveforms.
2. To determine if complete cancellation of the direct-path signal could be achieved.

Procedures

1. Again, the arrangement shown in Figure 48 was the starting point for this experiment. The same hardware was used in this experiment as in the first multipath experiment. The direct path had an initial path loss of 70 dB with variable attenuator set to 0 dB. The delayed path had an initial path loss of 80 dB. The section of variable length coaxial cable in the direct path was initially set in the closed position.
2. The system was operated in the Range mode with continuous commands. The range pulse was the only portion of the signal waveform that was of interest in this experiment.
3. The variable attenuators of both paths were set such that the signal strength of the delayed path was from 12 dB less to 9 dB greater than the signal strength of the direct path. At each setting the variable length section was adjusted for maximum range pulse distortion. Pictures were taken of range pulses detected at both the A station and the E unit.
4. By setting the variable attenuator in the direct path to 10 dB the signals of the two paths were as equal as could be measured or calculated. The variable length section was

adjusted for a minimum range pulse signal and the results were recorded.

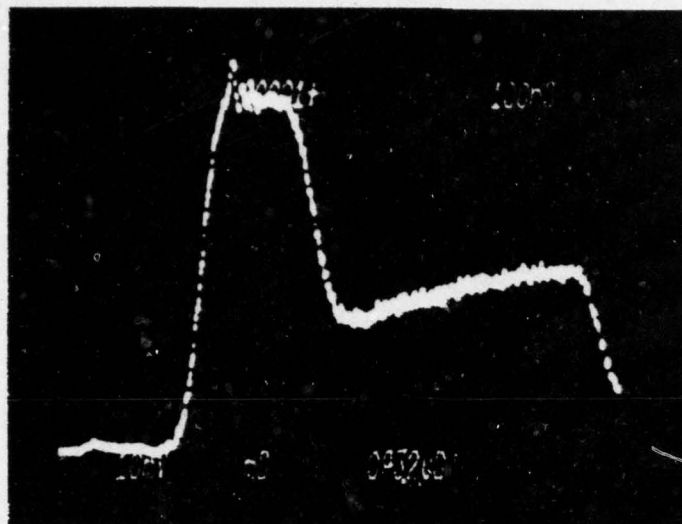
Results

The results of this experiment are shown in table D-4. The table indicates the total path attenuation settings for each path, the average range response for at least 20 single command interrogations, the response stability and the setting for the variable length coaxial cable section. The numbers in the response stability column indicate the percentage of proper responses for that setting. The remaining percentage of interrogations resulted in either wild range or 'no B response' results. The variable length section was calibrated in millimeter increments and the settings indicate the amount of extension from the closed position. As indicated, there were several instances where the system gave a 'no B response' result. Some of the more severe cases of range pulse distortion are presented in Figures 60-62. Each figure consists of two pictures of range pulses, one detected at the A station and one at the B unit. The amount of distortion was about equal for the two types of range pulses. Figure 28 presented previously and Figure 63 show the most severe distortion achieved. Both figures are pictures of range pulses detected at the B unit.

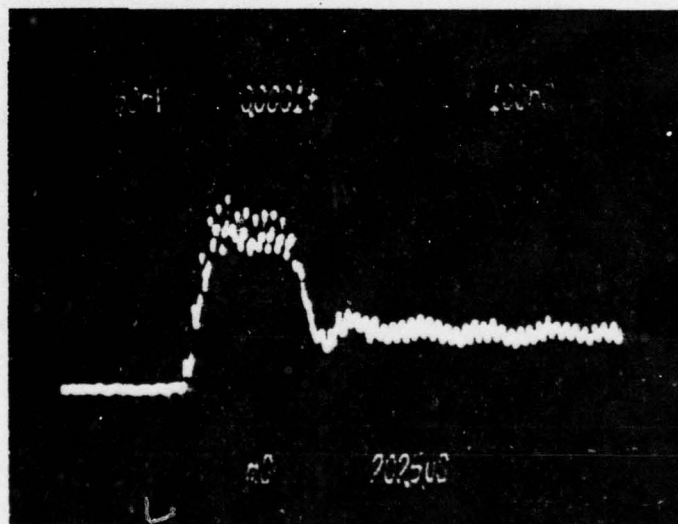
Complete cancellation of the direct-path signal was never achieved. Although minimum signals caused distortion of the signal waveforms, the combined signal was always large enough to trigger the B unit. When the system was operated at the maximum specified operating range, that is with both paths set at 105 dB of attenuation, it was possible to cause the system to give a 'no B response' result. In this case, the strength of the combined signal was too low to trigger the B unit.

Table D-4 RANGE MODE PHASE ADDITION TEST

DIRECT-PATH ATTENUATION (DB)	DELAYED-PATH ATTENUATION (DB)	AVERAGE RANGE (METERS)	RESPONSE STABILITY (%)	VARIABLE LENGTH (cm)
70	80	74	80	4.0
70	80	74	95	5.0
70	80	74	100	11.5
70	80	74	100	23.0
73	80	75	60	3.0
73	80	74	99	6.0
73	80	74	100	11.5
73	80	74	100	23.0
76	80	76	70	4.0
76	80	74	100	6.0
76	80	74	100	11.5
80	80	NO B RESPONSE	100	4.0
80	80	NO B RESPONSE	100	6.0
80	80	NO B RESPONSE	100	8.0
80	80	75	90	11.5
83	80	454(WILD)	100	6.0
88	80	122	100	6.0
88	80	124	100	11.5

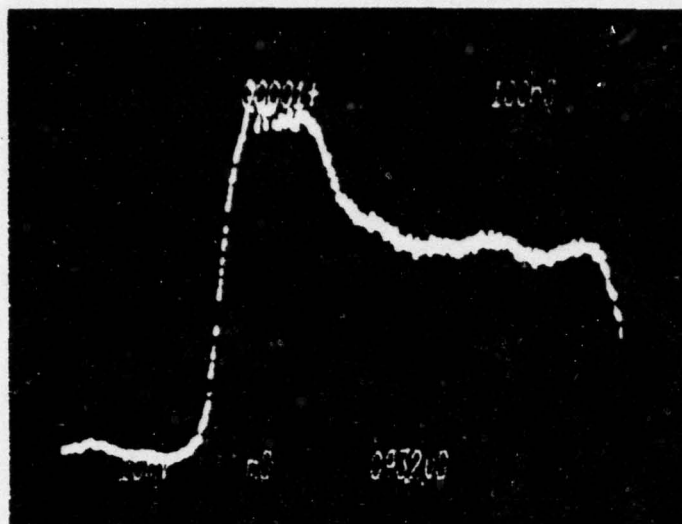


(A)
Detected at the
A Station

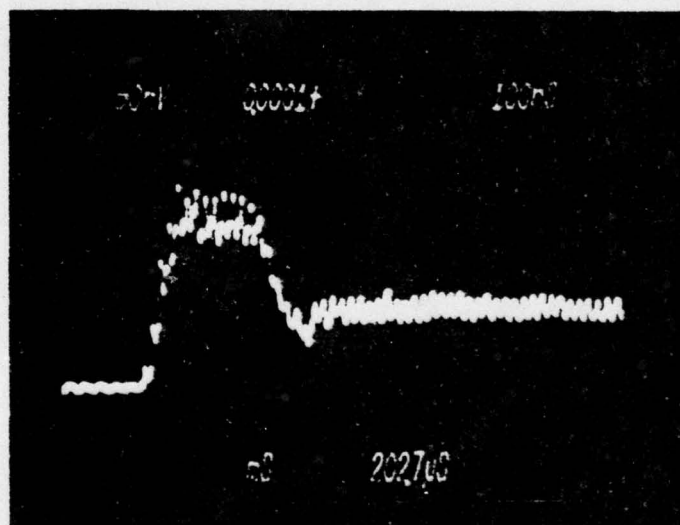


(B)
Detected at the
B Unit

Figure 60 - SEVERE RANGE PULSE DISTORTION

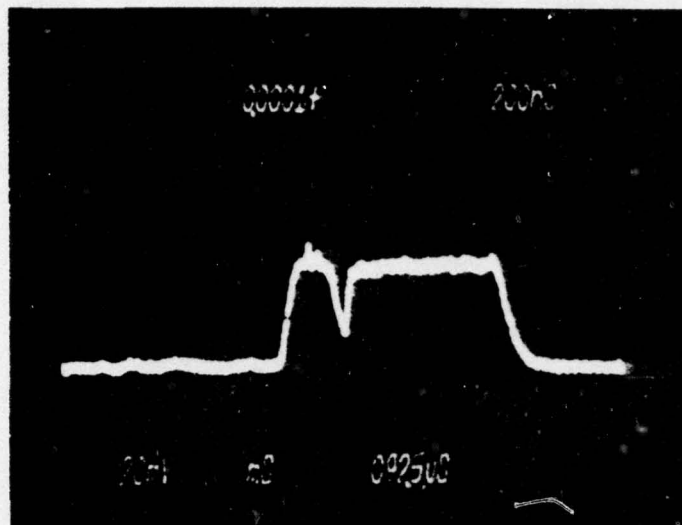


(A)
Detected at the
A Station

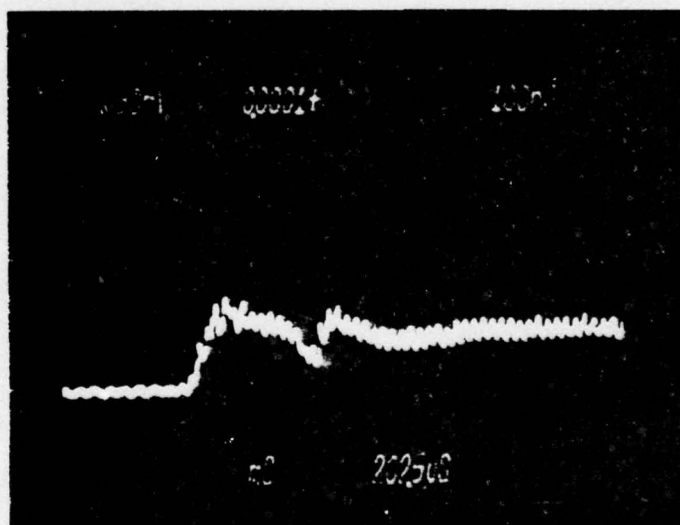


(B)
Detected at the
B Unit

Figure 61 - SEVERE RANGE PULSE DISTORTION



(A)
Detected at the
A Station



(B)
Detected at the
B Unit

Figure 62 - SEVERE RANGE PULSE DISTORTION

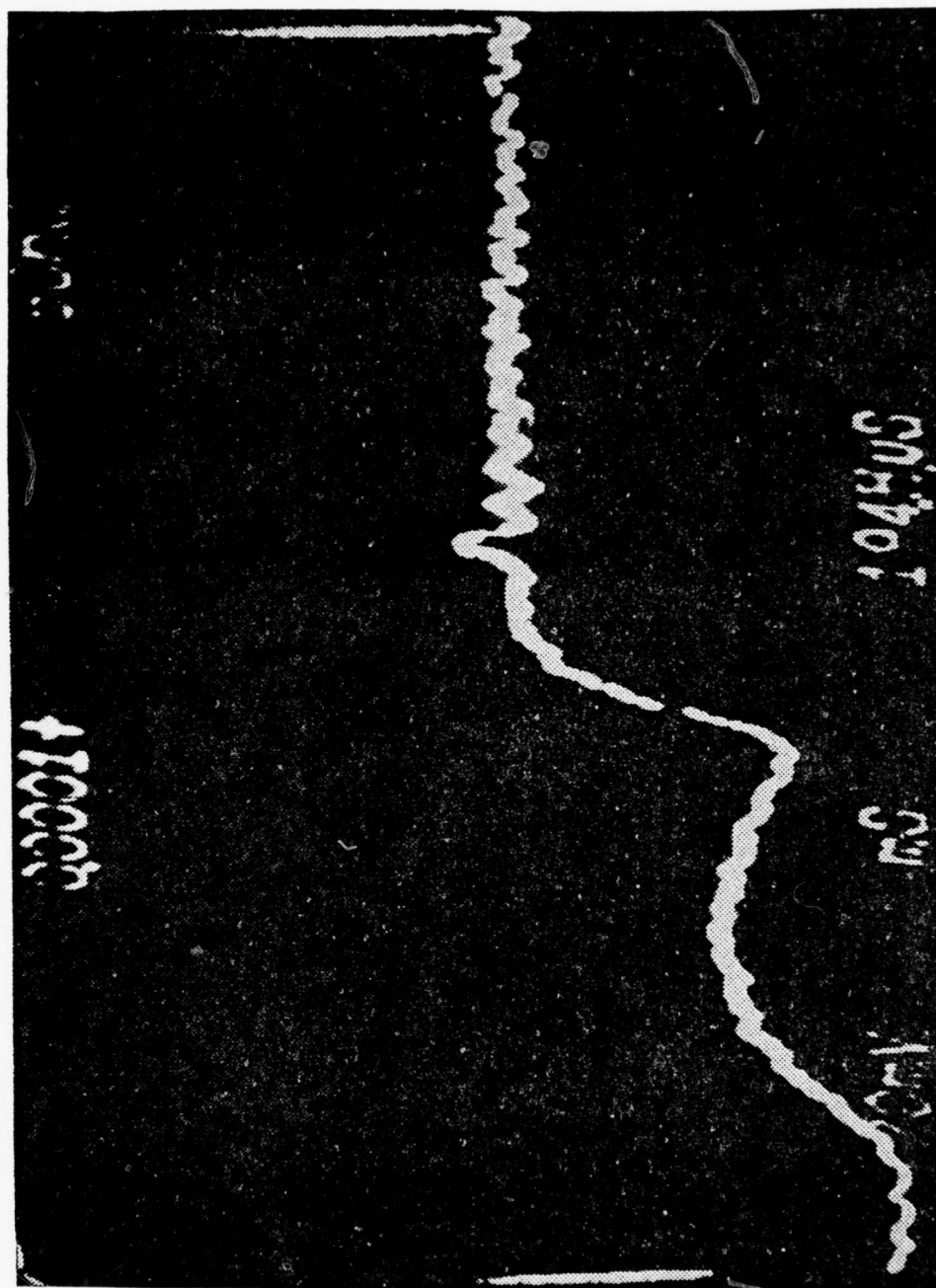


Figure 63 - SEVERE RANGE PULSE DISTORTION

Experiment 3

Objectives

1. To determine the effect of the multipath simulation on data bits in the signal waveforms of the SCCM messages.
2. To determine if bit shifting can be caused under the multipath simulation.

Procedures

1. The same multipath simulation arrangement (Figure 49) was used as that employed in the first two multipath simulation experiments.
2. Prior to commencing the multipath portion of the experiment, the effects of path attenuation on the SCOM mode signal waveforms for each individual path were measured. Operating in the SCOM mode with single commands, the message data bits detected at the B unit were monitored. The total path attenuation for each path was incremented over the specified operating range of the system and the responses recorded. For each attenuation setting, several single commands were initiated at the B checkout set. For each command, the four bit SCOM message transmitted by the A station and the four bit SCOM message received by the B unit as indicated on the B unit I/O device were recorded as well as the response lights of the B unit checkout set.
3. In the multipath simulation portion of the experiment the same information was monitored and recorded as in 2 above. Operating initially with the variable length section of the direct path in the closed position, the path attenuations were varied and the responses at each setting were recorded.
4. The variable length section of the direct path was set to 10 cm and step 3 of this procedure was repeated.
5. Several path attenuation combinations were selected. For

each combination, the variable length section was set to several positions and the system response recorded as before.

Results

In the single-path tests, whenever the path attenuation was greater than 105 dB the B unit failed to display the message transmitted by the A station. Although the system did work properly within its specified operating range, it had worked over a larger range of path attenuation in the Range mode. Table D-5 shows the results for the single-path tests. Figure 64 is a picture of the detected video signal of the B unit and shows three message bits for a command that resulted in correct response. The picture of Figure 65 shows similar message bits for a command where a 'no B response' resulted. This picture shows a large noise spike in the middle bit. There were no instances of bit shifting or wrong messages being displayed during this test. Only one instance occurred where the B unit received and displayed the correct transmitted message and then failed to respond to the A station. It was concluded that path attenuation in a single path would not cause errors in the SCOM mode provided the system was operated within its designed operating range.

Table D-5 SCOM SINGLE-PATH TEST

SCOM SINGLE PATH RESULTS					
DIRECT-PATH ATTENUATION(DB)	DELAYED PATH ATTENUATION(DB)	MESSAGE TRANSMITTED	MESSAGE RECEIVED	CHECKOUT SET INDICATION	VARIABLE LENGTH (CENTIMETER)
70	-	1111	1111	MSG COMPLTE	-
70	-	0001	0001	MSG COMPLTE	-
80	-	0011	0011	MSG COMPLTE	-
90	-	0111	0111	MSG COMPLTE	-
100	-	0110	0110	MSG COMPLTE	-
105	-	1000	0110	NO B RESPNS	-
110	-	1010	0110	NO B RESPNS	-
115	-	1001	0110	NO B RESPNS	-
120	-	0100	0100	NO B RESPNS	-
-	70	0110	0110	MSG COMPLTE	-
-	80	0000	0000	MSG COMPLTE	-
-	90	0001	0001	MSG COMPLTE	-
-	100	0011	0011	MSG COMPLTE	-
-	105	0010	0011	NO B RESPNS	-
-	110	0111	0011	NO B RESPNS	-
-	115	1111	0011	NO B RESPNS	-
-	120	010	0011	NO B RESPNS	-

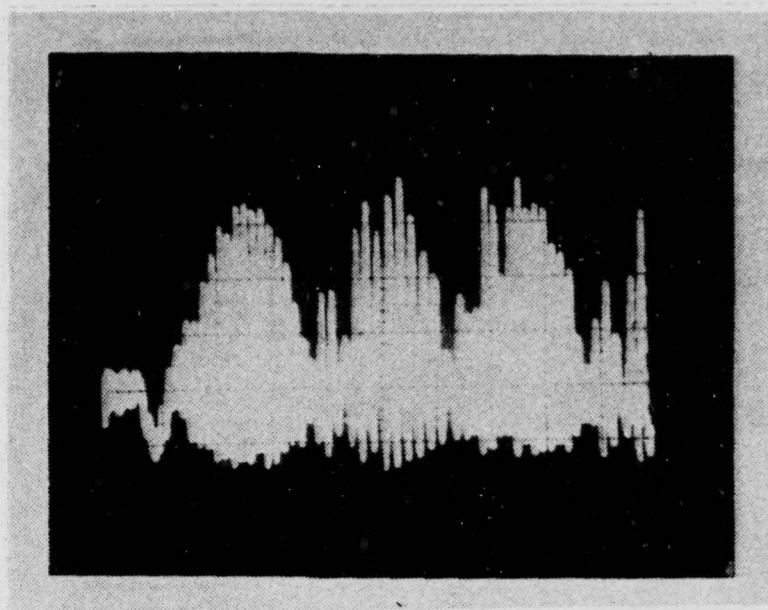


Figure 64 - SCOM MESSAGE BITS

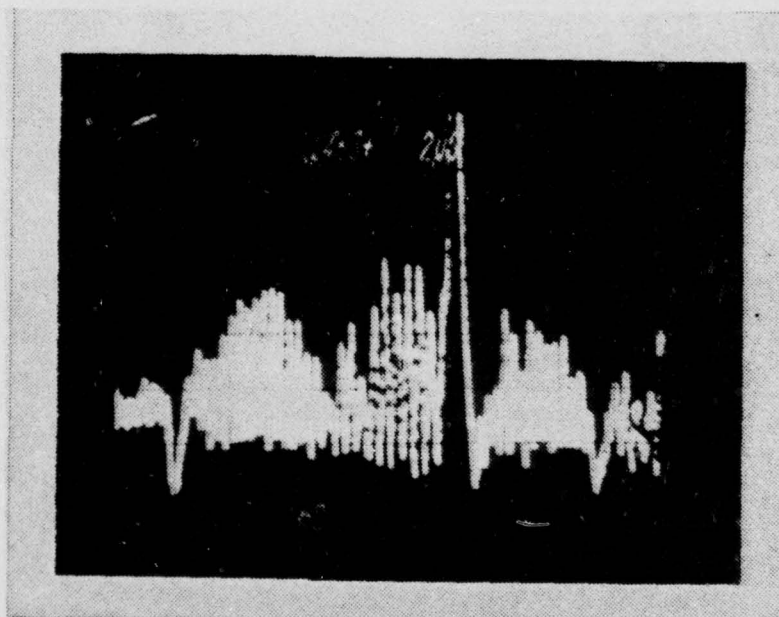


Figure 65 - DISTORTED SCOM MESSAGE BITS

In the multipath simulation, for a fixed direct-path length, which does not result in phase cancellation, the system operated properly for all attenuation combinations selected, Table D-6. The pictures of Figures 66 and 67 show that distortion of the message bits did occur, but not enough to cause errors. However, when the variable section of the direct path was adjusted for a near cancellation condition, the B unit failed to respond to the A station, while at the same time the B unit correctly detected and displayed the SCOM message transmitted by the A station. This type of response happened several times as is indicated in Table D-7. The signals shown in Figures 68 and 69 correspond to two instances where the B unit correctly received and displayed the SCOM message but failed to respond to the A station. There were no case where the B unit displayed an incorrect SCOM message nor was bit shifting evident.

Table D-6 SCOM MULTIPATH ATTENUATION TEST

DIRECT-PATH ATTENUATION(DB)	DELAYED-PATH ATTENUATION(DB)	MESSAGE TRANSMITTED	MESSAGE RECEIVED	CHECKOUT SET INDICATION	VARIABLE LENGTH (CENTIMETER)
70	80	0000	0000	MSG COMPLT	-
70	90	0001	0001	MSG COMPLT	-
70	100	0100	0100	MSG COMPLT	-
70	110	0110	0110	MSG COMPLT	-
70	115	0101	0101	MSG COMPLT	-
70	120	0111	0111	MSG COMPLT	-
80	80	0000	0000	NO B RESPONSE	-
80	80	0001	0001	NO B RESPONSE	40
90	80	0100	0100	MSG COMPLT	10
100	80	0110	0110	MSG COMPLT	10
105	80	0101	0101	MSG COMPLT	10
110	80	0111	0111	MSG COMPLT	10
115	80	1100	1100	MSG COMPLT	10
120	80	1001	1001	MSG COMPLT	10

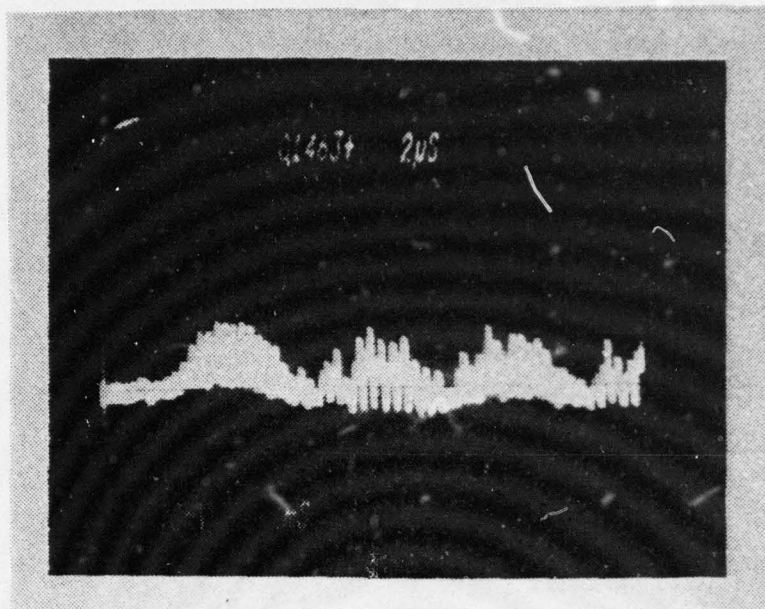


Figure 66 - DISTORTED SCOM MESSAGE BITS

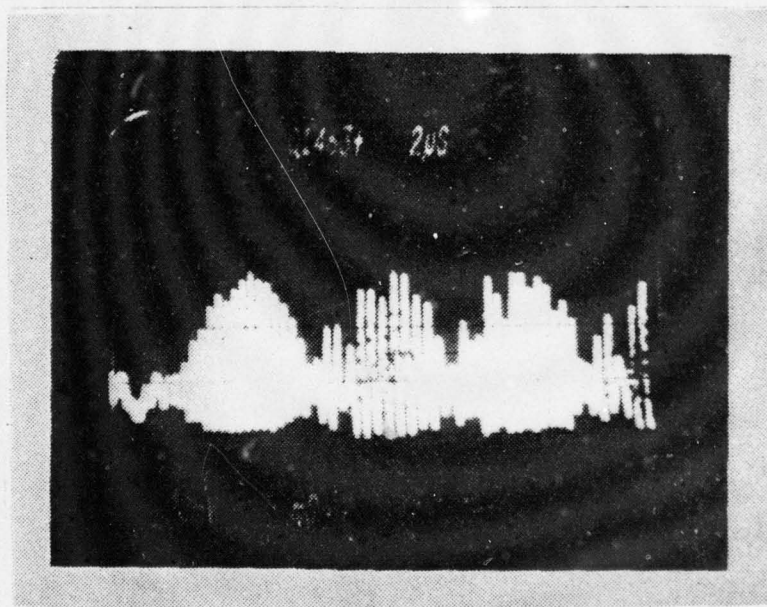


Figure 67 - DISTORTED SCOM MESSAGE BITS

Table D-7 SCOM PHASE ADDITION TEST

DIRECT-PATH ATTENUATION(DB)	DELAYED-PATH ATTENUATION(DB)	MESSAGE TRANSMITTED	MESSAGE RECEIVED	CHECKOUT SET INDICATION	VARIABLE LENGTH (CENTIMETER)
80	90	0000	0000	MSG COMPLTE	2
80	90	0001	0001	MSG COMPLTE	4
80	90	0100	0100	MSG COMPLTE	6
80	90	0110	0110	NO B RESPONSE	10
90	80	0101	0101	MSG COMPLTE	10
90	90	0011	0011	NO B RESPONSE	10
100	90	1000	1000	MSG COMPLTE	2
100	90	1100	1100	MSG COMPLTE	6
100	90	1001	1001	MSG COMPLTE	10
100	95	1001	1001	NO B RESPONSE	10
100	95	1001	1001	NO B RESPONSE	19

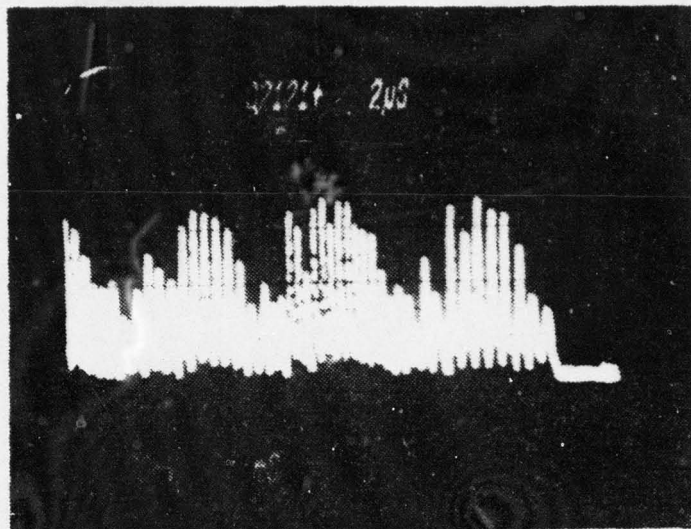


Figure 68 - SCOM MESSAGE BITS THAT GAVE A NO B RESPONSE

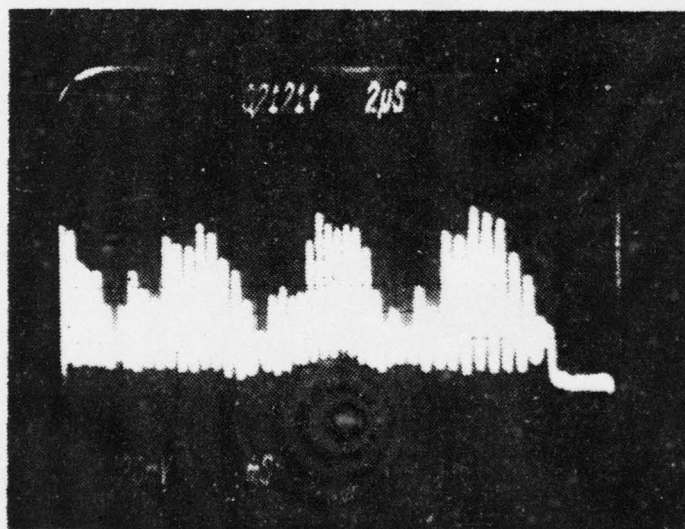


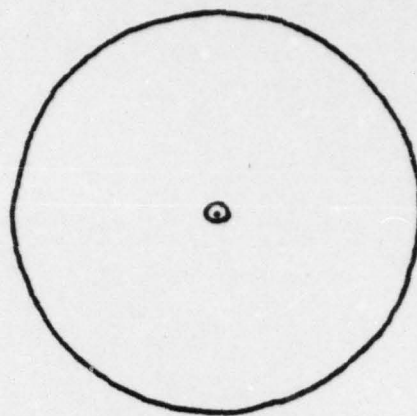
Figure 69 - SCOM MESSAGE BITS THAT GAVE A NO B RESPONSE

APPENDIX E

HELMET ANTENNA MODIFICATIONS

The objective of this section was to design modifications to the basic helmet antenna that would significantly alter the antenna pattern. Three basic horizontal antenna patterns were desired and are shown in Figure 70. Configuration C is the omnidirectional case and no modifications were needed. Configurations A and B clearly require some modification to the helmet antenna. Configuration A has a pencil beam pattern and thus can be used to limit signals to the direct path. Configuration B produces a horizontal pattern with a deep null in one direction thus can be used to block the direct path signal.

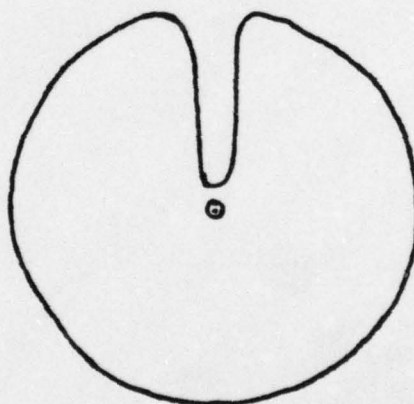
The design of the modifications was by trial and error. Aluminum shielding and RF absorbing material was used to alter the radiation pattern for the antenna. Once a modification had been made the horizontal pattern for the modified antenna was measured. Figure 71 is a diagram of the setup used to measure the antenna patterns. For testing and convenience purposes, configuration C consisted of the helmet antenna mounted on a 12 in. by 15 in. sheet of aluminum with one and one-half inches thick piece of absorbing material between the antenna and the aluminum (Figure 72). Figure 73 is the resulting horizontal pattern, which is nearly the omnidirectional case. The maximum gain was used as a reference and set to 0 dB.



CONFIGURATION C



CONFIGURATION A



CONFIGURATION B

Figure 70 - IDEAL HORIZONTAL PATTERNS FOR THE HELMET
ANTENNA

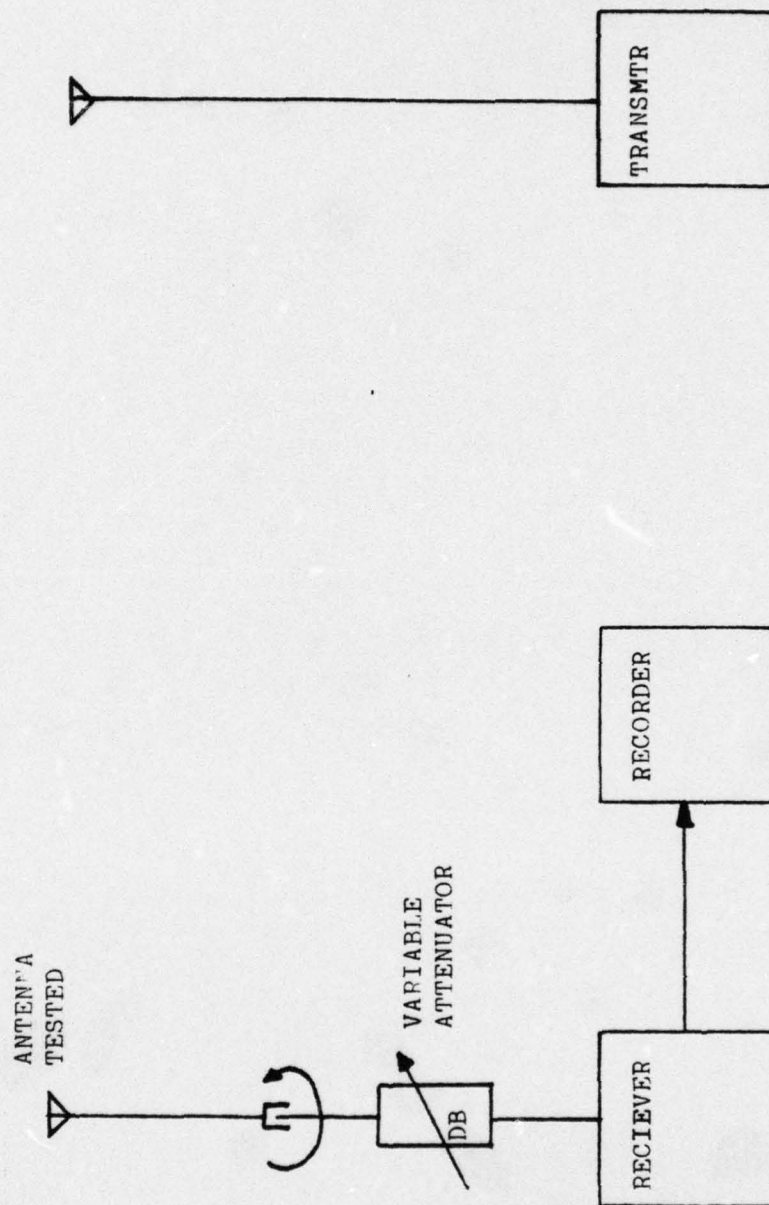


Figure 71 - ANTENNA PATTERN MEASUREMENT ARRANGEMENT

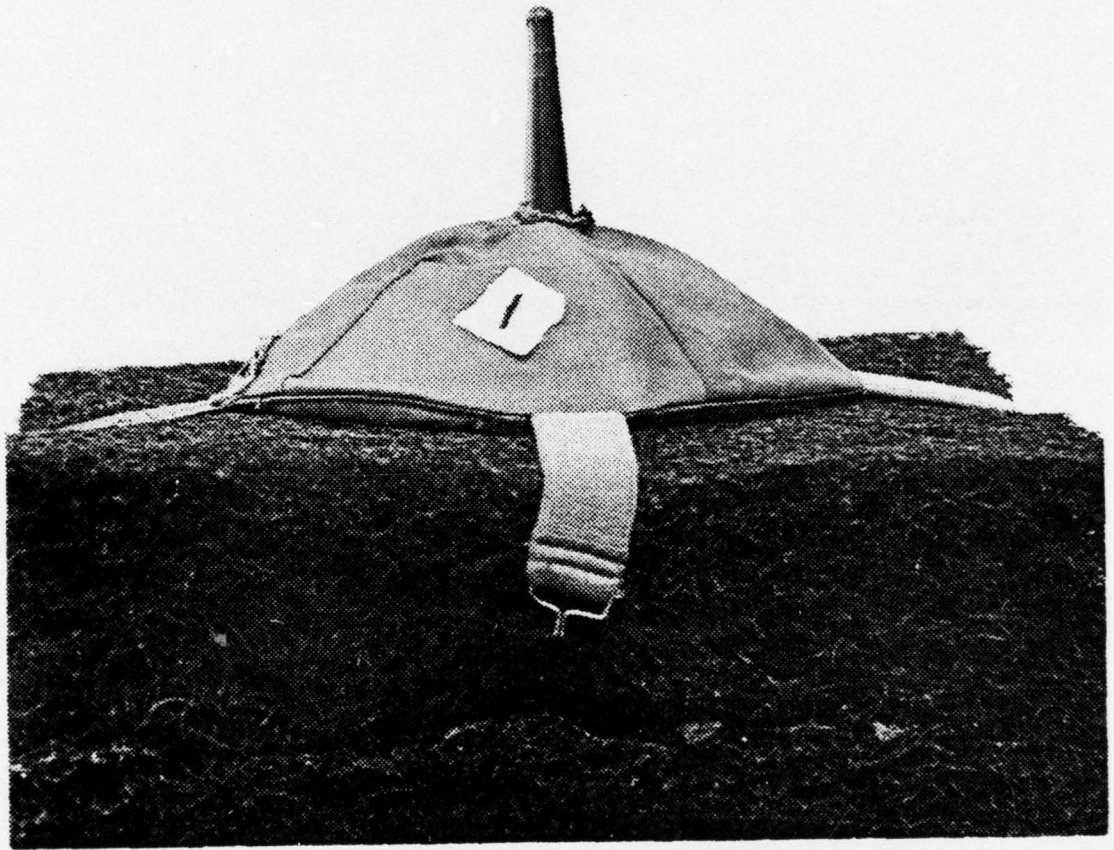


Figure 72 - FIELD CONFIGURATION C

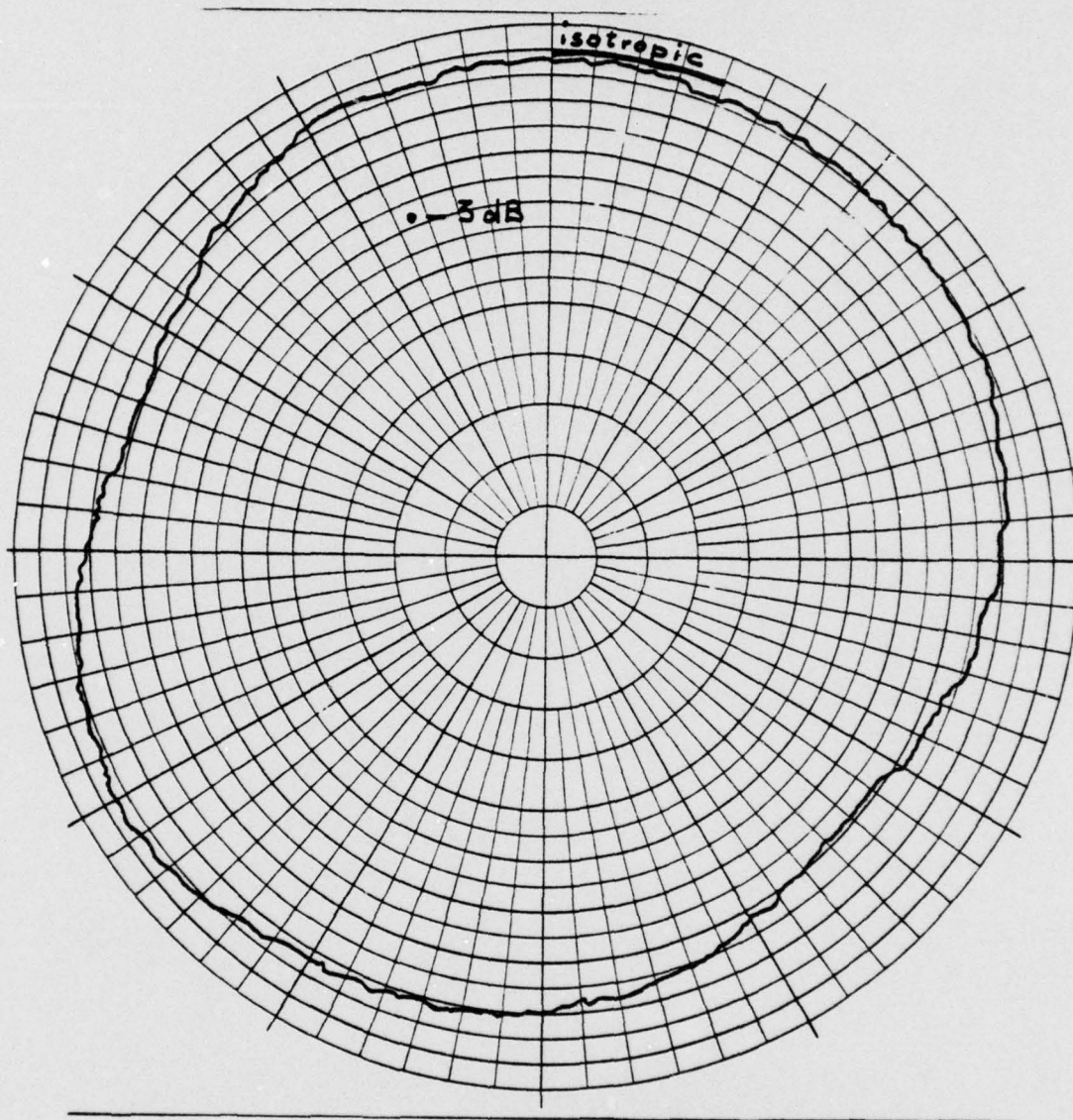


Figure 73 - HORIZONTAL PATTERN CONFIGURATION C

For configuration A an aluminum box with a one inch wide slit, vertically oriented, was placed over the helmet antenna in configuration C (Figure 74). Additionally, absorbing material was packed between the box and the antenna. Figure 75 is the horizontal pattern for configuration A. The maximum gain in the forward direction was approximately -6 dB with respect to the omnidirectional case. This gain reduction was not considered significant since the desired sideward gain reduction was achieved.

Configuration B is shown in Figure 76 and consists of a one and one-half inches wide strip of aluminum vertically oriented placed in front of the antenna of configuration C. The space between the antenna and the metal was filled with absorbing material. The horizontal pattern for configuration B is shown in Figure 77. The desired maximum gain in the sideward directions was about 1 dB below that of the omnidirectional antenna. The gain reduction achieved in the forward direction was almost 6 dB relative to the sideward level.

Equipment limitations precluded taking exact vertical patterns for configurations A and B. However, from the patterns that were available it was concluded that no severe gain reduction occurred up to 40 degrees above the horizontal plane. This agreed with the results of previous tests (Ref. 1).

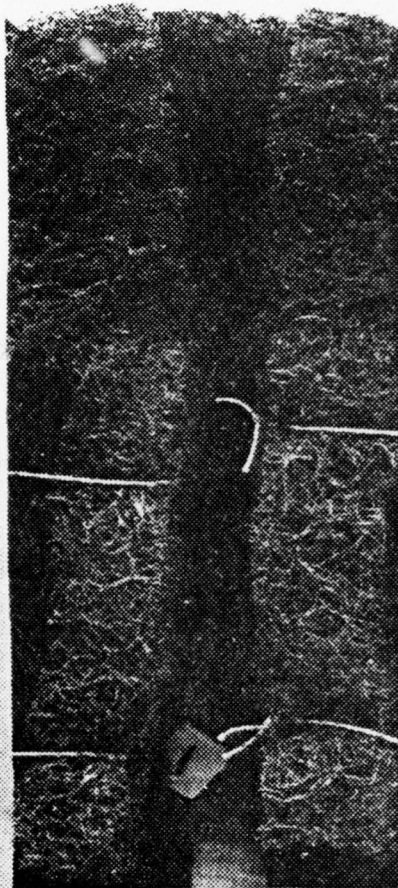


Figure 74 - FIELD CONFIGURATION A

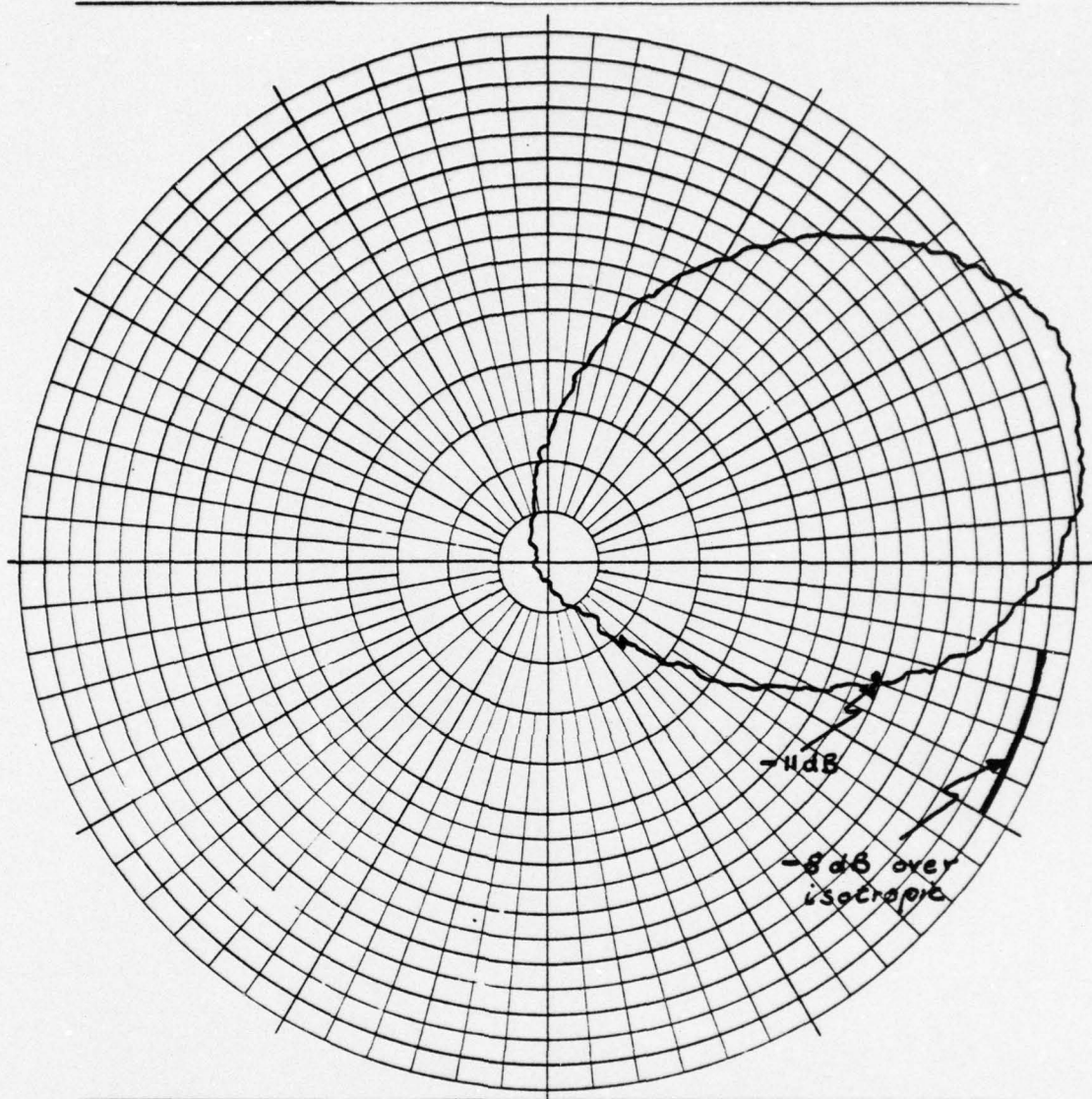


Figure 75 - HORIZONTAL PATTERN CONFIGURATION A

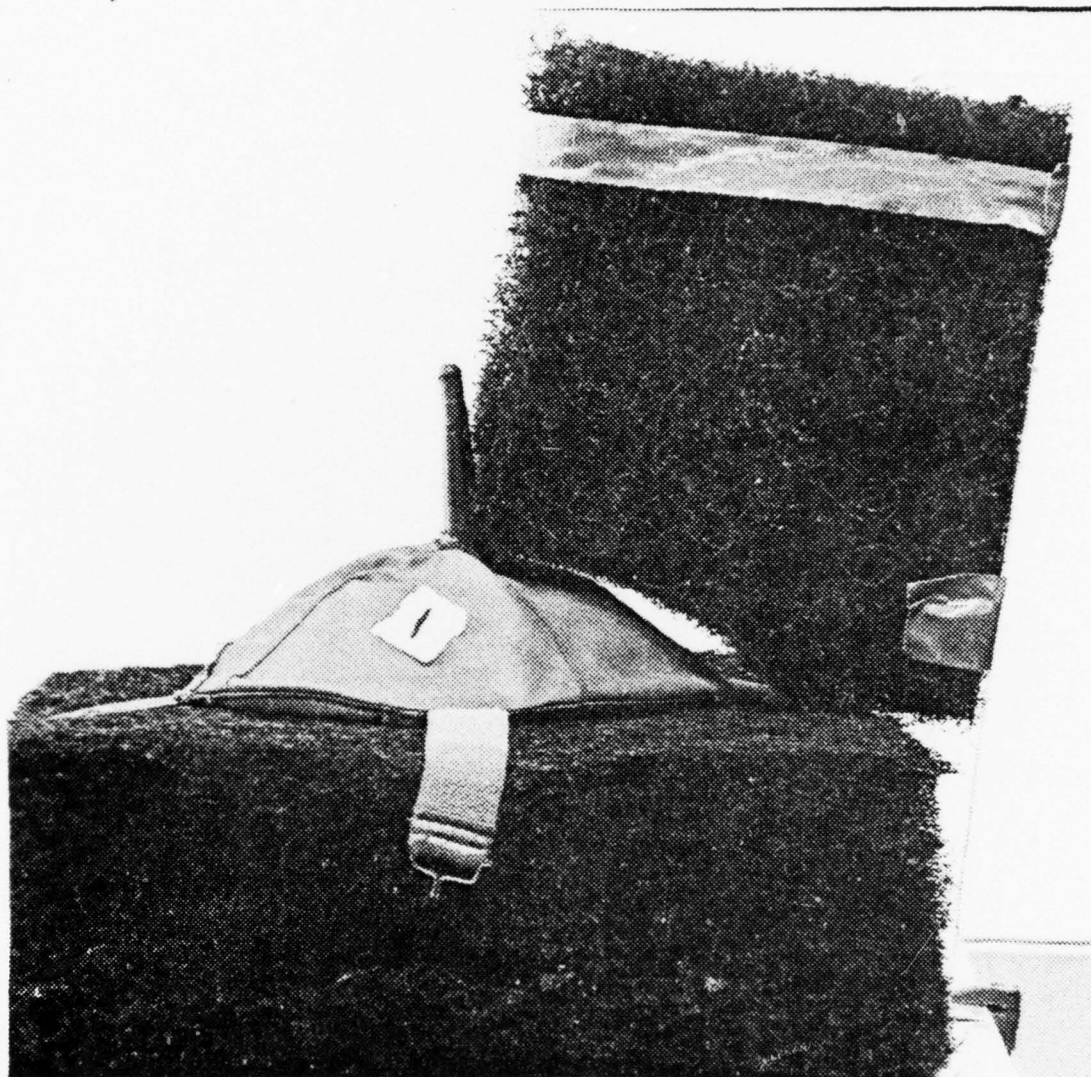


Figure 76 - FIELD CONFIGURATION B

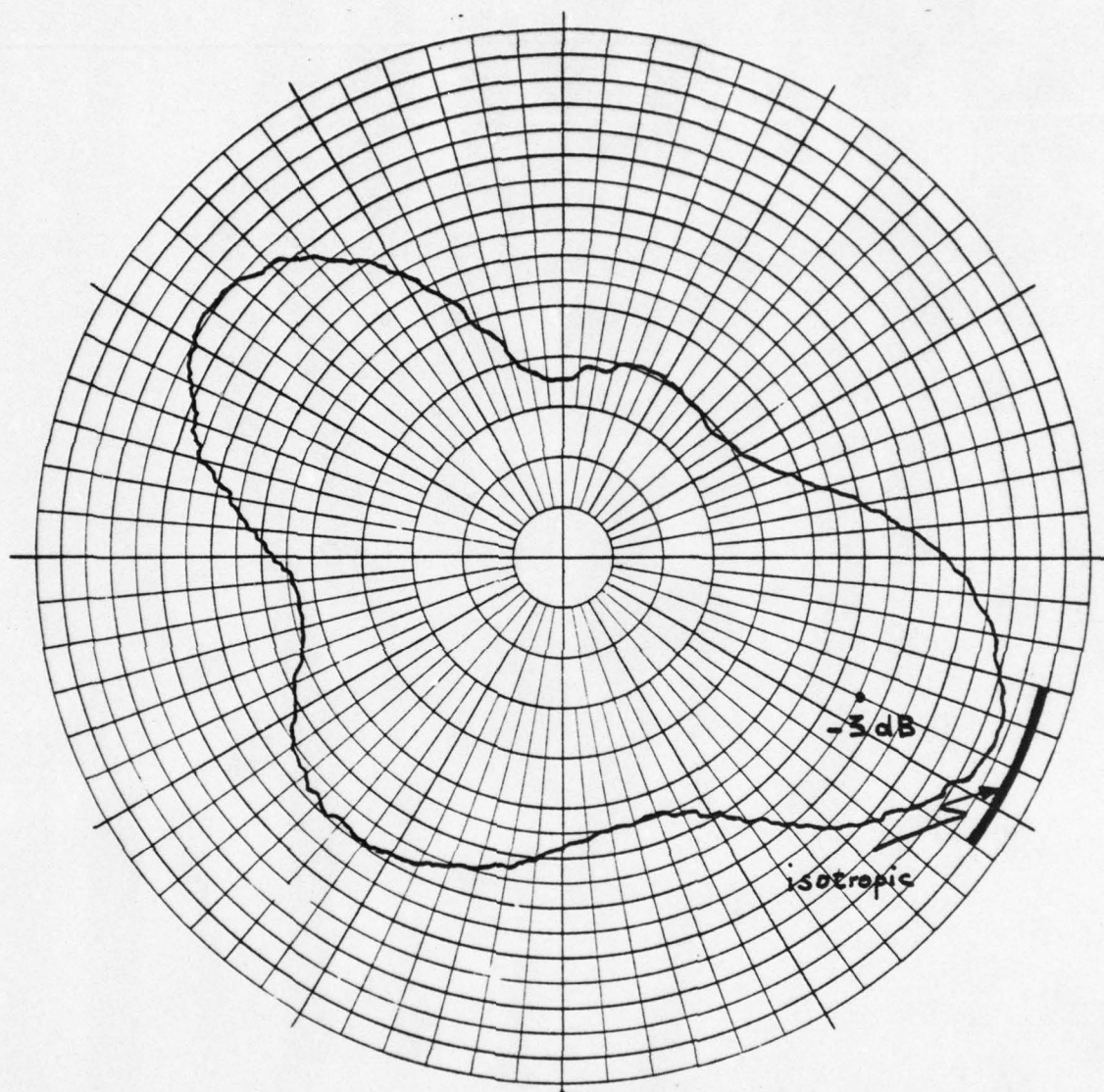


Figure 77 - HCRIZONTAL PATTERN CONFIGURATION E

APPENDIX F

FIELD TESTS

The first series of tests used the A station site J05 near the Ft. Hunter Ligett airfield. The three B unit locations are shown in Figure 23.

Field Tests A1B1, A1B2 and A1B3 (Range mode) The objective of these experiments was to become familiar with the intended measurement procedures for the field. It was expected to determine additional requirements and to report abnormal results. The test setup used was the standard AB configuration of Figure 21.

In test A1B1 the B unit was at a distance of about 270 meters from the A station. Since reflecting objects were located at a large distance from either the A station or the B unit, it was expected that the direct-path signal would be dominant. The data collected and significant signal waveforms are shown in Table F-1 and Figures 78-82. The range pulse transmitted from the A station was checked frequently and showed no distortion, Figure 78. After about two hours of operation the B unit responded only intermittently to interrogations from the A station. The ambient temperature had climbed to about 40°C.

Figure 79 shows a returning waveform detected at the A station, which was determined to be IF noise. Since any video detected RF carrier showed IF leakage, Figures 81 and 82, it was concluded that this waveform represented either a

very low power signal or one which was off center frequency due to alignment fluctuations caused by high temperatures. The A station ranged on these signals at random resulting in wild range readings as shown in Figures 79 and 80. Since these wild ranges occurred at antenna configuration B, elevation 72 inches, it was concluded that in addition to the reasons indicated above, antenna gain reductions might have caused power loss also. Range pulse waveforms for good range results are shown in Figures 81 and 82. Only slight envelope variations could be observed at different antenna configurations not affecting the leading edge of a range pulse.

Experiment A1B2 was performed to compare the results in A1B1 against another B unit, set up for test purposes at a known distance. This test B unit responded during 30 interrogations with a good return range pulse. A typical range pulse is shown in Figure 83. Envelope variations did not affect the leading edge in any of the observed cases.

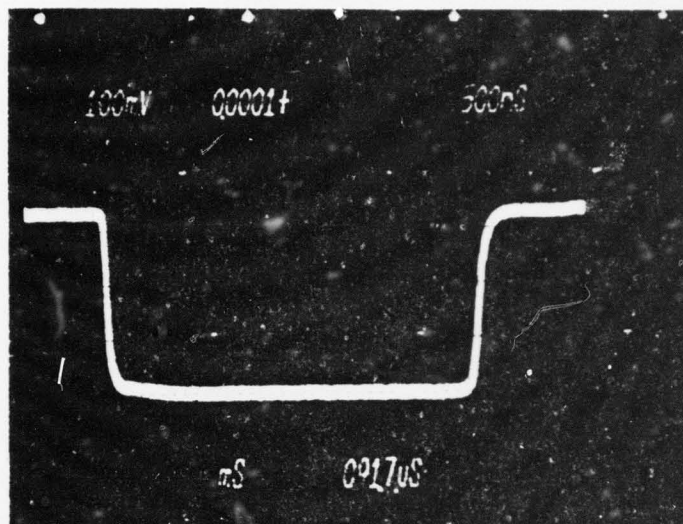


Figure 78 - A STATION TRANSMITTED RANGE PULSE

For experiment A1B3 the B unit used in A1B1 was located about 800 meters away against gentle rolling hills. For this deployment multipath propagation could occur. The objective was to determine whether due to the short range in A1B1 the B unit might have been in an A station antenna null, which effects would have been more serious at antenna configuration B. At this time however the B unit failed to respond at all. Since another B unit was not readily available the experiment had to be postponed to the next day. The B unit was checked out later using the single path simulation test setup. It was found that the B unit responded only over a path attenuation range from 30 dB to about 65 dB.

The next day experiment A1B3 was continued with a different B unit using only a time period from 6 am to 10 am, while the ambient temperatures were relatively low. The acquired data for experiment A1B3 are shown in Table F-2. Figure 84 shows a typical range pulse return. All range readings were acceptable. Slight range pulse envelope variations did not affect the leading edge of the range pulse, as shown in Figures 84 and 85.

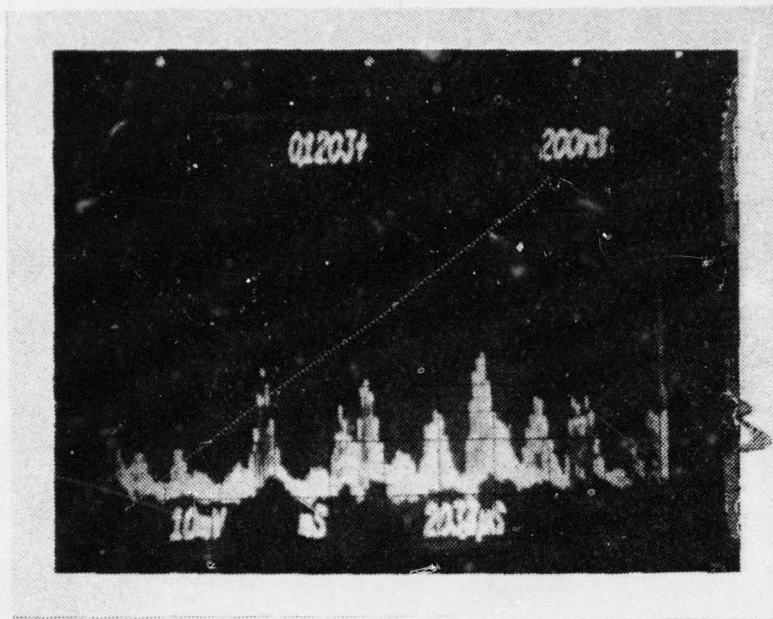


Figure 79 - SIGNAL AT THE A STAON SHOWING IF NOISE
SLANT RANGE INDICATED 2 M

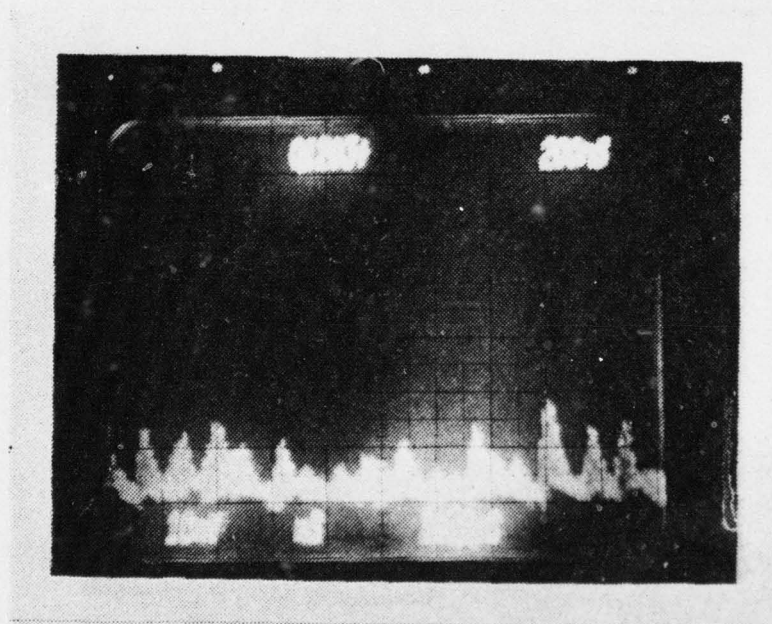


Figure 80 - SIGNAL AT THE A STATITION SHOWING IF NOISE
SLANT RANGE INDICATED 4190 M

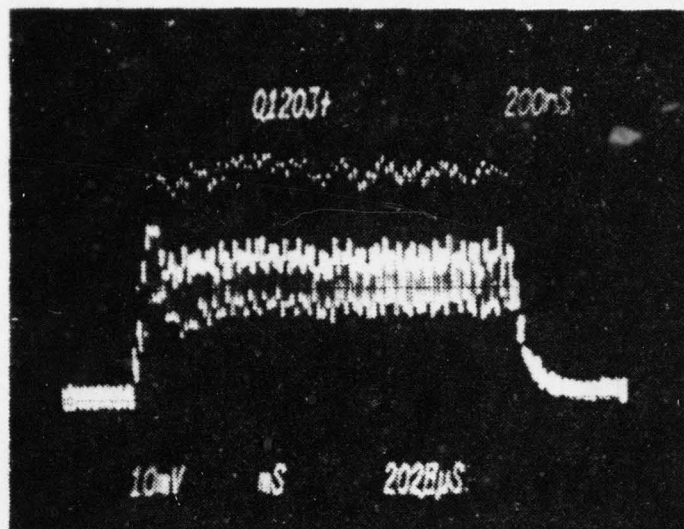


Figure 81 - RANGE PULSE DETECTED AT THE A STATION
ANTENNA CONFIGURATION A-36 INCHES, RANGE 266 M

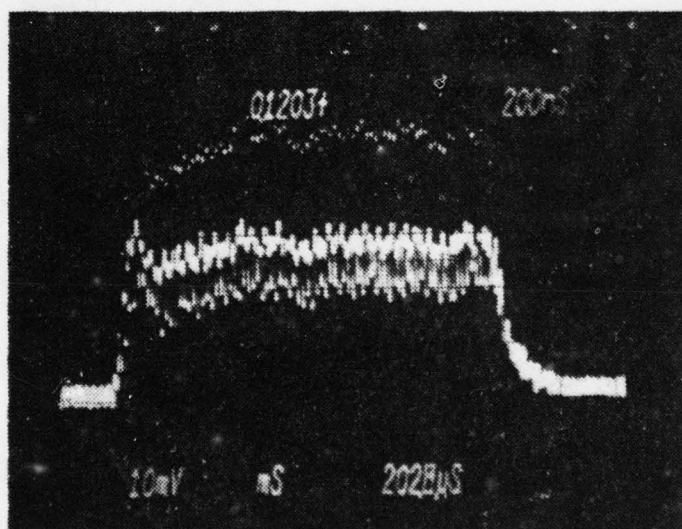


Figure 82 - RANGE PULSE DETECTED AT THE A STATION
ANTIENNA CONFIGURATION C-72 INCHES, RANGE 270 M

During experiments A1B1 to A1B3 the following general observations were made: The B unit I/O device failed, when SCOM mode experiments were attempted. Without the I/O device connected the B unit represented insufficient load to the batteries. The B unit had to be connected to a regulated DC power supply, fed by an AC generator.

From these initial familiarization experiments it was concluded that

1. More B units had to be made available to extend total test time.
2. Tests had to be conducted during low ambient field temperature periods to avoid B unit failures.
3. Further investigations were required to determine why the B unit failed after a relatively short time of operation in a high temperature environment, while it had worked for the entire laboratory experiment phase.

Table F-1 RANGE MODE DATA FOR TEST A1B1

B-UNIT ANTENNA CONFIGURATION	72 INCHES		ANTENNA HEIGHT ABOVE GROUND	36 INCHES		18 INCHES
A	264	264		264		264
	262	260		264		266
	262	262		266		264
	260	260		262		264
	262	262		266		266
B	266	264			270	266
	264	8190		266		264
	264	2		264		270
	124	264		266		268
	264	62		266		266
C	264	270		266		266
	264	266		264		264
	266	264		266		264
	264	266		264		266
	264	264		262		264

Table F-2 RANGE MODE DATA FOR TEST A1B3

B-UNIT ANTENNA CONFIGURATION	ANTENNA HEIGHT ABOVE GROUND		
	72 INCHES	36 INCHES	18 INCHES
A	810 812	814	812
	812 812	814	802
	812 814	812	808
	812 812	818	804
	812 808	808	802
B	810 808	810	810
	808 810	810	804
	808 808	810	804
	808 810	812	802
	808 810	814	806
C	808 804	806	806
	810 806	804	800
	806 808	804	802
	804 806	800	810
	808 808	804	800

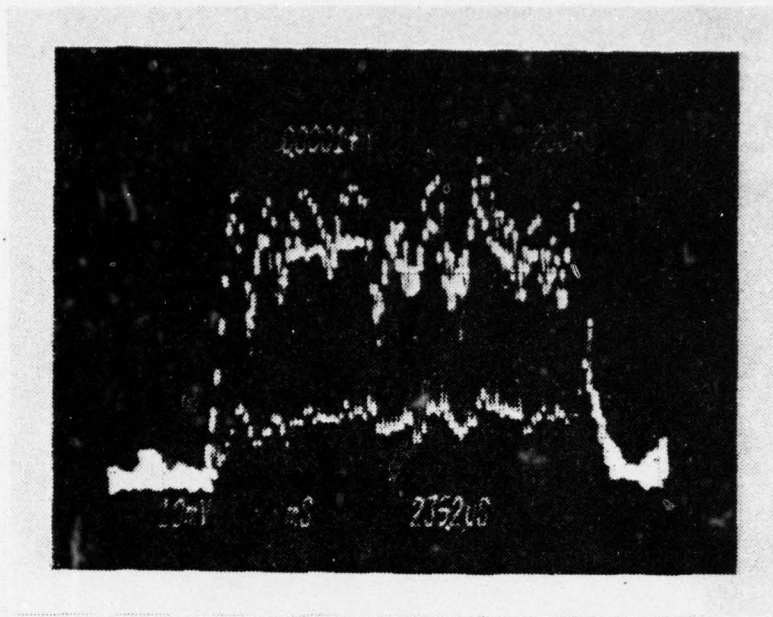


Figure 83 - RANGE PULSE DETECTED AT THE A STATION
ANTENNA CONFIGURATION C-72 INCHES, RANGE 4958 M

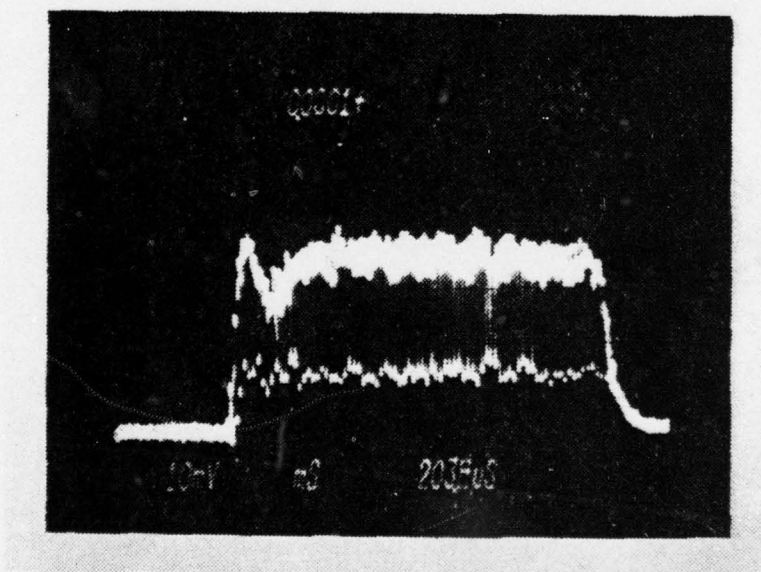


Figure 84 - RANGE PULSE DETECTED AT THE A STATION
ANTENNA CONFIGURATION C-72 INCHES, RANGE 808 M

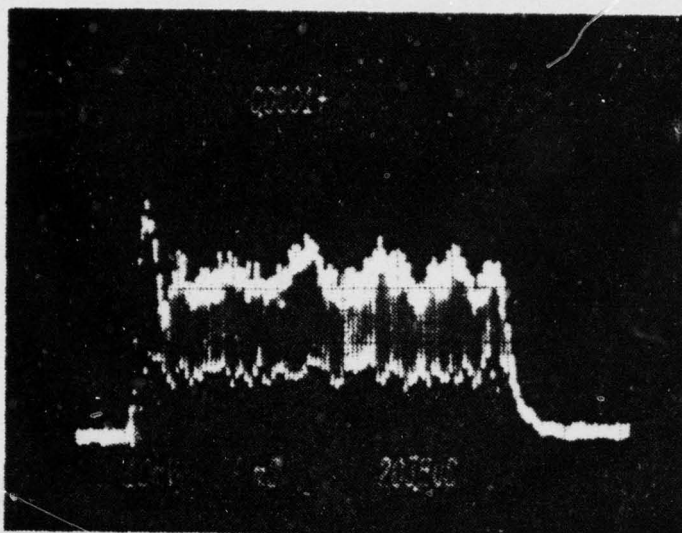


Figure 85 - RANGE PULSE DETECTED AT THE A STATION
ANTENNA CONFIGURATION A-18 INCHES, RANGE 808 M

Field Test A3B1

Field test A3B1 was performed at Camp Roberts Military Reservation. The standard AB test setup was used to find out whether a stable RF link could be established. A station and B unit locations are shown in Figure 25.

Using all three B unit antenna configurations and two pretested helmet antennas as well as one highly directional circularly polarized Helix antenna, the following results were obtained: The B unit with helmet antenna unshielded responded steadily for about 45 minutes. Then it started to respond intermittently. Varying the antenna height, the configuration as well as the position within a wavelength did not improve the response. Using the helix antenna (9 dB gain over isotropic) regained steady responses for about 10 minutes. Finally after about 2 hours the B unit failed to respond at all. A hard wired single-path simulation verified that the B unit receiver sensitivity had degraded. Steady responses could be obtained only from 30 to 65 dB of path attenuation. The following conclusions were drawn:

1. The B units checked out and aligned by maintenance personnel at Ft. Hunter Liggett generally decayed in receiver sensitivity after a short time of continuous operation at field temperatures between 25 and 45°C.
2. They decayed slowly or rapidly depending upon the particular B unit. In this experiment as well as in test A1B4 the sensitivity reduction could be balanced using higher gain antennas.
3. A spuriously responding B unit turned off may recover for a short time as observed during the single-path test following test A2B4.
4. Laboratory temperature sensitivity tests had to be done to investigate whether amplifier circuit breakdown or RF center frequency drift was causing this sensitivity

degradation.

5. The B unit found decaying in receiver sensitivity using the standard single-path test were returned to the maintenance facility. There they checked out to operate according to specifications. Therefore a comparison test had to be made between checkout procedures. The results of the temperature and checkout comparison tests are given in Appendices G and H.

Field Tests A2B1, A2B2, A2B3, A1B3 and B1A1

The objective of the first three of this second series of experiments was to investigate RF link signal waveforms in an environment likely for multipath propagation. The test setup was the same as described in test A1B1. This time however a preliminary 'room test' was performed to ensure proper A station and B unit operation. At room temperature it was found, that the two B units #220 and #234 operated satisfactorily, over a path attenuation range from 65 dB to about 105 dB. A new A station was used in this test, #027, and it displayed the same IF leakage in the video detected range pulse waveforms, for which the other A station had been exchanged. Since this IF ripple did not affect the range pulse leading edge it was accepted as a system feature. Further investigations into the detector circuitry were not attempted.

A station site E20 was chosen for the subsequent field tests. Its location and those for the B units are shown in Figure 24. Although for A2B1 and A2B2 the distances from the A station to the B unit were well within the system coverage not a single B unit response could be obtained for both units. At this time it was not clearly understood why the RF link was working so badly. Therefore the objective of the test was changed into a continuing hardware reliability investigation. Since broken B unit antenna elements as well as bad cables and connectors could have caused a RF link failure those components were interchanged frequently without any improvement. Parallel to this the A station power output and signal waveform were checked and compared with the specifications. No malfunctions of the A station could be detected.

In test A2B3 the B unit was moved as close as 300 meters to the A station. The objective was to determine whether

the B unit performance depended on the AB separation, which would have explained a similar receiver sensitivity degradation found during test A1B1. At this short distance the B unit responded spuriously to about every 50th interrogation regardless of antenna configuration. Figure 86 shows the transmitted range pulse from the A station, Figure 87 a 'no B response' signal cycle and Figure 88 one of the few but accurate range pulse return waveforms.

The next experiment, B1A1, was conducted at the A station site J05, used earlier, for two reasons. It was desired to observe the received range pulse at the B unit under spurious response conditions. At that time only one AC generator was available to be used at the B unit location for the BA arrangement. Only site J05 provided an AC outlet to power the B unit checkout set and the A station itself. Also, it was known from earlier tests, that the A station antenna at J05 was working properly, such that the malfunctioning AB link could be related to the B unit. The test was set up using the standard BA arrangement. The B unit location was the same as in test A1B1. At this close range B unit 234 responded spuriously for all antenna configurations to every 50th interrogation. Address and range pulses were detected at a very low RF carrier level such that noise spikes could distort both waveforms. Figure 89 shows a received B unit address sample with almost no RF carrier level. The high amplitude noise spike had passed the video filter and might have changed an address bit such that the B unit could not respond. Figure 90 shows a severe distortion of the envelope of a low signal range pulse. Since the signal level was so low, the AGC was set to its maximum gain such that slight envelope variations as observed earlier had a very pronounced effect. Since the A station and its antenna were tested to operate properly by interrogating the test B unit, the malfunction could be limited to either the RF path, the B unit antenna or the B

unit itself. It was therefore logical to exclude both the RF path and the antenna and use the single-path simulation arrangement for further B unit sensitivity tests. The waveforms observed at the B unit video detector agreed in distortion with those observed in the field. Moreover, the B unit receiver sensitivity had degraded such that it responded only between 30 dB and 60 dB of path attenuation.

From the first series of tests it was expected that B unit receiver sensitivity would decay with increasing operating time and increasing ambient temperature. It was not understood why both units started to fail immediately in the field. Both units were turned in for an operational check and realignment. It was decided to continue the hardware reliability tests in order to find out whether these results applied to a large number of available B units.

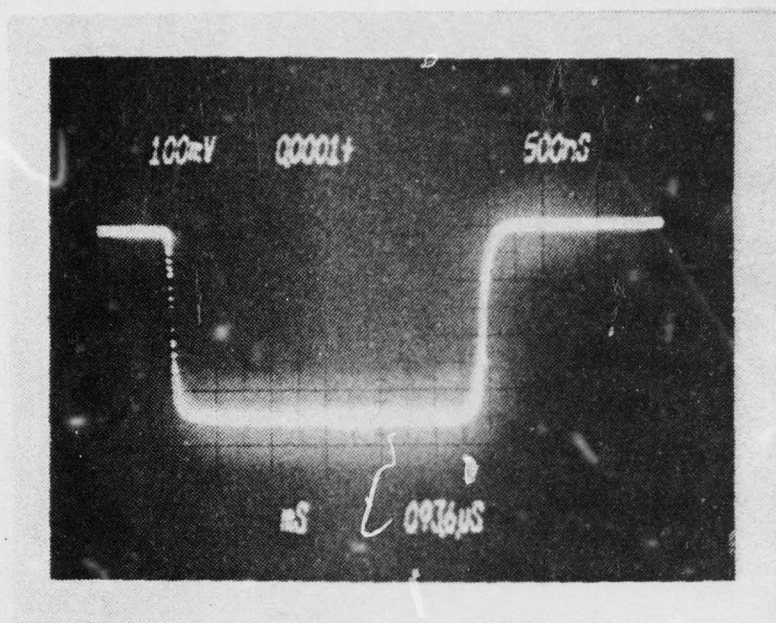


Figure 86 - A STATION TRANSMITTED RANGE PULSE

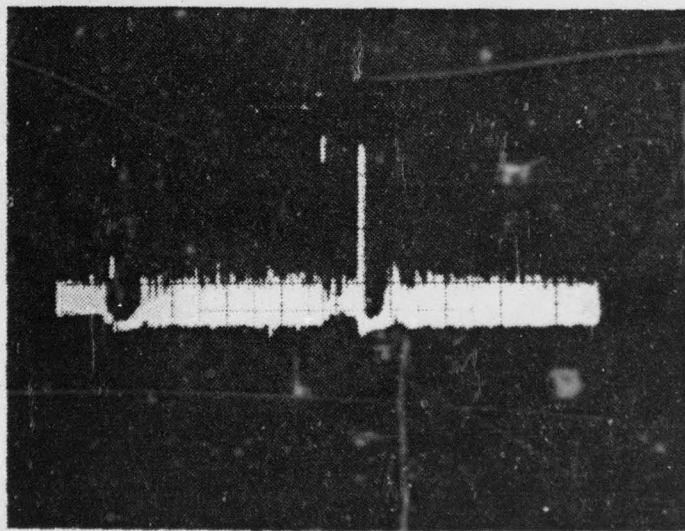


Figure 87 - RANGE MODE WAVEFORM, NO E RESPONSE

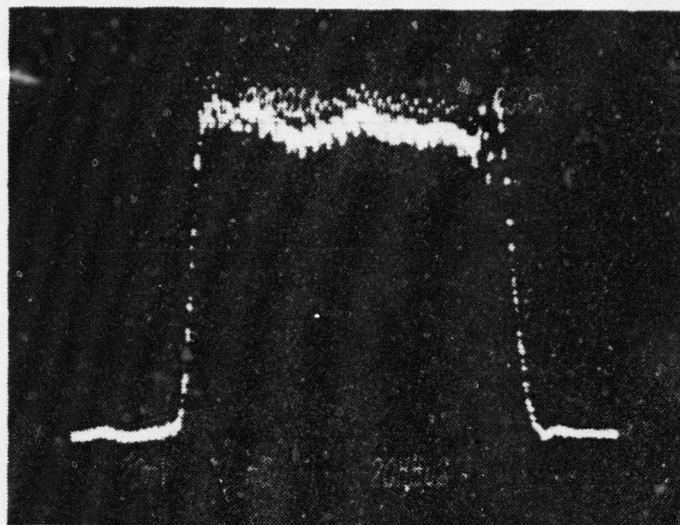


Figure 88 - RANGE PULSE DETECTED AT THE A STATION
ANTENNA CONFIGURATION C-18 INCHES, RANGE 312 M

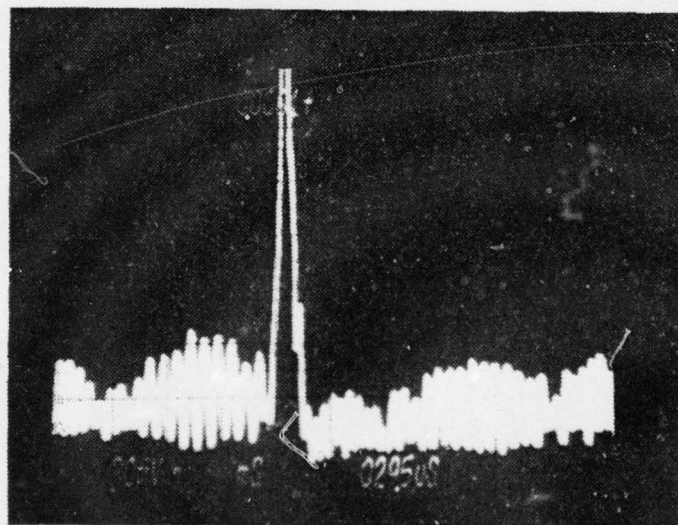


Figure 89 - DATA BITS DETECTED AT THE B UNIT
RANGE MODE, NO B RESPONSE

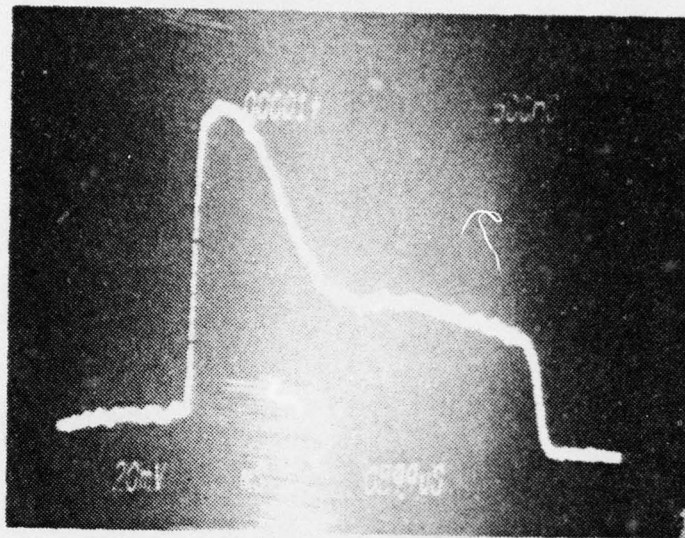


Figure 90 - RANGE PULSE DETECTED AT THE B UNIT

Field Tests A2B4 and A1B4

These tests were a continuation of tests A2B1-A2B3. The objective was to find out whether the results from the last tests could be duplicated, using a different E unit (#231) and different antennas and antenna cables. The E unit location was the same as that used for test A2B1.

The B unit responded intermittently in all three antenna configurations where the number of responses decreased from about one out of five to about one out of 50 interrogations after 45 minutes of operation. Since a steady response was received from the test B unit, B unit 231 was taken to the A station site and tested for receiver sensitivity. The standard single-path setup was used. The results were surprising since it responded over the specified range of path attenuation from 65 dB to 115 dB. Therefore, it was assumed that the antennas and antenna cables were malfunctioning. This assumption was confirmed when the number of responses could be varied significantly just by twisting the antenna and/or antenna cable. The A station and the B unit were again tested using the standard single-path setup. No malfunctions occurred.

In test A1B5 the B unit was set up at the location used for test A1B1. The objective was to observe any change in the RF link quality using an ordinary halfwave dipole E unit antenna. The test had to be interrupted, since no shielding had been designed for the dipole antenna. The results of this experiment added another variable to the problem of RF link breakdown to those found earlier. It was decided to try another series of experiments using the same E unit (#231) with a pretested antenna and antenna cables.

Field Tests A3B2, A3B3, A3B4, B1A3 and B2A3

This final series of field tests was performed at Camp Roberts Military Reservation. The area actually used is shown in Figure 25. The overall objective was to observe multipath distortion effects on the shape of the range pulse received at the A station or the B unit. Equipment limitations restricted the observations to either the A station or the B unit. Therefore, it was intended after having observed the range pulse distortions at the A station to show whether similar distortions occurred under the same conditions at the B unit. Additionally, the transmitted range pulse from the B unit to the A station had to be monitored to show that previously observed distortions were not caused by a malfunctioning B unit. Both experimental arrangements, AB and BA, promised valid results, since the system hardware problems had been solved, thus establishing a reliable RF link.

In experiment A3B2 B unit #237 was located at a range of approximately 500 meters against rolling hills. For this distance and the A station antenna height above the B unit, it was expected that the B unit would be within the A station antenna main beam. After the initialization tests, range data was collected at various heights and B unit antenna configurations as described in section IV. The data is presented in Table F-3.

Shielding the helmet antenna backlobes resulted in accurate range data and undistorted range pulse waveforms. One time of arrival error was observed at 18 inches as shown in Figure 91. The time difference with respect to an accurate range pulse, shown in Figure 92, agreed with the range error. Similar results were obtained when blocking the direct path. The gain reduction in the forward direction was not sufficient to cause the reflected signal

to be dominant. The effects of the reflected signals being relatively stronger than in configuration A could be observed as envelope fluctuations as shown in Figures 93 and 94. The leading edges were not affected.

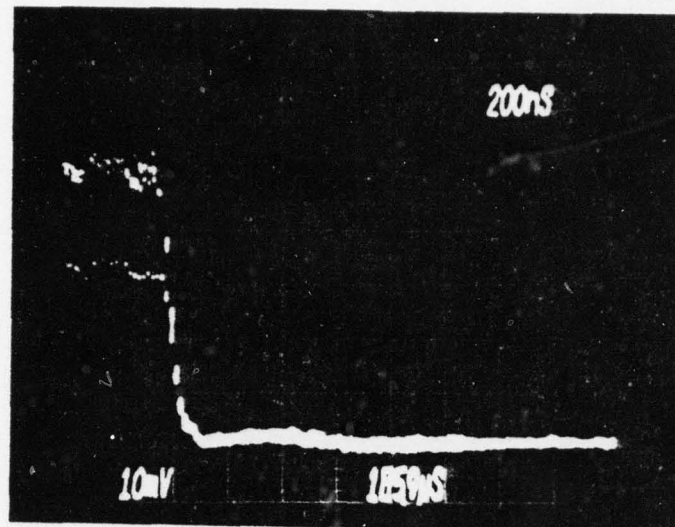


Figure 91 - RANGE PULSE DETECTED AT THE A STATION
ANTENNA CONFIGURATION A-18 INCHES, RANGE 288 M

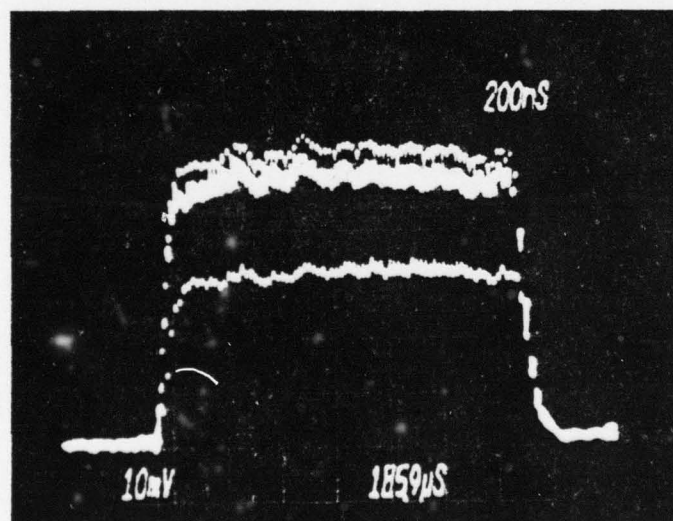


Figure 92 - RANGE PULSE DETECTED AT THE A STATION
ANTENNA CONFIGURATION A-36 INCHES, RANGE 506 M

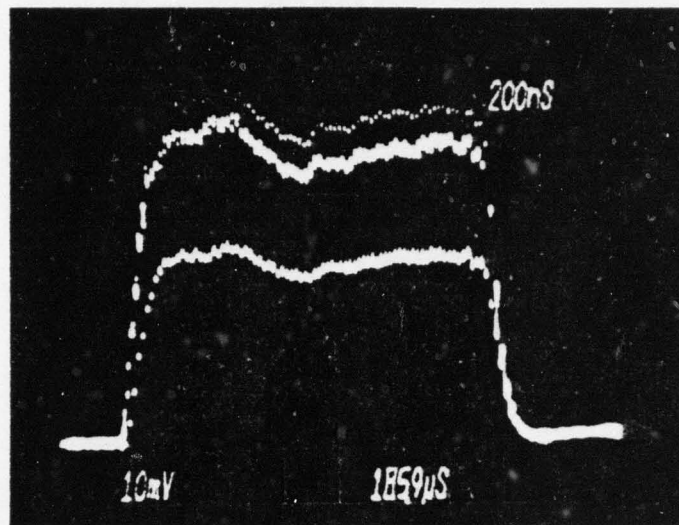


Figure 93 - RANGE PULSE DETECTED AT THE A STATION
ANTENNA CONFIGURATION B-72 INCHES, RANGE 510 M

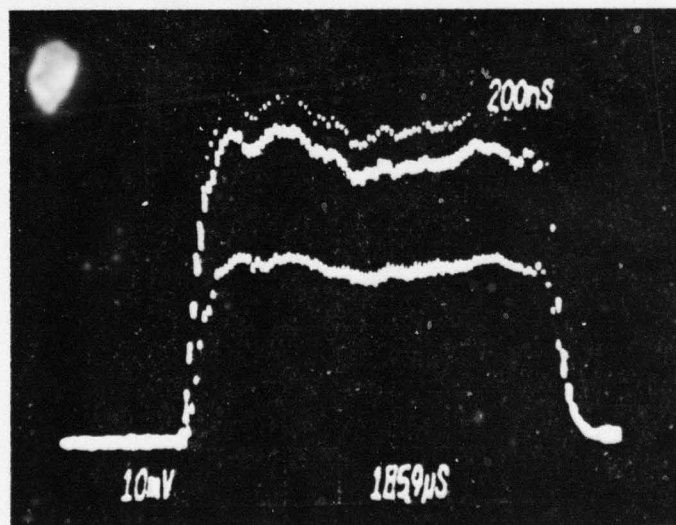


Figure 94 - RANGE PULSE DETECTED AT THE A STATION
ANTENNA CONFIGURATION B-36 INCHES, RANGE 504 M

Table F-3 RANGE MODE DATA FOR TEST A3B2

B-UNIT ANTENNA CONFIGURATION	ANTENNA HEIGHT ABOVE GROUND		
	72 INCHES	36 INCHES	18 INCHES
A	504	502	278
	502	504	504
	502	502	504
	500	500	502
	506	506	504
B	510	506	500
	504	504	502
	510	508	496
	506	506	504
	504	506	502
C	12	2	496
	498	492	502
	2044	2042	496
	58	42	496
	1994	2058	496

When allowing omnidirectional B unit antenna operation, severe multipath distortion occurred for antenna height 72 inches. Two such waveforms are presented in Figures 95 and 96. The distortions looked much like those obtained during the multipath simulation experiments. Table F-3 shows the resulting wild ranges, which could not be related to the time difference error caused by distortion of the leading edge. No range pulse distortion was observed at heights of 36 and 18 inches. Figure 97 is a picture of a sample range pulse with the helmet antenna set to 36 inches. It was demonstrated that the severe fading at antenna height 72 inches disappeared when the antenna location was changed slightly within a wavelength.

In experiment A3B3 B unit #237 was located at a range of approximately 4500 meters, against rolling hills. An automobile was located directly behind the B unit at a distance of about five meters to simulate the reflecting surface of a tank. The results of this test are given in Table F-4.

With the helmet antenna in configuration A, signal waveform distortion and no response messages were observed at an antenna height of 18 inches. This result was not clearly understood, although it could be related to reflected signals caused by multipath propagation within the relatively broad main beam of this configuration. Obviously data distortion occurred in some cases, such that no response messages were generated by the A station. Figure 98 shows a heavily distorted range pulse, where the leading edge seemed to be preserved, whereas the rest of the signal was significantly reduced in amplitude. Antenna configuration B resulted in good range pulse returns and accurate range readings.

When the direct and reflected paths were combined with configuration C, severe signal fading occurred. Figure 99 shows a distorted range pulse waveform, which still has a sharp leading edge. It was assumed that distortion of the data bits was so severe that the A station did not range on those pulses, thus the no B responses. Tests B1A3 and B2A3 showed later, that B unit #237 was operating to specifications, therefore, these results were not the result of a failing B unit. Using a different B unit for this antenna configuration produced similar results. Figure 100 shows a received range pulse from B unit #305. Comparing the constant IF leakage level to that of Figure 101, it can be seen, that the signal strength was very low. In the latter case, the data pulses were accepted by the A station, whereas it probably ranged on a noise spike occurring prior to the low signal level range pulse. The short range results are shown in Table F-5.

To obtain even more range pulse distortion, B unit #237 was moved in antenna configuration C-72 inches to another location until severe range pulse distortion was observed. Table F-6 presents the results. It was found that range pulse distortion resulting in wild ranges could be observed for all antenna configurations at 72 inches. For lower elevations, signal fading caused a constant 'no B response' result. Two distorted signal waveforms are shown in Figures 102 and 103.

Table F-4 RANGE MODE DATA FOR TEST A3B3

B-UNIT ANTENNA CONFIGURATION	ANTENNA HEIGHT ABOVE GROUND		
	72 INCHES	36 INCHES	18 INCHES
A	4448	4454	4270
	4448	4450	5706
	4448	4450	4450
	4448	4450	NR
	4448	4448	NR
B	4456	4454	4456
	4456	4456	4444
	4456	4452	4456
	4452	4456	4452
	4452	4452	4452
	5128	NR	NR
	NR	NR	NR
	NR	NR	NR
	NR	NR	NR
	NR	NR	NR

Table F-5 RANGE MODE DATA FOR TEST A3B3 (NEW B-UNIT)

B-UNIT ANTENNA CONFIGURATION	ANTENNA HEIGHT ABOVE GROUND		
	72 INCHES	36 INCHES	18 INCHES
C	352 252	352	352
	6 352	62	350
	356 352	352	98
	6 352	352	352
	782 352	352	350

Table F-6 RANGE MODE DATA FOR TEST A3B4

B-UNIT ANTENNA CONFIGURATION	ANTENNA HEIGHT ABOVE GROUND		
	72 INCHES	36 INCHES	18 INCHES
A	1022 2046	NR	NR
	876 862	NR	NR
	860 818	NR	NR
	846 632	NR	NR
	NR 132	NR	NR
B	348 1022	NR	NR
	348 350	NR	NR
	348 348	NR	NR
	346 348	NR	NR
	350 350	NR	NR
C	348 346	NR	NR
	350 344	NR	NR
	352 346	NR	NR
	348 352	NR	NR
	344 350	NR	NR

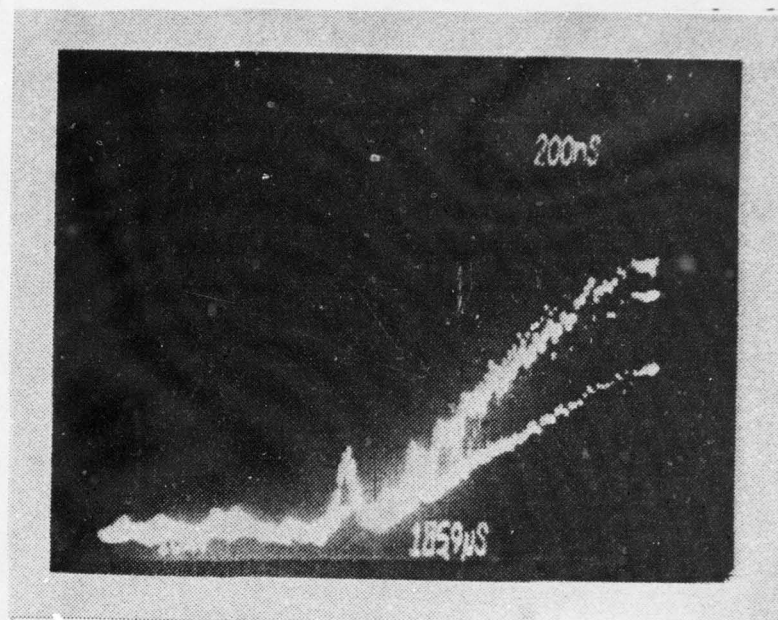


Figure 95 - RANGE PULSE DETECTED AT THE A STATION
ANTENNA CONFIGURATION C-72 INCHES, RANGE 42 M

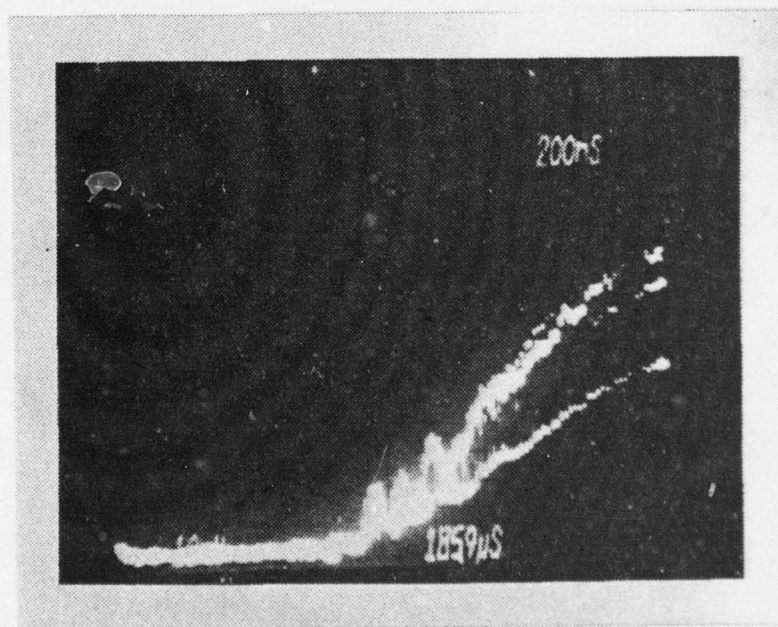


Figure 96 - RANGE PULSE DETECTED AT THE A STATION
ANTENNA CONFIGURATION C-72 INCHES, RANGE 2044 M

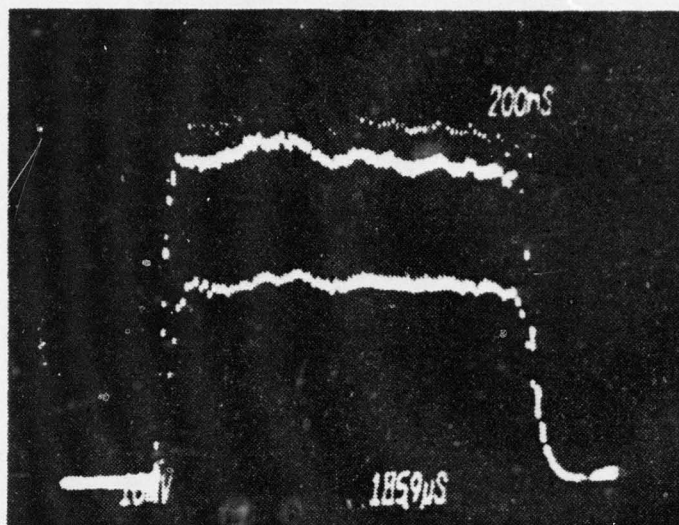


Figure 97 - RANGE PULSE DETECTED AT THE A STATION
ANTENNA CONFIGURATION C-36 INCHES, RANGE 504 M

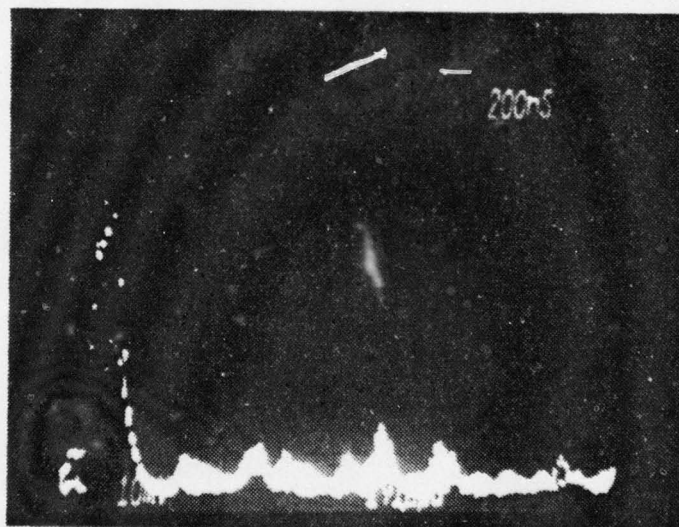


Figure 98 - RANGE PULSE DETECTED AT THE A STATION
ANTENNA CONFIGURATION A-18 INCHES, RANGE 4270 M

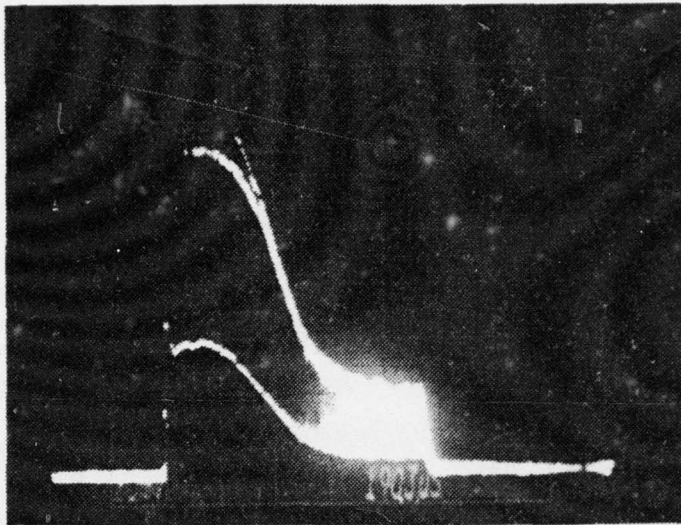


Figure 99 - RANGE PULSE DETECTED AT THE A STATION
ANTENNA CONFIGURATION C-72 INCHES, NO RESPONSE

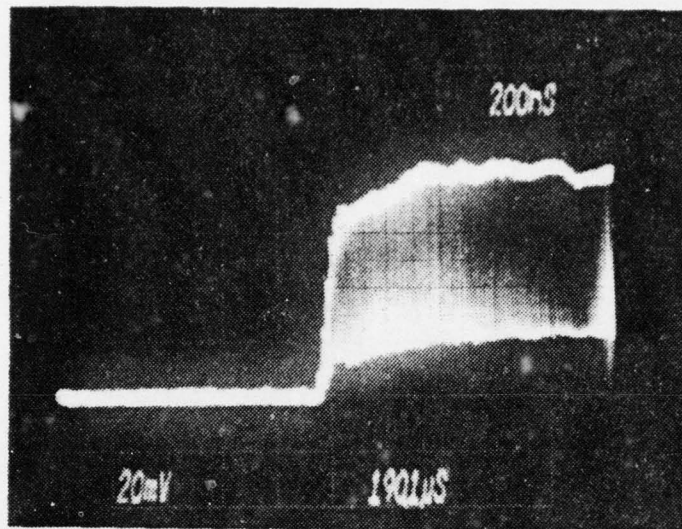


Figure 100 - RANGE PULSE DETECTED AT THE A STATION
ANTENNA CONFIGURATION C-72 INCHES, RANGE 352 M

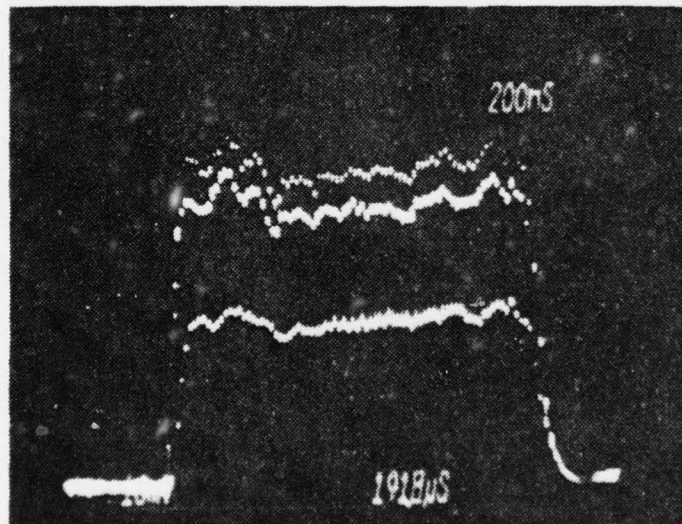


Figure 101 - RANGE PULSE DETECTED AT THE A STATION
ANTENNA CONFIGURATION A-36 INCHES, RANGE 4450 M

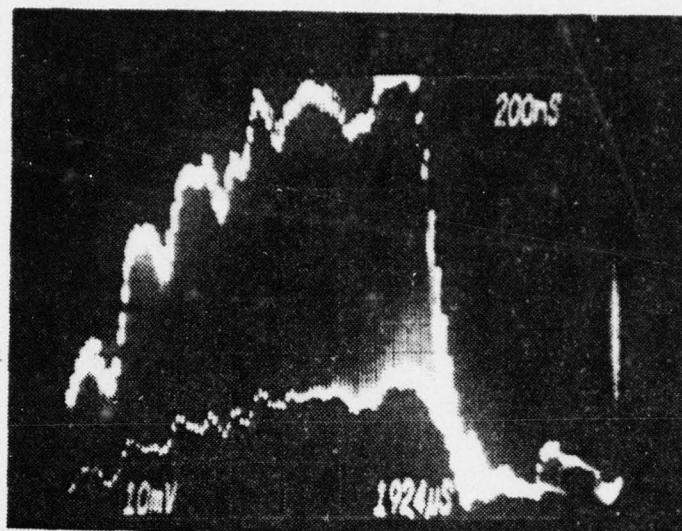


Figure 102 - RANGE PULSE DETECTED AT THE A STATION
ANTENNA CONFIGURATION C-72 INCHES, RANGE 846 M

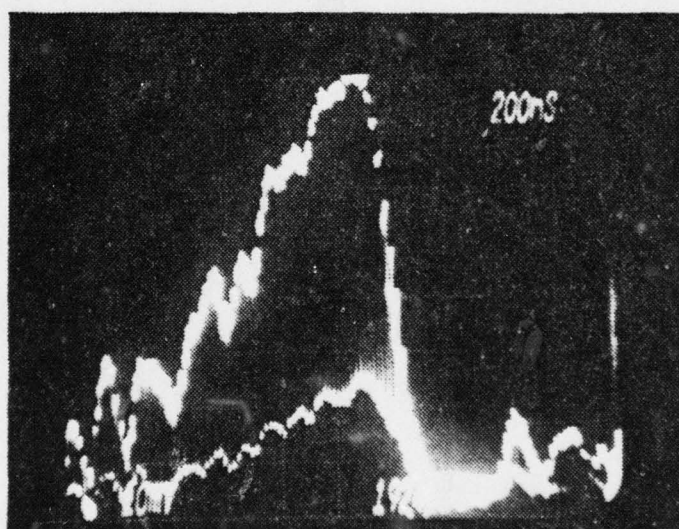


Figure 103 - RANGE PULSE DETECTED AT THE A STATION
ANTENNA CONFIGURATION A-72 INCHES, RANGE 1022 M

Field test B1A3 resembles test A3B2 with B unit #237 being located about 500 meters away from the A station. The data that was obtained is shown in Table F-7. No range errors were observed at any of the antenna configurations including configuration C-72 inches, where range errors had occurred in test A3B2. However no attempts were made to move the helmet antenna into a position to cause fading. The radio communication link between operators had broken down, so there was no way for the B unit operator to know that moves should be made.

It could be clearly shown, that B unit #237 transmitted a clean range pulse at the specified power level and that no multipath fading occurred at the B unit location. This agreed with the theoretical assumption that for non planar reflectors multipath propagation from A to B is a nonreciprocal phenomenon. Figures 104 and 105 show a typical range pulse received at and transmitted by the B unit. Therefore, the observed range pulse distortion in test A3B2 could be clearly related to multipath fading at the A station antenna.

Field test B2A3 resembled test A3B4 with B unit #237 located about 4500 meters away from the A station. The data obtained is shown in Table F-8. In agreement with test A3B4 short ranges of response messages were obtained for all antenna configurations. It was assumed that similar range pulse distortion occurred at the A station as observed in test A3B4. The received range pulses as well as those transmitted by the B unit were never significantly distorted. Typical transmitted and received range pulses are shown in Figures 106 and 107. As pointed out in the results of test B1A3, no critical multipath distortion occurred at the B unit, which operated within specifications for over five hours in the field.

Table F-7 RANGE MODE DATA FOR TEST B1A3

B-UNIT ANTENNA CONFIGURATION	ANTENNA HEIGHT ABOVE GROUND		
	72 INCHES	36 INCHES	18 INCHES
A	506 508	504	508
	506 510	504	508
	506 506	510	506
	506 504	500	508
	506 508	510	506
B	510 512	508	510
	514 510	508	510
	510 514	508	508
	508 510	508	506
	510 514	508	508
C	508 506	506	508
	512 506	506	508
	506 506	504	508
	502 502	510	508
	506 504	504	504

Table F-8 RANGE MODE DATA FOR TEST B2A3

B-UNIT ANTENNA CONFIGURATION	ANTENNA HEIGHT ABOVE GROUND		18 INCHES	NO RESPONSE (NR)
	72 INCHES	36 INCHES		
A	350 352	928		
	352 352	984		
	354 352	976		
	140 164	936		
	198 244	952		
B	342 358	NR		358
	352 352	362		358
	354 354	356		356
	352 352	362		356
	352 354	NR		356
C	352 354	362		358
	354 354	358		352
	352 352	358		358
	352 352	356		356
	354 350	356		358

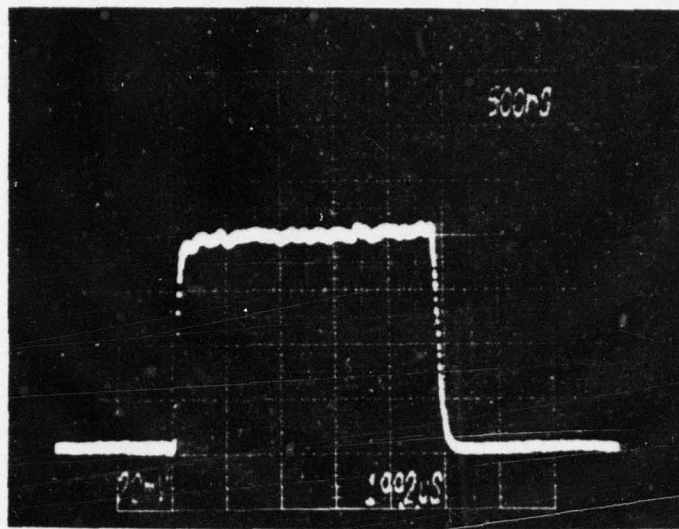


Figure 104 - B UNIT TRANSMITTED RANGE PULSE
ANTENNA CONFIGURATION C-72 INCHES

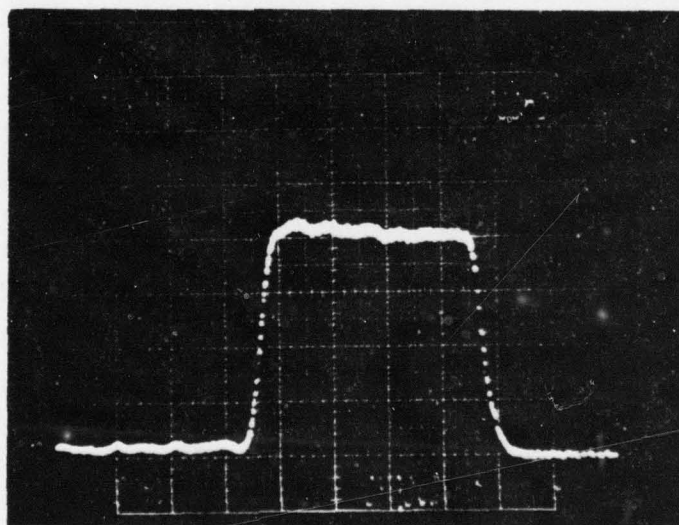


Figure 105 - RANGE PULSE DETECTED AT THE B UNIT
ANTENNA CONFIGURATION C-72 INCHES

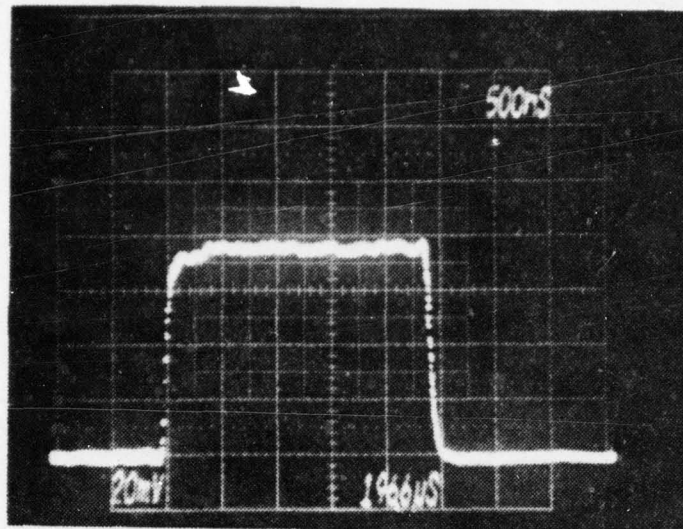


Figure 106 - B UNIT TRANSMITTED RANGE PULSE
ANTENNA CONFIGURATION C-72 INCHES

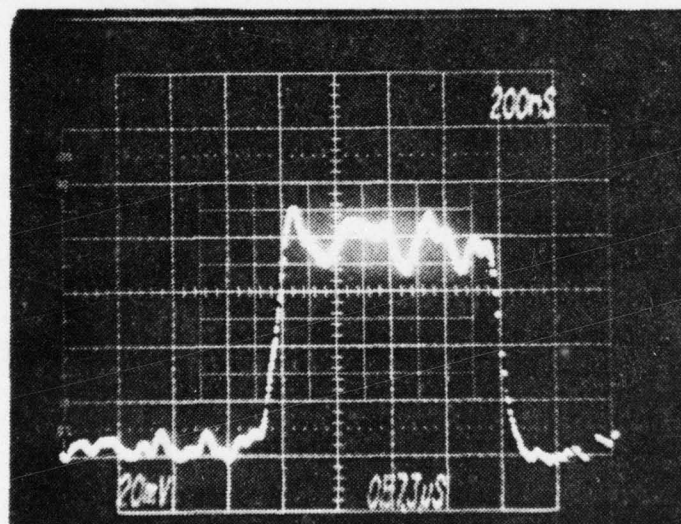


Figure 107 - RANGE PULSE DETECTED AT THE B UNIT
ANTENNA CONFIGURATION C-72 INCHES

APPENDIX G

A STATION/B UNIT TEMPERATURE TESTS

E Unit Receiver Sensitivity Test

It had become apparent during the RMS reliability field tests that B units which had worked properly at room temperature degraded in receiver sensitivity rapidly at higher field temperatures. This decay in receiver sensitivity shortened the usable interrogation range drastically. The objective of these experiments was to simulate a high ambient temperature environment for the B unit and test its performance against that at room temperature.

The experimental procedure consisted of three phases. First the B unit was continuously interrogated in the Range mode for about one hour at room temperature. Then, the B unit was put into a high ambient temperature box. There it was again continuously interrogated in the Range mode for almost an hour or until it failed to respond. Finally, after the B unit had completely cooled off, phase one and phase two of the test were repeated for recovery check. Periodically during each phase of the test the following characteristics were recorded.

- Room temperature (Room)
- Case temperature of the B unit (Case)
- Ambient temperature of chamber (Chamber)
- Maximum path attenuation with steady response (High)

- Minimum path attenuation above receiver saturation (Low)
- B unit average power out (B)
- A station average power out (A)

The experimental setup was the same as that used for the single path tests. In addition, a temperature control and measurement arrangement was used as shown in Figure 108. Two B units (#s 267 and 305) were tested. The results are tabulated in Tables G-1 through G-4. B unit 305 was tested only at room temperature since it had not recovered from a previous failure in the field.

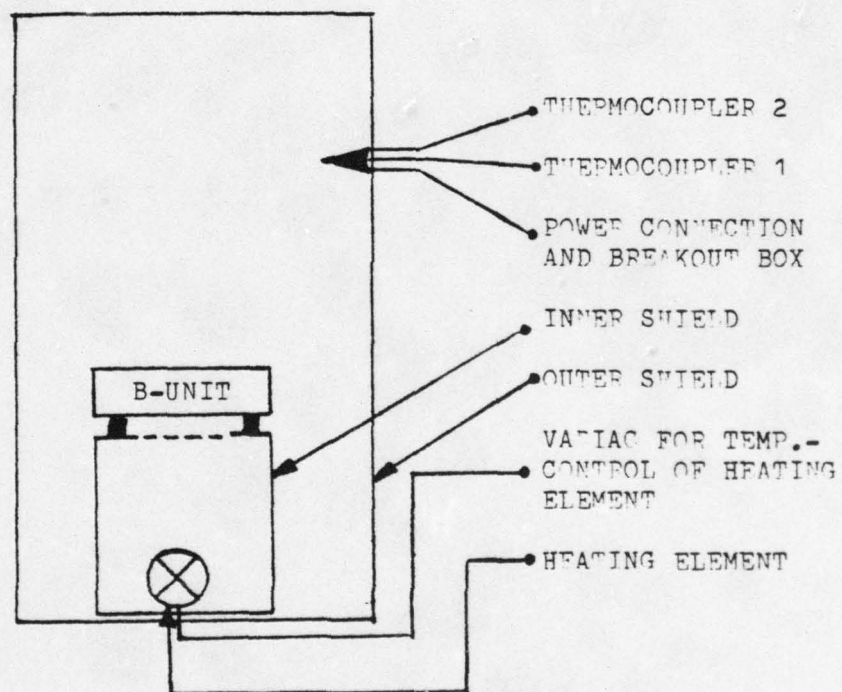


Figure 108 - B UNIT AMBIENT TEMPERATURE CONTROL ARRANGEMENT

Table G-1 TEMPERATURE SENSITIVITY TEST

TIME	TEMPERATURES (C)			B-UNIT SENSITIVITY (DB)		POWER OUT (DBM)	
	ROOM	CASE	CHAMBER	LOW	HIGH	A	B
1050	19	19	-	30	105	14.5	8
1055	19	23	-	30	99	14.5	8
1105	19	26	-	30	99	14.5	8
1115	19	29	-	30	99	14.5	8
1120	19	32	-	30	99	14.5	8
1130	19	34	-	30	99	14.5	8
1140	19	35	-	30	99	14.5	8
1145	19	36	-	30	99	14.5	8
1150	19	36	-	30	99	14.5	8

Table G-2 TEMPERATURE SENSITIVITY TEST

TIME	TEMPERATURES (C)			B-UNIT SENSITIVITY (DB)		POWER OUT (DBM)	
	ROOM	CASE	CHAMBER	LOW	HIGH	A	B
1300	19	41	50	35	57	15.0	8
1310	19	46	50	35	50	15.0	8
1315	19	51	50	35	50	15.0	8
1320	19	54	50	35	50	15.0	8

Table G-3 TEMPERATURE SENSITIVITY TEST

TIME	TEMPERATURES (C)			B-UNIT SENSITIVITY (DB)		POWER OUT (FRM)	
	ROOM	CASE	CHAMBER	LOW	HIGH	A	B
1130	22	23	-	32	65	15.5	7.5
1140	22	26	-	32	65	15.5	8.0
1150	22	31	-	32	63	15.5	8.0
1200	22	33	-	32	55	15.5	8.0
1210	22	36	-	32	56	15.5	8.0
1220	22	37	-	32	56	15.8	8.2
1230	22	38	-	32	56	15.8	8.2
1240	22	37	29	32	56	15.8	8.2
1250	22	42	49	32	56	15.8	8.2
1300	22	45	50	32	56	15.8	8.4
1303	22	46	50	32	56	15.8	8.4

Table G-4 TEMPERATURE SENSITIVITY TEST

TIME	TEMPERATURES (C)		B-UNIT SENSITIVITY (DB)		POWER OUT (DBM)	
	ROOM	CASE	CHAMBER	LOW	HIGH	A B
1605	22	27	-	38	85	16.0 9.7
1610	22	27	-	38	50	16.0 9.7
1625	22	28	-	38	43	15.8 9.8
1635	22	28	-	38	43	15.8 9.8
1645	22	30	-	38	39	16.0 9.9

A Station and B Unit Frequency Stability Test

It was assumed, that sensitivity degradation at higher temperatures could have been caused by RF carrier center frequency shifting in the A station and/or B unit. The objective of these tests was to determine whether any RF carrier center frequency was in fact drifting at higher operating temperatures. The experimental setup is shown in Figure 109.

The A station or B unit was put into a controllable ambient temperature chamber. The RF output signal was fed through a 20 dB loss dual directional coupler into the 7L13/TR 502 Tektronix Spectrum Analyser. The analyser had a specified 1 KHz to 1800 MHz range and a 2 KHz frequency stability over a one hour period after a two hour warm up period. Before and after each experiment the alignment of the analyser was checked against a stable signal source at 918 MHz. The analyser showed no observable internal oscillator drift.

The displayed A station or B unit frequency spectrum was observed over a four hour continuous Range mode period of operation. The ambient temperature was increased during this time period from room temperature to 48°C. The results are shown in Figures 110 to 116. The digital readout on the CRT displayed the following quantities:

Top left to right: Input RF attenuation
Center frequency
Resolution

Bottom left to right: Vertical scale in dB per division
Horizontal scale in KHz per division

No spectral analysis was done in this experiment since only the center frequency was to be observed.

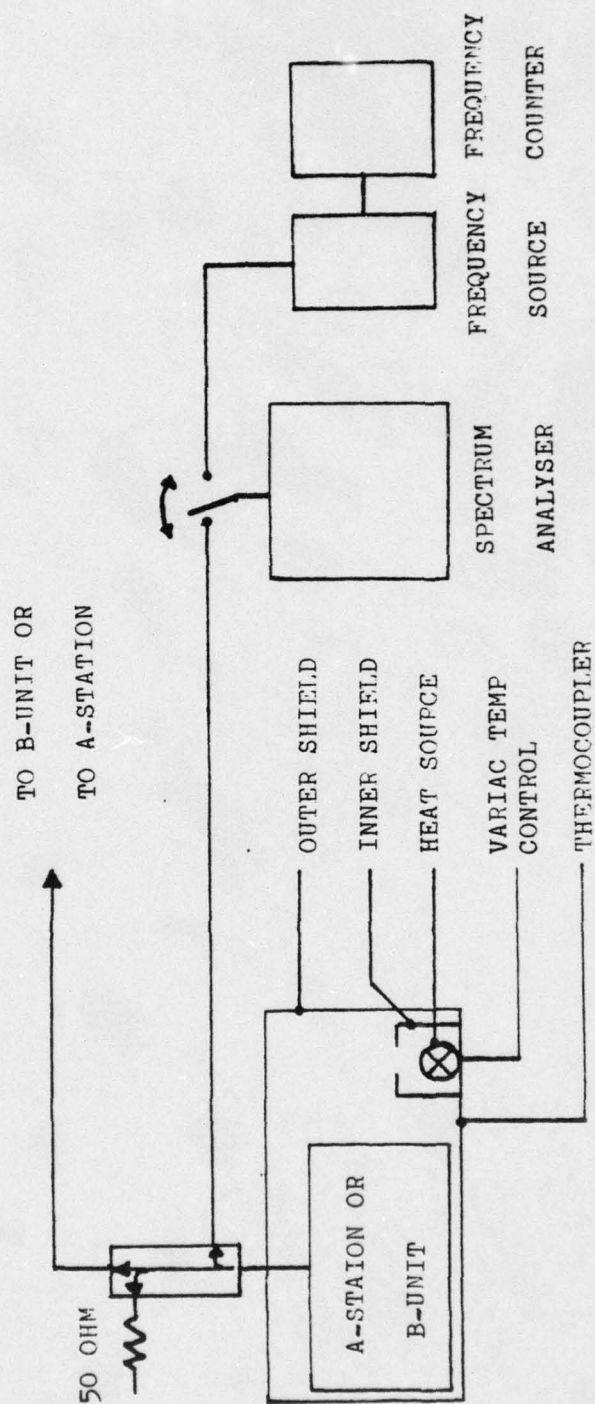


Figure 109 - A STATION/B UNIT FREQUENCY STABILITY TEST

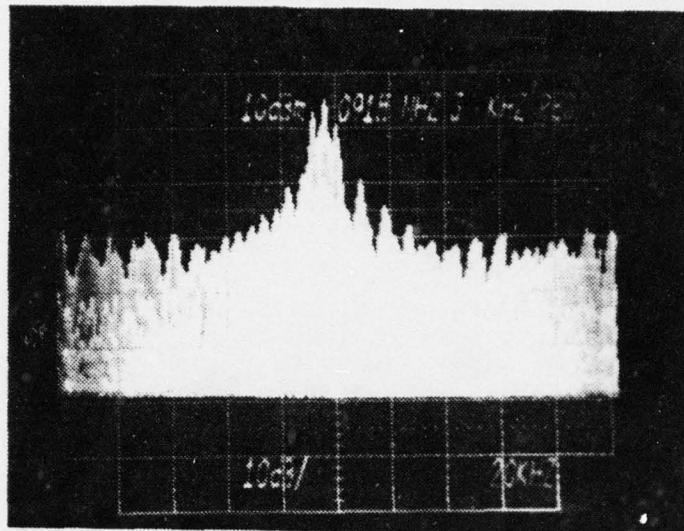


Figure 110 - A STATION FREQUENCY SPECTRUM
AFTER 5 MINUTES OF OPERATION AT 23°C

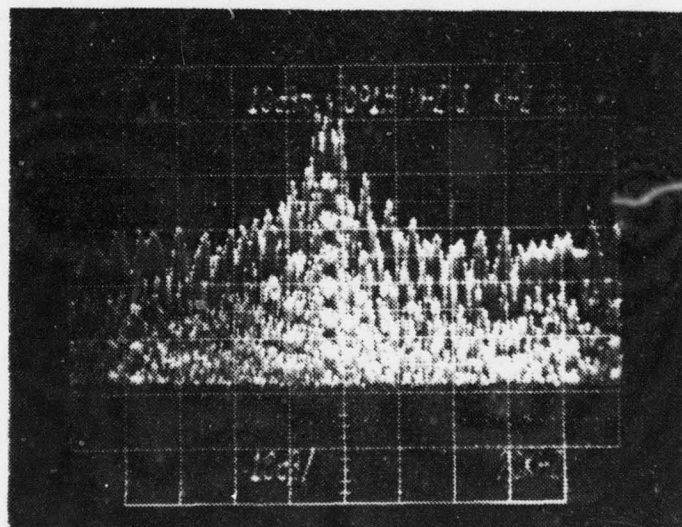


Figure 111 - A STATION FREQUENCY SPECTRUM
AFTER 2 HOURS OF OPERATION UP TO 33°C

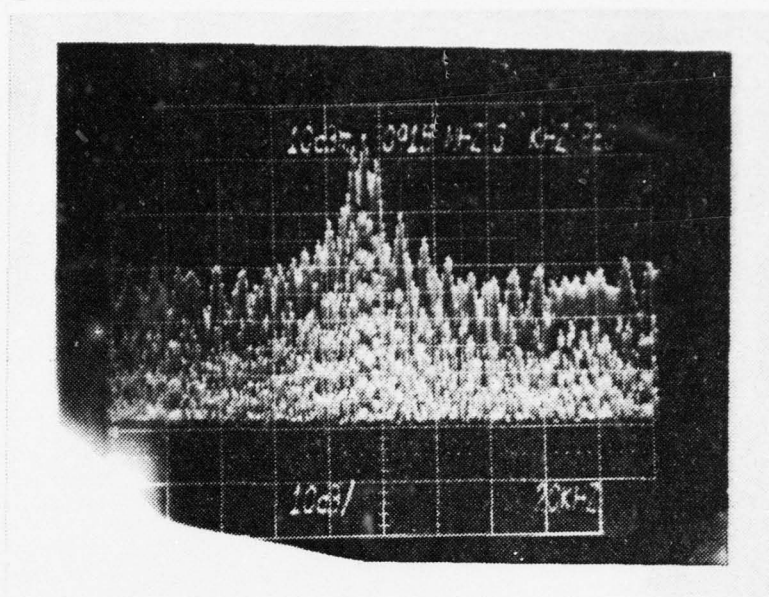


Figure 112 - A STATION FREQUENCY SPECTRUM
AFTER 4 HOURS OF OPERATION UP TO 48°C

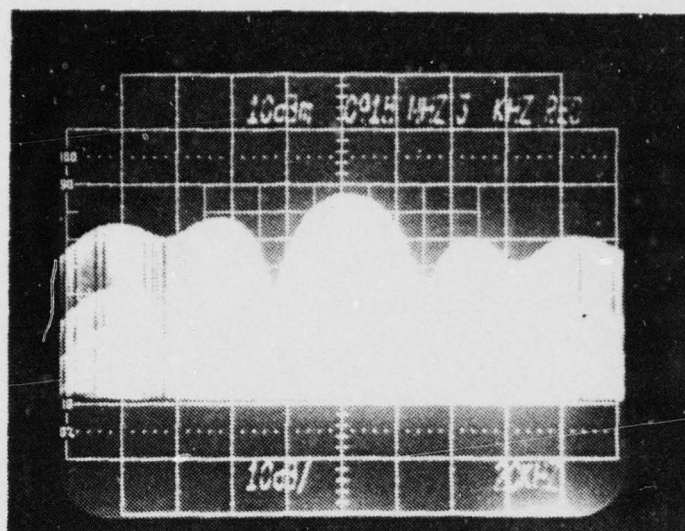


Figure 113 - OUTPUT SPECTRUM B UNIT 305
AFTER 5 MINUTES OF OPERATION AT 23°C

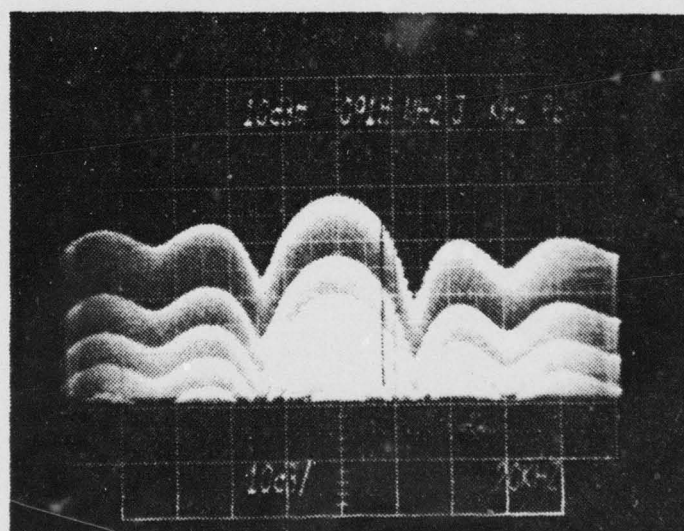


Figure 114 - OUTPUT SPECTRUM E UNIT 305
AFTER 4 HOURS OF OPERATION UP TO 48°C

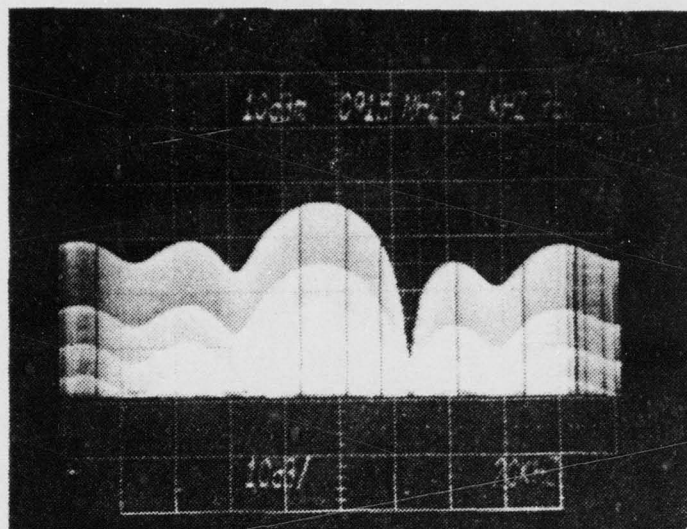


Figure 115 - OUTPUT SPECTRUM B UNIT 267
AFTER 5 MINUTES OF OPERATION AT 23°C

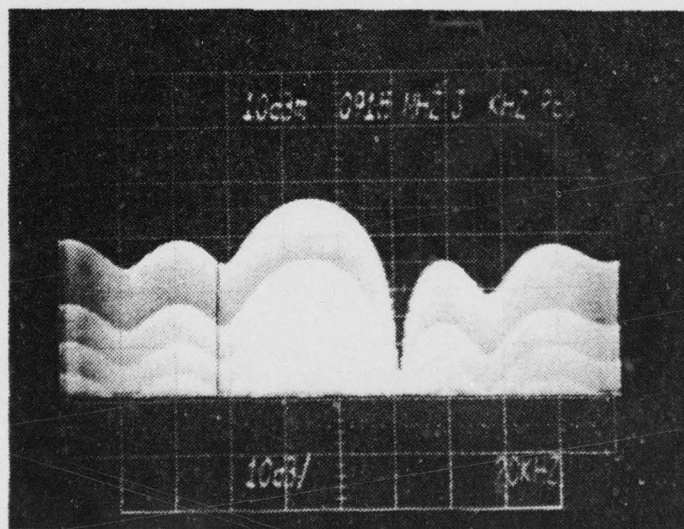


Figure 116 - OUTPUT SPECTRUM B UNIT 267
AFTER 4 HOURS OF OPERATION UP TO 48°C

APPENDIX H

ALIGNMENT INVESTIGATIONS AT FHL/BDM

The laboratory experiments initially conducted and the temperature sensitivity tests described in Appendix G, had shown that all B units aligned by maintenance personnel at Ft. Hunter Liggett worked satisfactorily only at low or room temperatures. It was therefore decided to compare the B unit checkout procedure used in single path experiments with that employed at the maintenance facility at Ft. Hunter Liggett. Moreover it had become apparent, that multipath propagation phenomena could only be observed with a reliable A to B RF link.

The test procedure is shown schematically in Figure 117. Four B units were available (#s 213, 267, 237, 305). Only B unit 213 worked satisfactorily at room temperature. After failing the high temperature test it was realigned in the same manner as B units 267, 237 and 305, which did not operate properly over the specified sensitivity range. The test setup used by maintenance personnel at Ft. Hunter Liggett is shown in Figure 118. The B unit was directly interrogated by the test C station and then aligned as described in ref. 2. This test setup was then modified to that shown in Figure 119 which resembled the single path B unit checkout setup used in Appendix C. A E unit which was first aligned directly to a C station, failed to respond to an A station, which in turn was interrogated by the C station. After the B unit was realigned to the A station, the low and high temperature tests were repeated.

If the unit worked over the specified sensitivity range it was taken out for the next field experiments.

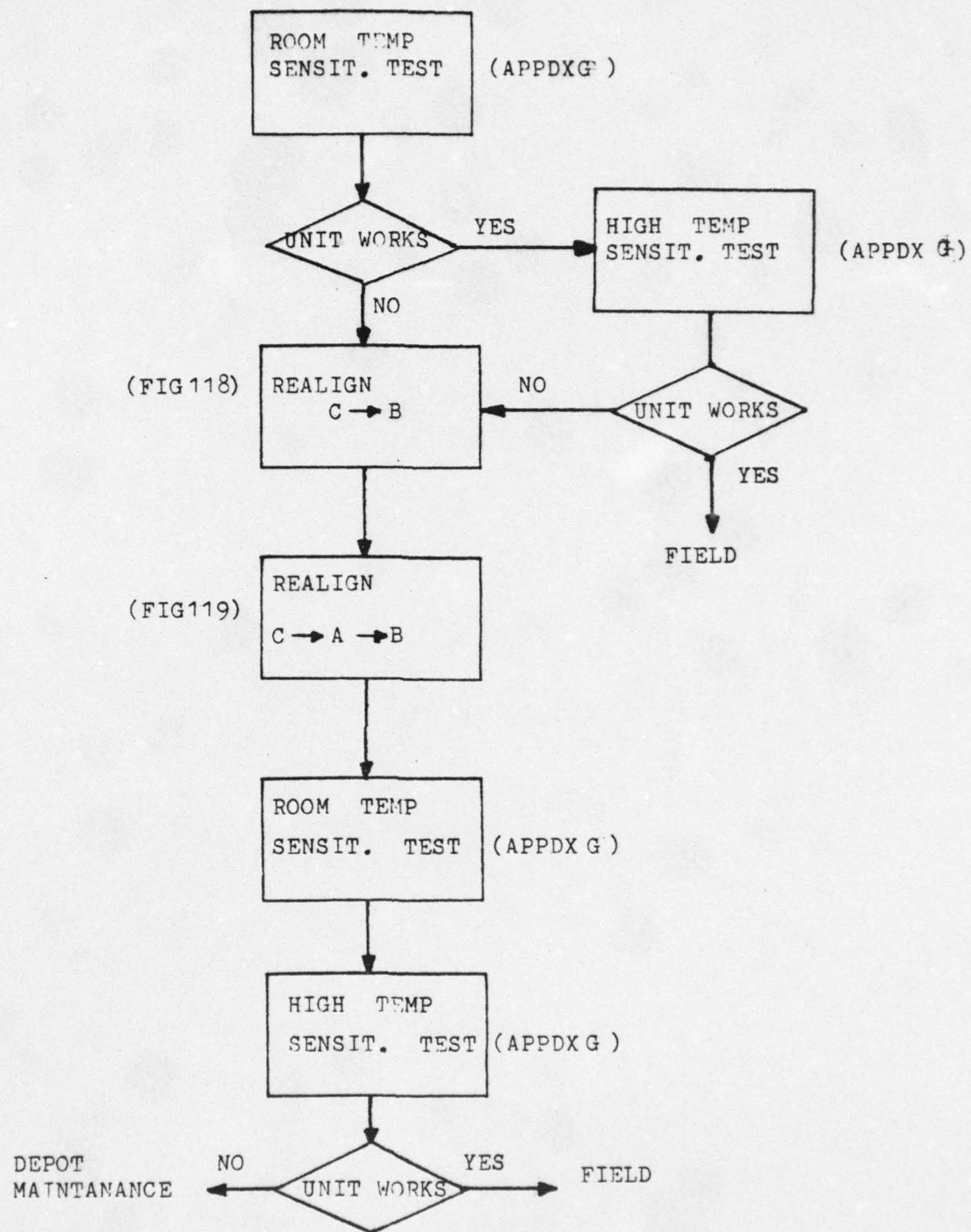


Figure 117 - ALIGNMENT TEST PROCEDURE

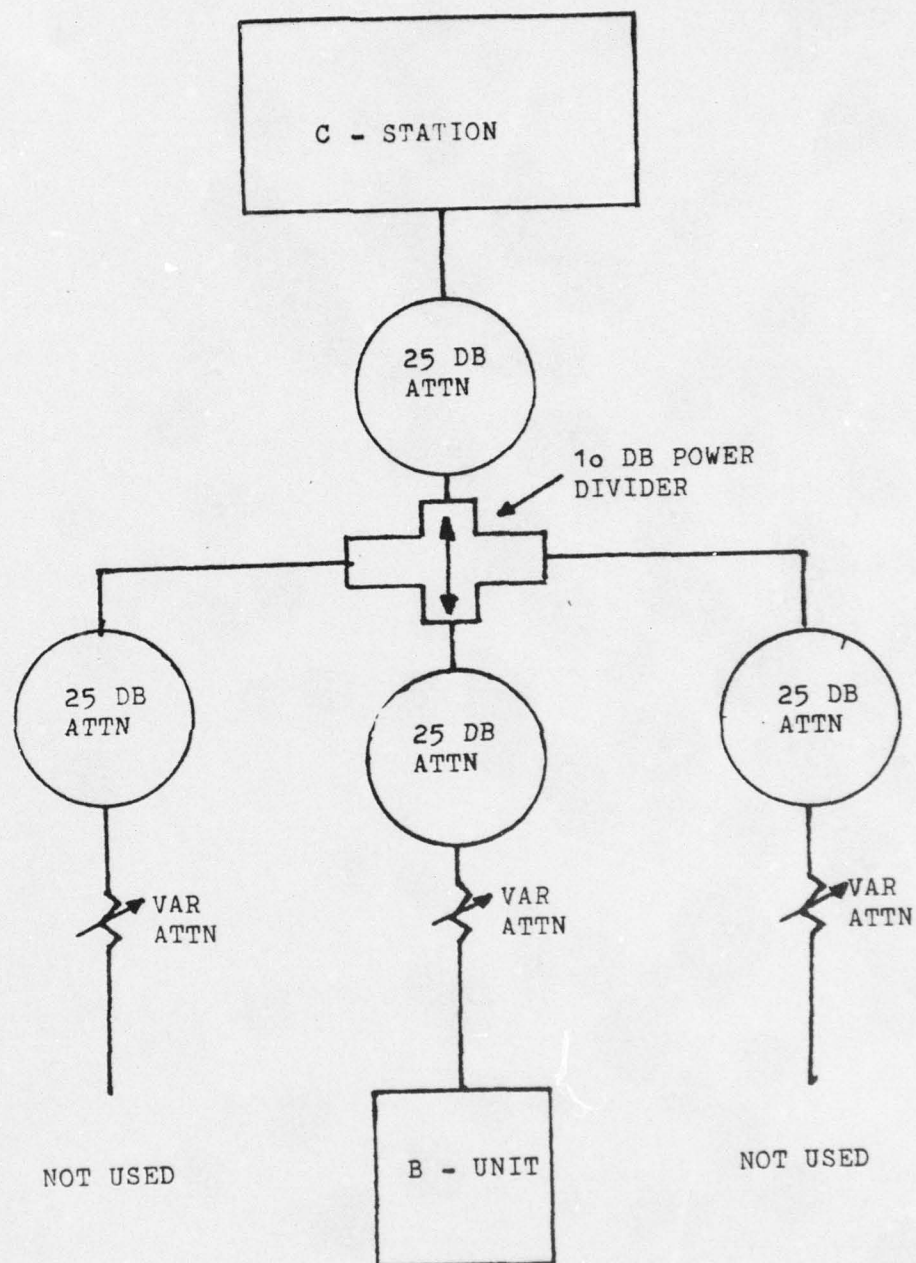


Figure 118 - FORMER B UNIT CHECKOUT SETUP

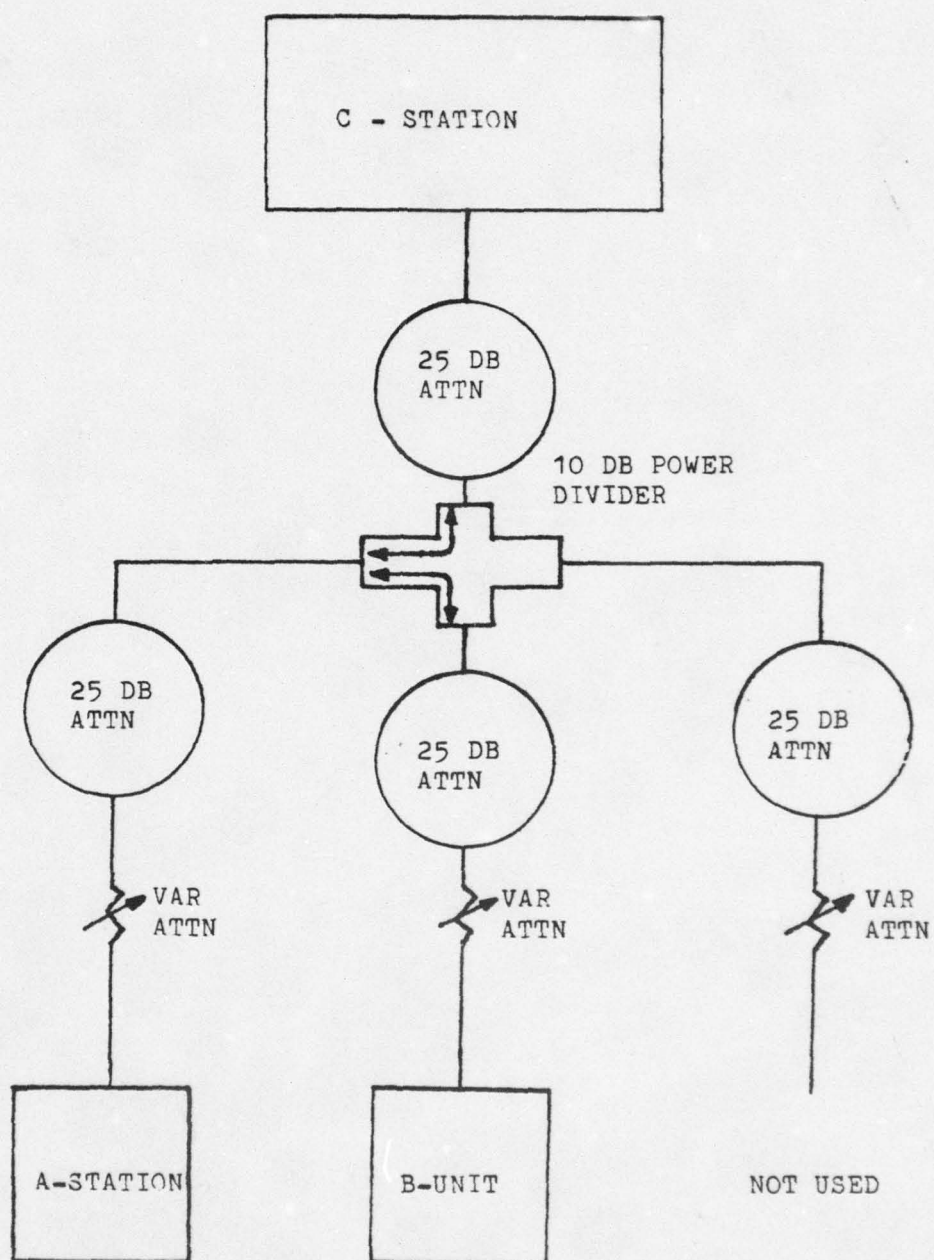


Figure 119 - B UNIT CHECKOUT SETUP

LIST OF REFERENCES

1. Berthiaume, William, B. H., Introductory Investigation of the Range Measuring System/Data Collection System (RMS-2/ECS), M.S. Thesis, Naval Postgraduate School, Monterey, Ca., March 1977.
2. General Dynamics, Electronics Division, Maintenance Instructions, Micro-B Unit, GDE-BGR-74-012, July 1974.
3. General Dynamics, Electronics Division, RMS-2/DDS, System Description and Operation, GDC-BGR-68-001, June 1968.
4. General Dynamics, Electronics Division, Software Documentation Mobile Test Station, GDE-BGR-74-017, September 1974.
5. ITT Corporation, Reference Data for Radio Engineers, Howard W. Sams, 1975.
6. Price, R. and Green, P. E., Jr., 'A Communication Technique for Multipath Channels,' Proceedings of the IRE, v. 46, p. 555-569, March 1958.
7. Schmid, Hermann F., 'A Prediction Model for Multipath Propagation of Pulse Signals at VHF and UHF Over Irregular Terrain,' IEEE Transactions on Antennas and Propagation, v. AP-18, March 1970.
8. Jakes, William C., Jr., Microwave Mobile Communications, Wiley, 1974.
9. Turin, George L., 'Communication Through Noisy, Random-Multipath Channels, paper presented at IRE